University of Zurich[UZH]

Reliability of Multi-day Precipitation Estimates from Climate Models

GEO 511 Master's Thesis

Author
Désirée Montalbetti
12-934-329

Supervised by
Dr. Ilja van Meerveld

Faculty representative
Prof. Dr. Jan Seibert

30.09.2021
Department of Geography, University of Zurich

Universität Zürich[UZH]

Geographisches Institut

Reliability of Multi-day Precipitation Estimates from Climate Models

GEO 511 Master's Thesis

Author
Désirée Montalbetti
12-934-329

Supervised by
Dr. Ilja van Meerveld

Faculty representative
Prof. Dr. Jan Seibert

30.09.2021
Department of Geography, University of Zürich

Abstract

The aim of this work is the analysis of reliability of multiday precipitation estimates from climate model, more precisely from the chain model simulations that compose CH2018, the most up to date tool for climate simulations in Switzerland. The analysis was carried out through the statistical study of the correlations of the CH2018 outputs with the historical data recorded by SwissMetNet (SMN) network, an integrated automatic monitoring network of MeteoSwiss which collets observations resulted from a centralized modernization of the meteorological monitoring system between 2003 and 2015 (previous 2003 the different meteorological variables were split into different monitoring networks). CH2018 includes 68 EURO-CORDEX simulations running three different future scenarios: RCP2.6, RCP4.5, and RCP8.5. The different scenarios or Representative Concentration Pathways (RCPs) describe the possible increase in radiative forcing values in W/m^{-2} by 2100 (CH2018,2018), covering from a reduction in emissions up to the point where global warming is kept below 2°C (RCP2.6) to unabated emissions (RCP8.5) with a possible intermediate scenario, where even with due care, global warming fails to stay below 2°C. (CH2018, 2018).

Data analyses and temporal correlations were performed with R, a free software environment for statistical computing (Rstudio Team, 2021). Later spatial analyses were also done using the free and open-source cross-platform desktop geographic information system application QGIS (QGIS.org, 2021).

Changes in precipitation patterns, storms and cyclones, and locally heavy rains around the world have recently conspired to bring down structures and power grids, cause flooding, and result in deaths. There are numerous variables that link flooding to climate change, and it's becoming a growing problem as more countries experience unprecedented flash floods. This is where climate models come in, created to help prepare for the consequences of climate change, as they are designed to project weather conditions into the future, but being systems of physical and mathematical formulas and procedures that aim to represent real-life conditions, they are far from perfect and as a result are constantly being improved and revised.

However, precipitation products to date have primarily been evaluated in terms of rainfall totals, but for hydrologic concerns and forecasting, other precipitation characteristics are also important to evaluate. For example, for the prediction of drought duration and severity, the number of consecutive days with little precipitation or the minimum monthly precipitation amounts are important or for forecasting large flood events, three-day precipitation or above-average moisture conditions are an important factor to consider.

Due to the importance of climate change on precipitation and hydrological extremes in particular therefore in this work the mean, maximum, 95th percentile and 99th percentile of 3, 7, 30 and 90 day multi-day precipitation were analyzed. The starting point were the daily outputs so that we have the same inputs that CH2018 uses for simulations. The daily precipitation results were then summed for each chosen multi-day precipitation for both the SMN observations and CH2018 outputs. At the temporal level, the analysis was conducted in three different periods: the first one starts from 1981 and goes up to 2020, the second one goes

from 2021 to 2060 while the third one covers from 2061 to 2099. The first period is the one in which historical data are available, the other two periods were chosen accordingly to have an average of 40 years per period each.

In furtherance of the correlations for the first period, SMN observations were analyzed only for the RCP8.5 scenario, as the scenario with no change in emissions is the closest to the current situation. For future periods, however, the analysis was performed for all three scenarios, comparing the outputs of each scenario in the future with the outputs of the corresponding scenario in the first period.

The study of the chosen statistical variables highlighted the inability of CH2018 to accurately simulate the median of SMN. About the extremes, i.e., the 95th and 99th percentiles, the correlation between the two datasets is quite good, especially for longer multiday precipitation windows, i.e., 30 and 90 days. The spatial analysis also highlighted the underestimation of the extremes along the Alps and a general overestimation of the SMN data in the rest of Switzerland. In addition, the 99th percentile has a higher overestimation of SMN data than the 95th percentile. Analyses on projected future data also show the same trend as found for the first period analysis although there are some small differences between scenarios, visible especially in the shorter time windows.

The analysis of the maxima shows a general overestimation that becomes more accurate the wider the time window, but the area of Ticino and Walensee are more affected by maximum precipitation. The analysis of the future has fewer clear results both statistically and spatially.

Beside the fact that the data analyzed are few to make an accurate general consideration on the reliability of CH2018 simulations about precipitations patterns, this work highlights how the simulations are not yet able to accurately predict extreme events. The tendency is in fact to standardize the data (Edwards, 2011) and we can have an idea of how the rainfall will evolve, but not having accuracy and adequate warning time in case of disasters such as floods or droughts. The multi-day analysis turns out to optimize this lack, since it can monitor the sequence of days with precipitation (or lack thereof) that are the discriminating factor to predict problematic situations related to precipitations (whether there are present or not).

In conclusion, this work shows that it is also worthwhile to do multi-day precipitation analysis. Their knowledge can help to improve the warning and prediction of extreme events that in recent years are becoming less rare. Moreover, it turns out to be a valid solution to have an overview of the general trend of heavy rains and thus improve the management of their consequences, and possibly also make the reading of CH2018 more sensitive to the sequence of multiple rainy days or their absence.

Acknowledgement

Above all, I would like to thank my supervisor Dr. Ilja van Meerveld, who always remained available during the realization of this work through stimulating discussions, constructive ideas and corrections, especially when I was not clear on how to proceed.

In addition, I would like to thank Marc J. P. Vis for his endless patience and helpful advice in debugging the R code used for the analyses.

A thank you also goes to MeteoSwiss for the availability of the SwissMetNet and CH2018 data.

In particular, I would like to thank everyone who sacrificed their time to help me proofread the work and encouraged me throughout the thesis process.

Above all, I would like to thank my family who not only allowed me to study, but also supported me in all situations in life. Thank you so much!

Index

List of Figure

List of Tables

1 Introduction

Climate change does not only refer to the increase in temperature but also changes in weather characteristics, including extreme events. Extreme events such as heat waves, cold waves but also heavy precipitation and droughts are becoming more frequently and severe (Huber et al., 2011). Region with low elevation on the Swiss Plateau, Ticino and the lower Alps are already experiencing an increase in temperature extremes and tropical nights (CH2018, 2018). These of extreme events will become less rare and rather normal, which is consistent with our theoretical understanding and climate models (Prudhomme et al., 2002). This trend will likely continue in the years to come, and it is especially the rarer and more extreme events that will be most affected (Alexander et al., 2006).

Predictions for the coming decades is an increase in global temperatures due to the absorption of longwave radiation by greenhouse gases, going on to affect the distribution of water resources. (Kothavala et al., 1997). The higher the temperature, the more the atmosphere can retain moisture due to the exponential relationship between temperature and saturation vapor pressure described by the Clausius-Claperyron equation and since an increase in temperature is directly consequent to higher evaporation rate, precipitation is as well in a rising trend. As previous research suggests possible occurrence of summer droughts would be directly proportional to increased evaporation (Manabe et al., 1981).

Moreover, Changes in rainfall patterns, storms and cyclones, and locally severe rain across Asia have recently conspired to bring down structures and power grids, cause flooding, and result in deaths. Extreme weather, rising sea levels, and other climate change consequences are not just affecting Asian countries. European countries are also witnessing flooding as a result of extreme weather, rising sea levels, and other climate change impacts. There are numerous variables that link flooding to climate change, and it is becoming an increasing problem as more countries experience unprecedented flash floods. According to a recent study by Anderson et al. (2015), precipitation changes were responsible for 36 % of all U.S. flood damages from 1988 to 2017. Models demonstrate how climate change increases the likelihood of intense rain events, which contribute to most of the flood damage, according to Wilhelm et al. (2012). Hydrological studies have concluded that as climate change accelerates, changes in precipitation will become more intense. The connection between climate change and extreme weather events has been thoroughly documented in various parts of the world. Coastal flooding has grown as sea levels have risen, while torrential rainfall and urban floods have increased as a result of the warmer atmosphere's capacity to retain more water.

The hydrological data is highly speculative. This is true even for the most fundamental values, such as rainfall at a specific location, discharge at a specific location, and accurate evapotranspiration variations. It is significantly more difficult if we are concerned in the hydrological cycle over a catchment region, because precipitation, snowpack, evapotranspiration gradients, and measurement tools are all subject to uncertainty. The problem is exacerbated because, in most cases, the uncertainties are caused by a lack of expertise rather

than variability. Hydrologic modelling is used to address environmental mobility concerns including water shortage, excess, or dissolved or solid content. There is no single optimum model for environmental predictions due to the nature of the subject. Rather, depending on the objective and required complexity, there are a variety of viable options. For this and other reasons, hydrologic modelling has tended to rely too heavily on mathematical concepts at the expense of genuine knowledge, and there is a need for more thorough assessment of appropriateness. In most cases, model selection is based on familiarity rather than suitability. Hydrologic modelling is complicated by process uncertainties as well as the disproportionate influence of variabilities and other understudied and poorly characterized natural phenomena. As a result, a large range of hydrologic models exist, all of which are insufficient and unreliable in all but the most basic scenarios.

Climate models are used to project weather conditions into the future but being system of physical and mathematical formulas and procedure that aim to represent real-life conditions, they are far from perfect and consequently are constantly improved and revised.

Global climate models (GCMs) are considered one of the most reliable tools for the study of climate change (Shine et al., 1990), they consider five basic variables, such as: temperature (determined by the thermodynamic equation), humidity and surface pressure (determined by equations for the conservation of substances and mass of water), and the NS and EW wind components (determined by the Navier-Stokes equation). Moreover, sea surface temperature is derived from climate data and coupled with solar zenith angle variation by day and season, GCMs can be considered numerical weather prediction models adapted for long periods (decades) (Mitchell, 1989).

Despite their potential catastrophic impact, both economically and as a hazard to humans, animals, and vegetation (Aon Benfield, 2017) extreme precipitation changes in the literature have received limited attention (Gordon et al., 1992; Rind et al., 1989) furthermore it is argued that in analyses of climate impact relative to the mean, is the variability that carries more significance (Katz et al., 1992).

Model predictions for temperature tend to agree with reality but their predictions of precipitation are more variable and uncertain (Neelin, 2010). Evaluation of climate models' outputs for precipitation has mainly focused on rainfall totals which data from daily, monthly or annual scale (Wilby, 2010). For hydrological predictions, other precipitation characteristics are important as well. For example, for prediction of large flood events, the three-day or 30-day total precipitation data is needed to obtain information on the wetness conditions that can significantly affect the response to large precipitation events. Many floods are the consequence of several consecutive days of rain. For example, in August 2021, heavy rainfall in Kanzaki, Saga prefecture, Japan caused floods and landslides (Jones, 2021). Storms were triggered by deep tropical moisture, resulting in severe flooding and landslides, prompting the evacuation of more than one million residents. Several people are thought to have died, with the Kyushu region taking the worst of the damage, with some weather records indicating more than 1,000mm of precipitation in five days. In climate modelling to predict

the duration and severity of future droughts, the number of consecutive days with very little rainfall or monthly minimum rainfall amounts is important because droughts are the results of long periods with little rain.

Climate change may exacerbate hydrological extremes, altering the size as well as the timeframe of flood and drought occurrences. Understanding anticipated future trends in hydrological extremes at the state level is crucial for guiding national policies and ensuring suitable adaption measures are implemented. Hydrological models' process descriptions are simply generalizations to the real-world elements of surface and groundwater flows. It is also self-evident that the epistemic difficulties with hydrological data imply that even a flawless model would not be able to make perfect projections. Indeed, the predictions can appear to be poor at times, especially when models are deployed without validation, as if to an ungauged catchment. Calibration is often useful in identifying parameter sets that, at least during the calibration period, produce forecasts that are comparable to the measurements. Whenever a split record analysis was conducted, it is usual to discover that the model's reliability is poor during the validation timescale or under other seasonal or climate patterns.

Droughts and floods can have devastating societal, environmental, and economic consequences. The California drought of 2012-2016, for instance, resulted in catastrophic crop yield declines and water rationing in large cities. These extreme weather events might have particularly serious consequences if they strike a vast area or occur in quick succession. Drought–flood transitions that occur quickly, such as the shift from the California drought of 2011–2016 to the winter of 2017 in the United States. Due to the opportunity cost between water storage and flood mitigation, the California floods prove problematic to water supply and dam operations. Management solutions that focus just on floods or droughts may hinder the ability to cope with other types of extremes. Droughts and floods ought to be evaluated together in order to build coordinated and efficient management methods. Our capacity to forecast floods and droughts at diverse time periods is critical for developing management methods to reduce the negative effects of droughts, floods, and rapid event changes. Flood and drought predictions at hourly to annual time periods are used to plan crisis measures and early warnings. Estimates of the frequency and size of severe occurrences, such as the likelihood of a 100-year flood event, are required effective water resource management. Long-term drought and flood forecasts that describe future climate are needed for the development of policy interventions.

Given the importance of climate change on precipitation and hydrological extremes, with this work, I would like to try to understand if multi-day precipitation statistics, such as 3, 7, 30 and 90 day total rainfall, minimum or maximum monthly rainfall, are well represented by climate models. I, therefore, compared global climate model with a regional climate model to estimate multi-day precipitation. More specifically, I aimed to answer the following research questions.

What is the reliability of climate models for Switzerland, in terms of different precipitation signatures and precipitation distributions, and since floods, respectively droughts often occur in response to long periods

with and without precipitation, are the models able to correctly simulate these extreme events with enough accuracy?

2 Literature Review

2.1 Precipitation measurements

Precipitation is a measure of the quantity of water reaching earth's surface's horizontal and horizontal ground projection plane and is represented as a vertical level of water or the water equivalent of snowfall. In Switzerland, the unit of measurement is millimeters, where 1 mm = 1 l/m^2 and 1 mm of water corresponds approximately to 1 cm of fresh snow (MeteoSwiss, 2021). Precipitation is usually measured in its liquid form, so in the case of solid precipitation, once it has melted the equivalent in water is calculated (MeteoSwiss, 2021).

The measurement of the amount and distribution of precipitation with respect to time and space can be acquired both directly and indirectly. Ground-based instruments such as rain gauges are used for direct measurement while indirect data collection is entrusted to remote sensing techniques (radar system, aircraft and Earth-observing satellites) (Jain et al., 2003). In this work the analyzed data came from direct measurement and more specifically from two types of rain gauges. The first one is a 1518 H3 and 15188 manufactured by Lambrecht and the second one is a Pluvio2 by OTT. The 1518 H3 is a type of rain gauge heated so in case of solid precipitation it is possible to calculate its contribution after the melting. Moreover, it is also equipped with a tilting device, meaning that when it is full, the collecting basin is automatically poured into a second one located at the base of the funnel. Then from the number of overturns in a given period of time it is possible to determine the amount of precipitation. In the case of the Pluvio2 rain gauge, the measurement is based on weight, all precipitation (whether solid, liquid or mixed) is determined by means of a closed weight scale inside the device. In contrast to the tilting device, this second instrument must be emptied regularly. Despite all the precautions that can be taken, the measurement of precipitation using rain gauges is not always accurate and carries a few systematic errors that lead to an underestimation of the actual volume of water falling to the ground and if the precipitation is solid the error is even greater (Lendvai et al., 2014). The main uncertain factor is the wind that induces perturbations in the trajectory of raindrops that prevents the funnel from collecting them accurately (Lendvai et al., 2014). these errors can essentially be grouped into two subcategories such as systematic and random errors, where systematic errors are essentially due to instrument malfunction, wrong exposure conditions or lack of observer knowledge (Jain et al., 2003); whereas random errors cover from possible losses in and out of the receiver to observer errors in handling the data.

All precipitation measurements, alongside other meteorological variables, besides being a valuable tool for research in terms of better understanding what happens in our atmospheric system are also the starting point for creating climate models as accurate as possible: climate models are useful tools for better understanding and forecasting climate behavior on seasonal, yearly, decadal, and centennial time scales (Buytaert et al., 2010). Models look into whether recorded climate changes are the result of natural variability,

human action, or a combination of both. Their findings and estimates give critical information for making better decisions about management of water resources, agriculture, infrastructure, and urban development at the federal, provincial, and local levels.

Temperature, moisture content, pressure, sun radiation, precipitation, and wind conditions are all continuously recorded by SwissMetNet standard monitoring station. The monitoring program and instruments deployed are tailored to the type of station in question. Some stations are dedicated to the study of climate and its long-term evolution; they are equipped with specific instruments that can be counted on to provide accurate data over an extended period. MeteoSwiss optimizes its measurement systems with SwissMetNet in order to meet the needs of its partners and customers in industries as diverse as air transport, meteorology, agricultural production, power generation, and infrastructure maintenance. As a result, the measurement program records various elements such as surface temperatures at various depths, sunshine length, radiation, radioactivity, visibility, and of course precipitation.

2.2 Precipitation signatures

Precipitation data was originally available at a daily resolution but is now available at an hourly or minute resolution. The most frequent used precipitation data is, however, the daily precipitation sum. The analysis of extreme values by MeteoSwiss (Kotlarski and Rajczak, 2018), for example, used daily precipitation data for the 1966 to 2015 period to determine climatic conditions. Multi-day metrics of precipitation that are used in the literature are the 3-day, 7-day, and monthly precipitation. The tangible impacts on the territory are a consequence of several consecutive days of torrential rains, dry periods, high temperatures, wind, humidity; and beside having most accurate information possible is also an advantage to have a clearer view of what happened and consider it for building models as accurate as possible is necessary and useful but a wider overview, especially in term of time is not to be underestimated.

2.3 Climate models

Climate models are vital instruments for bettering our understanding and forecasting of atmospheric, oceanic, and climate phenomena. They enable us to determine the unique influence of various climate aspects by allowing us to investigate climate sensitivity using experiments that cannot be carried out in the real world. For example, is possible to determine the influence of changes to one component in a climate model, such as natural variability sea floor temperatures, simply by changing the variable on the simulation.

Moreover, they can be also used for diagnosis and prognosis. Detection and attribution are two examples of diagnostic uses. Detection and attribution include proving that a measured variation is statistically meaningful before assigning it to non-natural causes, such as the importance of anthropogenic forces in twentieth-century climate change (Santer et al., 1995). Prognostic climate modelling uses current or historical

data such as ocean topography and solar radiation to forecast future climate. Seasonal variability, decadal forecasting, and 21st century forecasts are all timescales for projection. Finally, to test the validity and accuracy of the model simulations, it is run for a period in the past. The results are then compared with the observations obtained through the years testing the accuracy of the simulations and helps correct the equations that regulate it. Furthering improvement and new ideas came also from constant comparison with the results and the observations of other models already existing. (Sahoo et al., 2020).

Global Climate Models (GCMs) are computer-based simulations of the Earth's climate system. The models cover various aspects of the Earth's climate system and include the most important processes in the atmosphere, ocean, on land, and the cryosphere. They are used to reconstruct the climate in the past and to make projections for the future (National Centre for Atmospheric Science, 2020).

Despite the validity of GCM simulations, the information has low resolution, on the order of hundreds of kilometers. For areas where the models are largely dependent on orography, such as mountainous areas, the GCM information is transferred to a regional scale by downscaling procedures in order to increase the spatial resolution of the data. To achieve this goal, various downscaling techniques have been developed that can be classified into statistical and dynamic downscaling.

Underlying the design of downscaled climate variables (such as precipitation) by statistical downscaling is the assumption that statistical associations are valid even at different spatial resolutions (Wilby et al., 1997). With this assumption, typing schemes, transfer functions, or weather generators are then used for downscaling (Ayar et al., 2016). Although it is very simple to use, it has uncertainties as it relies on the assumption that the statistical relationships used remain unchanged over time (Hakala et al., 2019).

Dynamical downscaling, on the other hand, includes the use of RCMs with spatial resolution from 10 to 50 kilometers that are performed using the boundary conditions obtained from GCMs offering a more realistic view (Lafon et al., 2013). Regional Climate Models (RCMs) are embedded in global climate models, a combination often referred as GCM-RCM model chain and with their higher spatial resolution allow forecasts for smaller topography areas (Eden et al., 2014).

Despite the increase in accuracy a 10x10 km resolution is still too inaccurate for Switzerland, which is why the RCMs are additionally downscaled to 2x2 km resolution through bias correction. As Maraun et al. (2017) define a bias is “the systematic difference between a modeled property of the climate system and the corresponding real property”. In practical terms it includes all corrections to the outputs given by climate models through quantile mapping to reduce the effects of systematic errors in climate models and to make the output more suitable as guidance data for hydrological models, ensuring as well that the distribution of observed and simulated climate variables agree for past measurements (Hakala et al., 2019). The same corrections are applied for future forecasts at a daily temporal resolution (CH2018, 2018).

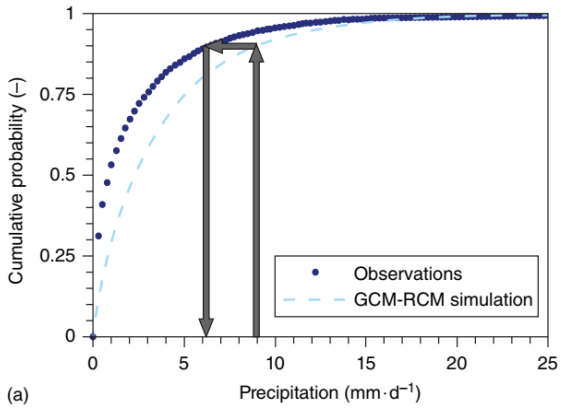

Figure 1: Transformation of the GCM-RCM-simulated values to the observed values through bias correction (Hakala et al., 2019).

3 Method

3.1 Datasets

3.1.1 Observed data

For the comparison of the climate scenarios for precipitation with the observations, the SwissMetNet (SMN) was selected because of the possibility for point-to-point comparisons. In addition, the long data time series of the SMN mean that it is more likely to include extremes events. The SMN is an integrated automatic monitoring network of MeteoSwiss which collets observations that resulted from a modernization of the meteorological monitoring system between 2003 and 2015. Prior to 2003 MeteoSwiss had multiple networks divided by observation type, but due the increasing demand of meteorological forecasting and climate observation, SMN was created. The base of the network is thereby the collection of the previous one that before 2003 were divided by observation type; to make some examples there is the ANETZ automatic monitoring network and the ENET supplementary measurement network, as well as conventional climate stations where parameters were measured three times a day, and "human" observations. With the standardization[1] of SMN, continuous records for temperature, humidity, air pressure, solar radiation, precipitation and wind strength and direction are available.

The studies region covers all of Switzerland. The data series for the different stations differs but were cut to the 1981 and 2020 since CH2018 simulation outputs are available starting from 1981. The SwissMetNet (SMN) network today includes 160 automatic meteorological station and 100 manual ones but only the 69 stations that were already active for daily precipitation record in 1981 were used for the analyses.

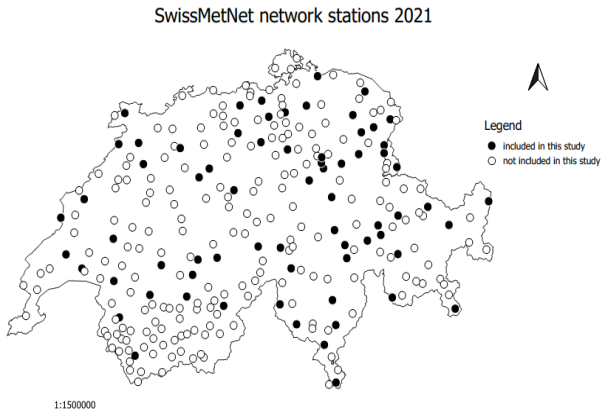

Figure 2 – SwissMetNew network station today 2021. Stations that it has been possible to use in this study are marked in black.

[1] From here on, any reference to standardization refers to Edwards, 2011 publication.

3.1.2 CH2018 scenarios

The CH2018 Climate Scenarios for Switzerland were published in 2018 and are the results of a combined effort by various Swiss institutions under the National Centre for Climate Services (NCCS): MeteoSwiss, ETH Zürich, the Centre for Climate System Modelling (C2SM), the University of Bern and the Institute for Snow and Avalanche Research (SFL/WSL). All the changes of meteorological variables in CH2018 rely on the European Coordinated Downscale Experiment (EURO-CORDEX) ensembles of regional climate simulation combined with Regional Climate Models (RCMs) (CH2018, 2018; Jacob et al., 2014). The CH2018 climate scenarios for Switzerland provides daily time series for the period 1981 - 2099 for precipitation and other meteorological variables at individual station on Swiss territory (DAILY-LOCAL) as well as a 2 km gridded data covering all Switzerland (DAILY-GRIDDED). Here the data for the stations that are part of the SwissMetNet are used. The data are the results of bias correction and downscaling (quantile mapping QM) of the original climate projection of EURO-CORDEX from which the different CH2018 scenarios have been derived. They consist of several climate predictions resulting from different combinations of global GCMs and regional RCMs climate models for three different greenhouse gas (GHG) scenarios: RCP2.6, RCP4.5 and RPC8.5. The three scenarios or Representative Concentration Pathways (RCPs) describe the possible increase in radiative forcing values in W/m^{-2} by 2100 (CH2018,2018). In practice the three possible alternatives of RCPs are based on anthropological impacts covering from a reduction in emissions up to the point where global warming is kept below 2°C (RCP2.6) to unabated emissions (RCP8.5) with a possible intermediate scenario, where even with due care global warming fails to stay below 2°C. (CH2018, 2018).

In total CH2018 scenarios are the result of 68 EURO-CORDEX simulations at two different resolutions: EUR11 and EUR44, with approximately 12 km respectively 50 km spatial resolution. For the RCP2.6 scenario there are 12 simulations, for the RCP4.5 25 simulations and finally for RCP8.5 31 simulations (Kotlarski et al., 2018). Each EURO-CORDEX combination of RCMs and GCMs that CH2018 utilize are performed for both two resolutions and the three RCPs scenarios according to the scheme [RCM]_[GCM]_[RESOLUTION]_[SCENARIO]. Table 3 contains the RCMs and GCMs abbreviations employed by the CH2018.

Full EURO-CORDEX RCM name	CH2018 abbreviation [RCM]
CLMcom-CCLM4-8-17	CLMCOM-CCLM4
CLMcom-CCLM5-0-6	CLMCOM-CCLM5
DMI-HIRHAM5	DMI-HIRHAM
ICTP-RegCM4-3	ICTP-REGCM
KNMI-RACMO22E	KNMI-RACMO
MPI-CSC-REMO2009 (r1i1p1)	MPICSC-REMO1
MPI-CSC-REMO2009 (r2i1p1)	MPICSC-REMO2
SMHI-RCA4	SMHI-RCA
Full EURO-CORDEX/CMIP5 GCM name	**CH2018 abbreviation [GCM]**
ICHEC-EC-EARTH	ECEARTH

MOHC-HadGEM2-ES	HADGEM
MPI-M-MPI-ESM-LR	MPIESM
MIROC-MIROC5	MIROC
IPSL-IPSL-CM5A-MR	IPSL
CCCma-CanESM2	CCCMA
CSIRO-QCCCE-CSIRO-Mk3-6-0	CSIRO
NCC-NorESM1-M	NORESM
NOAA-GFDL-GFDL-ESM2M	GFD

*Table 1 – RCM and GCM abbreviations utilized for the CH2018 data file names (**Kotlarski** et al., 2018)*

For the analysis all ten model chain outputs for EUR11 were used due its higher spatial resolution, resulting in the following 24 outputs for each station (each model chain output for each scenario, however, RCP2.6 is not available for every model chain resulting in 24 file pro station instead of 30) (Table 2).

CLMCOM-CCLM4_ECEARTH_EUR11_RCP45	MPICSC-REMO2_MPIESM_EUR11_RCP26
CLMCOM-CCLM4_ECEARTH_EUR11_RCP85	MPICSC-REMO2_MPIESM_EUR11_RCP45
CLMCOM-CCLM4_HADGEM_EUR11_RCP45	MPICSC-REMO2_MPIESM_EUR11_RCP85
CLMCOM-CCLM4_HADGEM_EUR11_RCP85	SMHI-RCA_ECEARTH_EUR11_RCP26
CLMCOM-CCLM4_MPIESM_EUR11_RCP45	SMHI-RCA_ECEARTH_EUR11_RCP45
CLMCOM-CCLM4_MPIESM_EUR11_RCP85	SMHI-RCA_ECEARTH_EUR11_RCP85
DMI-HIRHAM_ECEARTH_EUR11_RCP26	SMHI-RCA_HADGEM_EUR11_RCP45
DMI-HIRHAM_ECEARTH_EUR11_RCP45	SMHI-RCA_HADGEM_EUR11_RCP85
DMI-HIRHAM_ECEARTH_EUR11_RCP85	SMHI-RCA_IPSL_EUR11_RCP45
MPICSC-REMO1_MPIESM_EUR11_RCP26	SMHI-RCA_IPSL_EUR11_RCP85
MPICSC-REMO1_MPIESM_EUR11_RCP45	SMHI-RCA_MPIESM_EUR11_RCP45
MPICSC-REMO1_MPIESM_EUR11_RCP85	SMHI-RCA_MPIESM_EUR11_RCP85

Table 2

CLMCOM-CCLM4_ECEARTH_EUR11_RCP45	MPICSC-REMO2_MPIESM_EUR11_RCP26
CLMCOM-CCLM4_ECEARTH_EUR11_RCP85	MPICSC-REMO2_MPIESM_EUR11_RCP45
CLMCOM-CCLM4_HADGEM_EUR11_RCP45	MPICSC-REMO2_MPIESM_EUR11_RCP85
CLMCOM-CCLM4_HADGEM_EUR11_RCP85	SMHI-RCA_ECEARTH_EUR11_RCP26
CLMCOM-CCLM4_MPIESM_EUR11_RCP45	SMHI-RCA_ECEARTH_EUR11_RCP45
CLMCOM-CCLM4_MPIESM_EUR11_RCP85	SMHI-RCA_ECEARTH_EUR11_RCP85
DMI-HIRHAM_ECEARTH_EUR11_RCP26	SMHI-RCA_HADGEM_EUR11_RCP45
DMI-HIRHAM_ECEARTH_EUR11_RCP45	SMHI-RCA_HADGEM_EUR11_RCP85
DMI-HIRHAM_ECEARTH_EUR11_RCP85	SMHI-RCA_IPSL_EUR11_RCP45
MPICSC-REMO1_MPIESM_EUR11_RCP26	SMHI-RCA_IPSL_EUR11_RCP85
MPICSC-REMO1_MPIESM_EUR11_RCP45	SMHI-RCA_MPIESM_EUR11_RCP45
MPICSC-REMO1_MPIESM_EUR11_RCP85	SMHI-RCA_MPIESM_EUR11_RCP85

Table 2 – List of CH2018 data files available for each station and therefore used in this work analysis

For the period with the observed data (1981 – 2020), the data from all ten models for the RCP8.5 scenario were used, as for this period the CO2 concentrations are based on measured CO2 concentrations. For the period from 2020 onwards, the results from all three scenarios were compared, always including the same ten model combinations. The data were assessed for the stations for which the observed data were available for the 1981-2020 time period.

3.2 Data analyses

As mentioned in the previous section (3.1) the dataset consists of daily precipitation. The goal, however, is to assess multi-day precipitation amounts that are important for extreme events, such as floods or droughts. The chosen indices are the 3, 7, 30 and 90-day total rainfall, as well as the minimum and maximum monthly rainfall. These are referred to as P_3, P_7, P_{30}, P_{90}, P_3 as P_{min} and P_{max} in the remainder of the thesis. The 3 day rainfall (P_3) was chosen because synoptic weather systems can last longer than a day but usually don't last longer than 3 days (Jones, 2021). The 7 days correspond to a week, twice the time of the 3 days but rounded up to a more common temporal interval, whereas 30 and 90 days correspond respectively to at a month and a season.

3.2.1 Comparison measurements and climate models

The multi-day rainfall amounts were calculated for every day between 1981 and 2020 for both the observed data from SMN network weather stations and the ten models outputs time series for each RPC 8.5 scenario in the CH2018 dataset. For these multi-day precipitation time series, the 50th, 95th, 99th percentile, maximum and minimum values were extracted. The 50^{th} percentile summarize a distribution without excessive deviations from central values but concerning extreme events does not provide useful information. For this matter also the 95^{th} and 99^{th} percentile was calculated in the attempt to catch also the extreme event and include their contribution on the analysis. Finally, the maximum and minimum were useful to estimate how much they were different from the other statistical value calculated.

For the CH2018 dataset, the mean and standard deviation for these percentiles for the ten models were calculated. For each percentile and precipitation duration, the mean value for the models was then compared to that of the observed data. More specifically, I used the ratio between the mean value of the percentile for the models and the percentile for the observations, so that 1 indicates that the model represents the observations perfectly, a value less than 1 indicates that the models on average underestimate the real data and a result greater than 1 indicates that the models on average overestimates the real data. This analysis was done separately for all stations.

To analyze the data for all stations, a set of scatterplots with the value for the observations on the x-axis and the mean value for the ten models and an error bars corresponding to the standard deviation on the y-axis was used for each percentile and rainfall duration. In addition, I created a set of boxplots of the ratios to more easily compare the results for the different rainfall durations and the percentiles. Boxplots provide an overview of the variability of the values showing the median, upper and lower quartile, maxima and minima and eventual outliers in the dataset. The outliers can be indicative of errors or in the case of this work for unusual occurrences in the data.

Ultimately, I chose two stations for which I also did a frequency distribution plot in order to also have an example of what happen in a single station.

All analyses were done in the free software environment for statistical computing R (RStudio Team, 2021). More specifically, I used the packages: plyr, dplyr, naniar, lubridate, and ggplot2. In addition, I used the free and open-source cross-platform desktop geographic information system application QGIS (QGIS.org, 2021) to analyze the geospatial data and create maps of Switzerland with the location of the station and the value of the ratio between the mean model value for the percentile and that of the observed data.

3.2.2 Comparison current climate and future

For the future, i.e. the period between 2021 and 2099, the analyses were the same as for the past period except that the data that was compared are the outputs of the three RCPs scenarios. The analyses were repeated for the period from 2021 to 2060 and the period from 2061 to 2099. Since we no longer had the observations, the comparison term were the scenarios outputs from 1981 to 2020 as control period. For both future periods, the values of the statistical variables under consideration are compared for each RCP with the corresponding statistical variable during the control period. To give a practical example, the average 95th percentile of the period 2021 - 2060 for the RCP85 scenario is divided by the average 95th percentile of the period 1981 – 2020 of the RCP85. With R boxplots and scatterplots were made, to check the correlation of the datasets, completed by the frequency distribution of the two chosen station, for more insight into specific locations and with QGIS, maps were made with the relationship between each scenario outputs with the same scenario output in the past, to ultimately understand their spatial distribution.

4 Results

This chapter presents the results of the study. First, the results of the analysis of the comparison with the measured data (i.e., historic period) is presented and the second part includes the results of the analysis of the projected future climate for the three RCPs scenarios.

4.1 Historic data

4.1.1 Multi-day rainfall across Switzerland

Before diving into future simulations outputs, a quick look at the precipitation situation in Switzerland for the period from 1981 to 2020. Extreme rainfalls are registered in Ticino. Precipitation in Ticino is higher on annual time scales due to extreme rainfall however, precipitation occur only a few days per year. For shorter time window (daily to weekly) the Swiss plateau is likely to have more millimeters of rainfall as it undergoes low rains throughout the year (Bader et al., 2004).

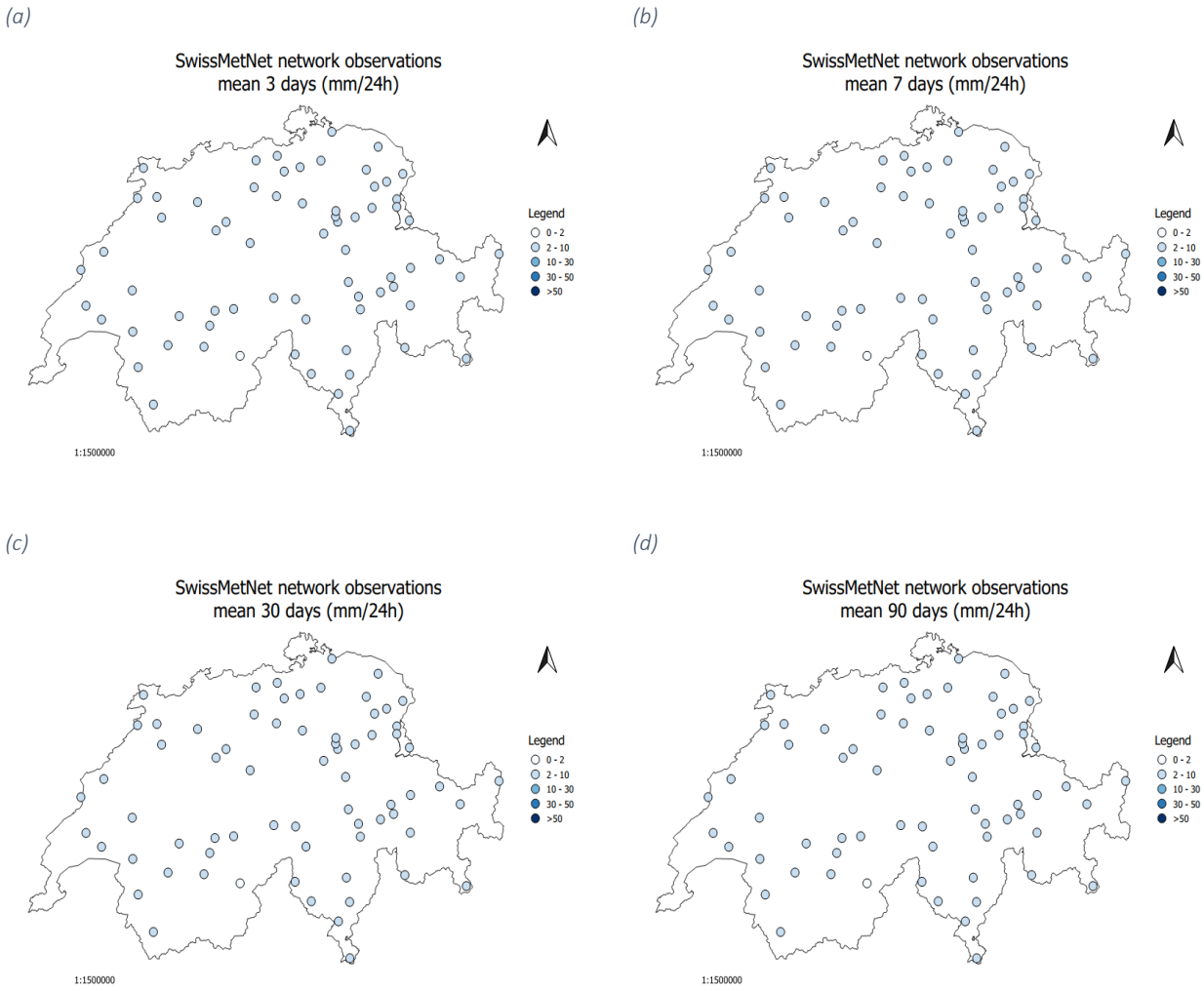

Figure 3 – Maps showing the mean of the SMN network for 3 (a), 7 (b), 30 (c) and 90 day precipitation (d) in the period between 1981 and 2020. Precipitation intensity in mm/24h is according to MeteoSwiss terms which owns the SMN network and its data.

In Figure 3 is presented the average rainfall recorded by SMN network for the period between 1981 and 2020. On average, no spatial differences are observed because the amount of perceived precipitation depends on the extremes and on how many rainy days each part of Switzerland perceives, therefore it is not surprising that when analyzing the average precipitation, no spatial differences are seen for all the time windows analyzed.

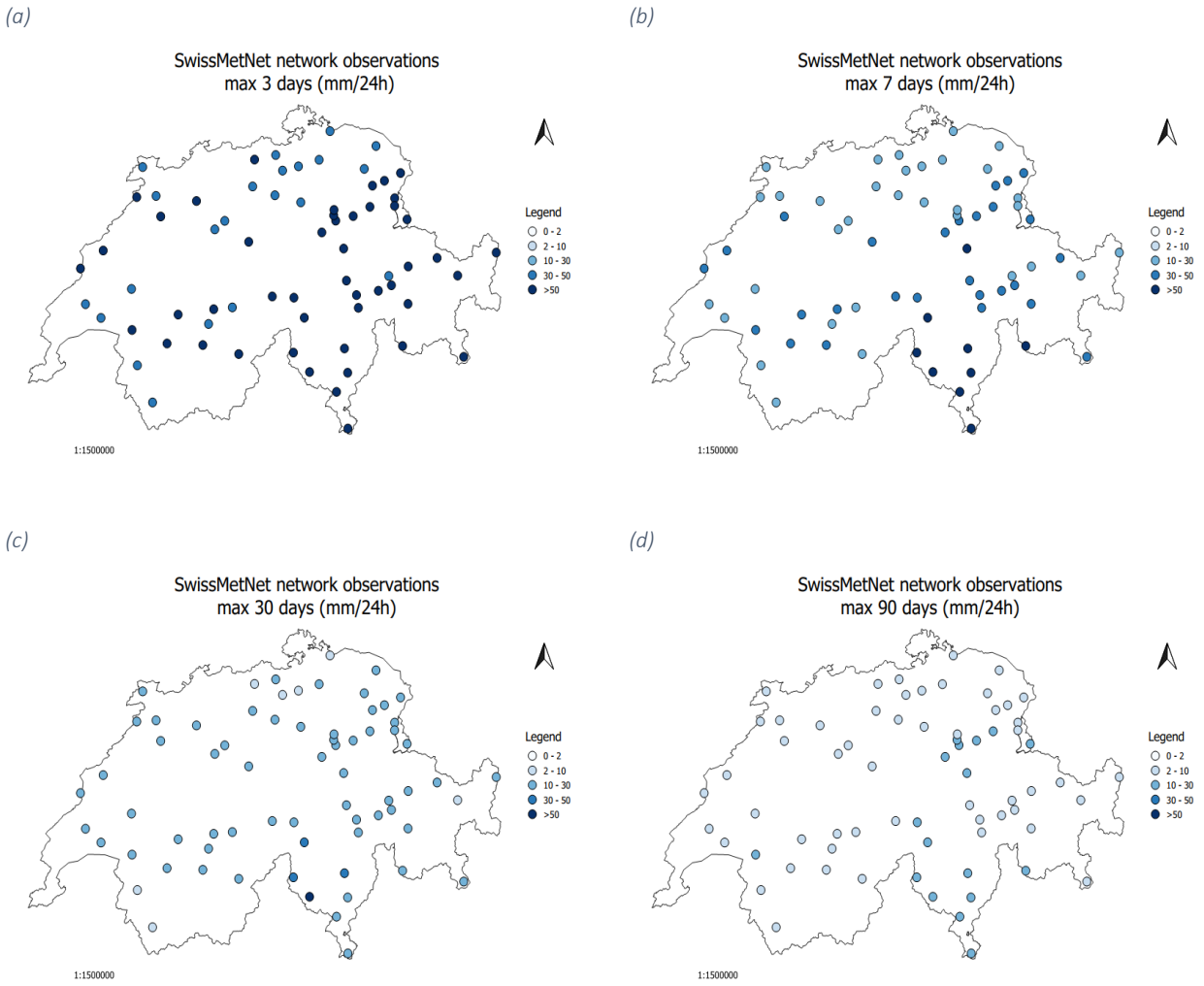

Figure 4 - Maps showing the maximum of the SMN network for 3 (a), 7 (b), 30 (c) and 90 day precipitation (d) in the period between 1981 and 2020. Precipitation intensity in mm/24h is according to MeteoSwiss terms which owns the SMN network and its data.

Figure 4 shows the recorded maxima rainfall recorded by SMN network for the period between 1981 and 2020. Maximum's precipitation as it could be expected are more evident in small time windows, maximum are events that occur occasionally (for now, although simulations predict an increase in their frequency) so it is more likely that they are more evident in the shorter time windows than in the long ones. Independentely of the time window analyzed a predisposition to the south of the Alps and in the area of Walensee going towards Lichtenstein can be seen. The singular analysis of the two stations below (Figure 5) support these entries and the total rainfall values are higher for the station of Coldrerio than for the station of Opfikon for all time windows. Based on the knowledge of Ticino climate, it is possible that having fewer days of rain but large quantities made the cumulative value of the frequency distribution for Coldrerio higher, although the number of rainy days is lower than that recorded for Opfikon. Opfikon, in fact, have on average less extreme rainfall but distributed in a more homogeneous way.

4.1.2 Comparison of the frequency distributions for two selected stations

To gain a more detailed overview at the distribution of the observed and simulated rainfall for the 3, 7, 30 and 90 day total precipitation, the distributions for two selected sites Coldrerio (COL) in Ticino and Opfikon (OPF) in canton Zürich are shown in Figure 5 and 6, respectively. The Coldrerio station in Ticino was chosen because in the last years, Ticino had big flood problems following torrential rains, These frequency distributions show that the model simulations result in a lower frequency of low total precipitation and a higher frequency of very high total precipitation, and that the differences increase somewhat as the period over which the total precipitation is calculated increases. In other words, the distribution of the modeled multi-day precipitation is "broader" than the observed distribution. It can be seen that as the number of observations increases all three scenarios overestimate the observations with an average value that increases as the time intervals increase. The values are presented in Table 3.

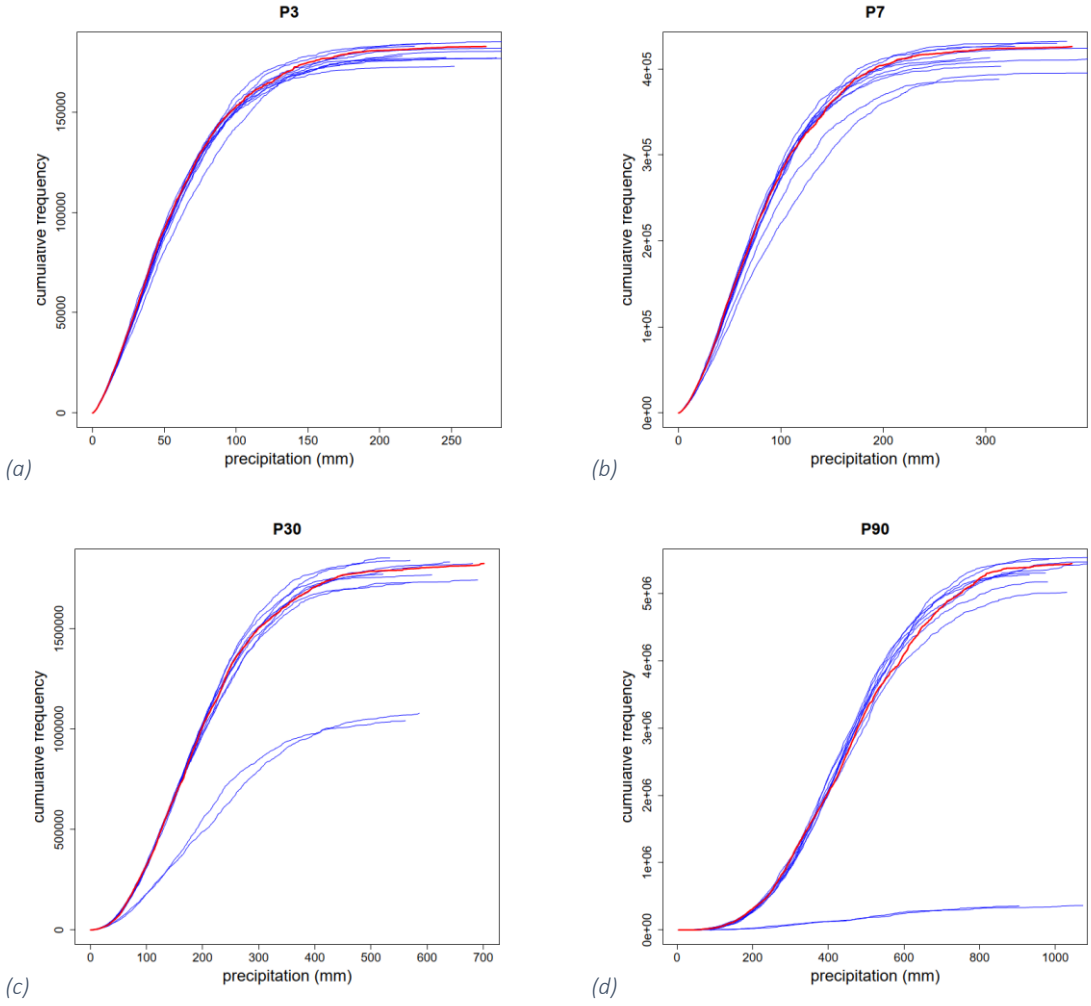

Figure 5 – Cumulative frequency of the 3 (a), 7 (b), 30 (c) and 90 days total precipitation (d) in millimeter for the Coldrerio (COL) station during the period between 1981 and 2020. The red line indicates the observations obtained from SMN, while the blue ones represent the result of the ten chain model simulations for the RCP8.5 scenario.

The station of Opfikon in canton Zürich was chosen because it was interesting to see how the model predict a station close to the university (Opfikon is the closest that was available from the stations selection). Similar to the Coldrerio station the distribution of the modeled multiday precipitation is broader than the observed precipitation. These differences in the frequency distributions are also reflected in the differences between CH2018 simulations for all ten chain model with RCP8.5 and SMN observed rainfall. For a clearer idea of the difference value see Table 3.

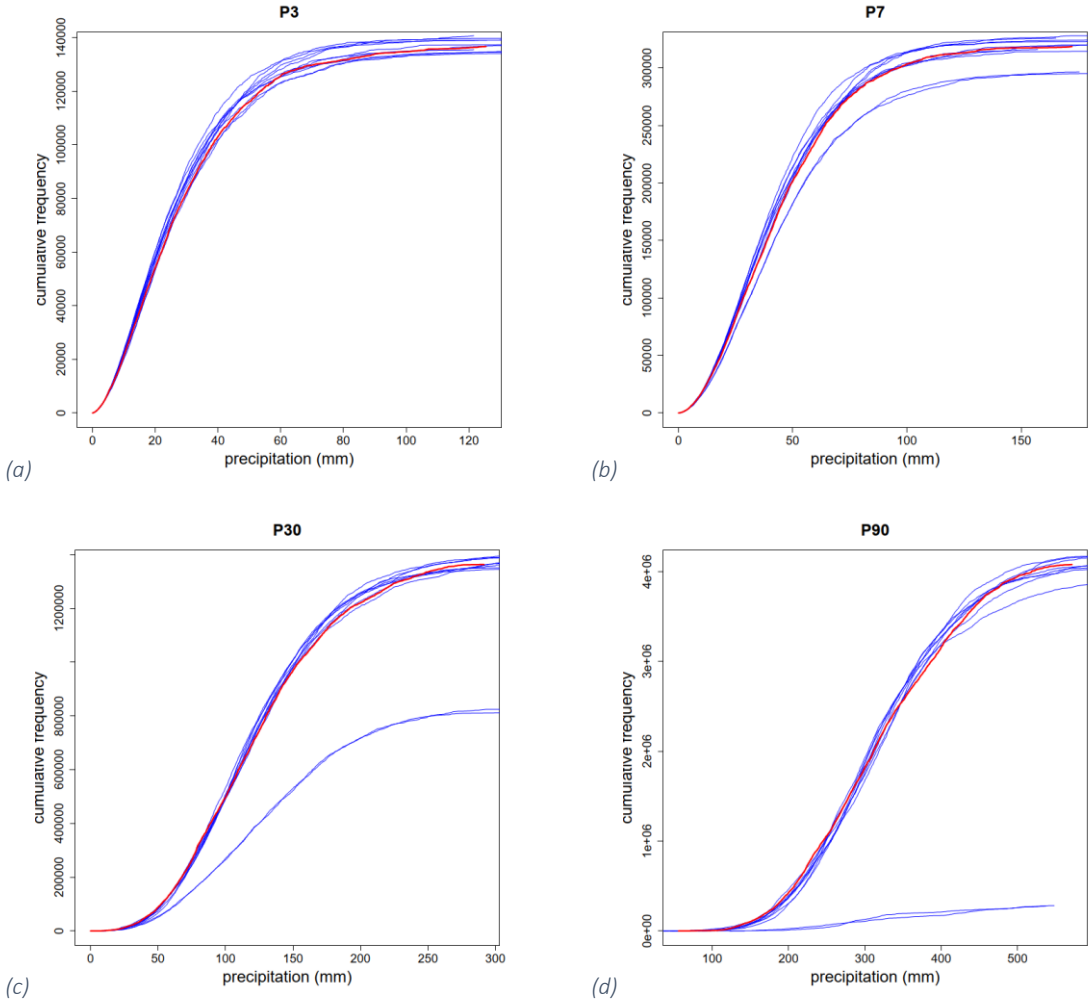

Figure 6 - Cumulative frequency of the 3 (a), 7 (b), 30 (c) and 90 days total precipitation (d) in millimeter for the Opfikon (OPF) station during the period between 1981 and 2020. The red line indicates the observations obtained from SMN, while the blue ones represent the result of the ten chain model simulations for the RCP8.5 scenario.

Difference (mm)	P3	P7	P30	P90
COL	99.96	151.77	290.95	467.76
OPF	50.35	75.01	153.06	252.54

Table 3: Average difference between the ten CH2018 simulations for RCP8.5 and SMN observations during the period 1981-2020 in millimeters of the multi-day precipitation for Coldrerio (COL) and Opfikon (OPF) stations.

4.1.3 Comparison of the percentiles for all stations

The four statistics analyzed (median, 95th percentile, 99th percentile, and maximum) were compared for the model results and observations for all stations. The correlation results are show in Figures 7 and 8 for the 95th and 99th percentiles and in Appendix Figure 50 and 51 for the median and maximum values.

The statistic for the observed precipitation in millimeter is plotted on the x-axis, while the chain model outputs are shown on the y-axis. The error bar length is equal to the standard deviation of the ten different chain model outputs.

The median for the two datasets for short durations, such as 3 and 7 days do not agree but for the results for the 30 and 90 day precipitation are closer to the 1:1 line and there are fewer stations for which the model results and observations differ considerably.

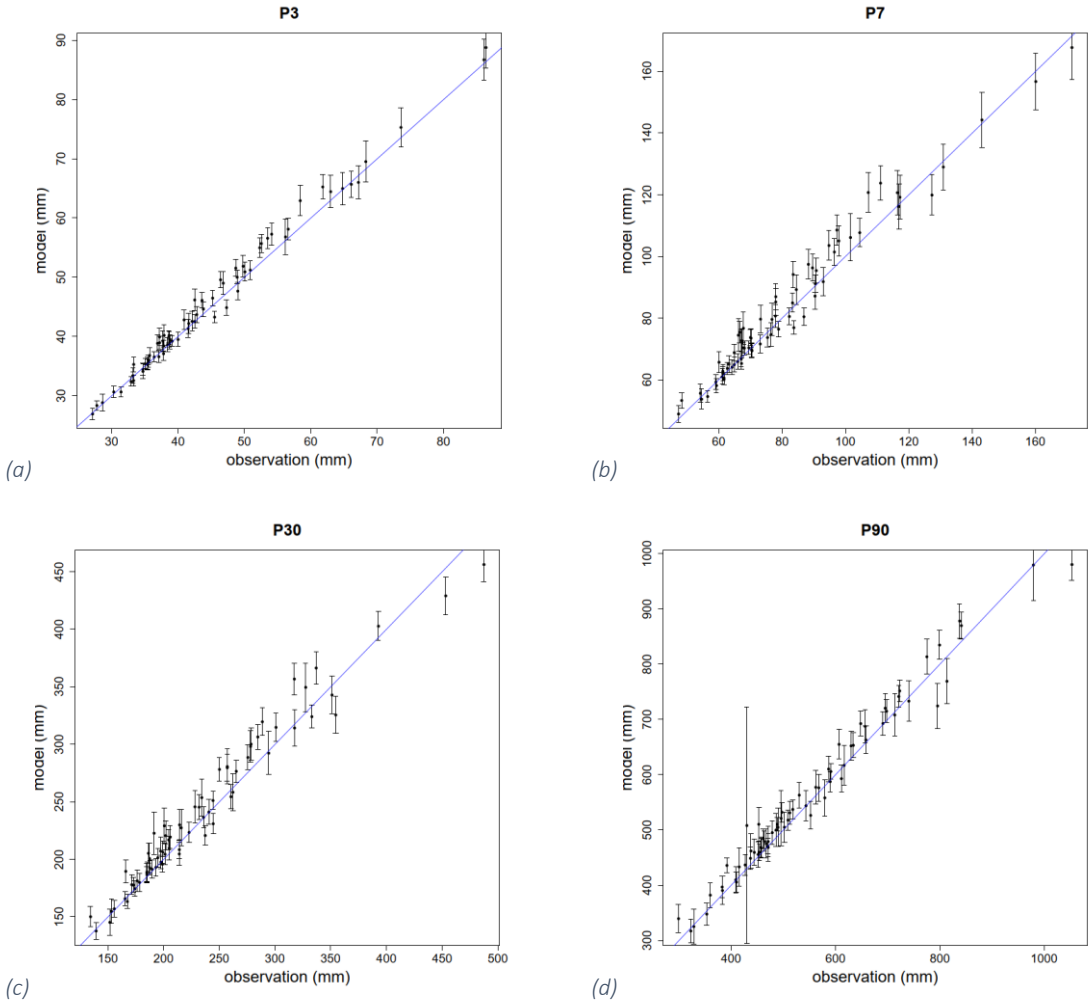

Figure 7 – Correlation between the 95th percentile of the observed and simulated 3 (a), 7 (b), 30 (c) and 90 day precipitation (d) in millimeters for the 69 SMN for the period between 1981 and 2020. The blue line displays the 1:1 line while the error bars indicate the standard deviation of CH2018 model results.

The 95th percentile values (Figure 7) however are closer to a 1-to-1 correlation. Note that for one station (Amriswil), the model results for the 90 day time precipitation differ significantly for this statistic (Figure 7.d). The results for the 99th percentile of the precipitation are similar but the differences between the model results are larger, as indicated by the much larger error bars in Figure 8. This effect is even clearer for the maximum values (see Figure 51 in the Appendix).

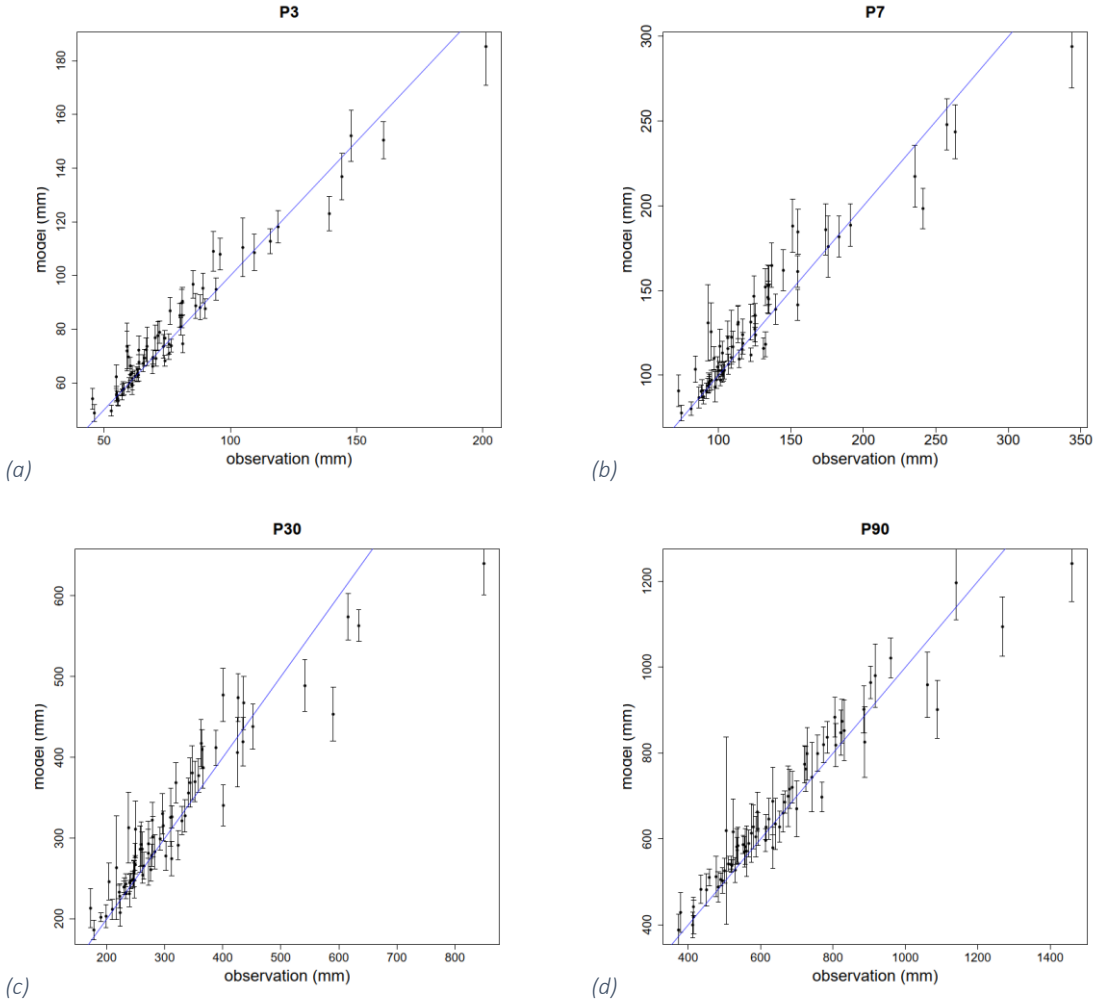

Figure 8: Correlation between the 99th percentile of the observed and simulated 3 (a), 7 (b), 30 (c) and 90 day precipitation (d) in millimeters for the 69 stations for the period between 1981 and 2020. The blue line displays the 1:1 line while the error bars indicate the standard deviation of the ten CH2018 model results.

The boxplots of the ratio between the chain model mean value of the statistic and the statistic for the observed value (Figure 9) and maps (Figures 10 and Figures 11) show a similar result, moreover the maps show the spatial distribution on the territory of the results.

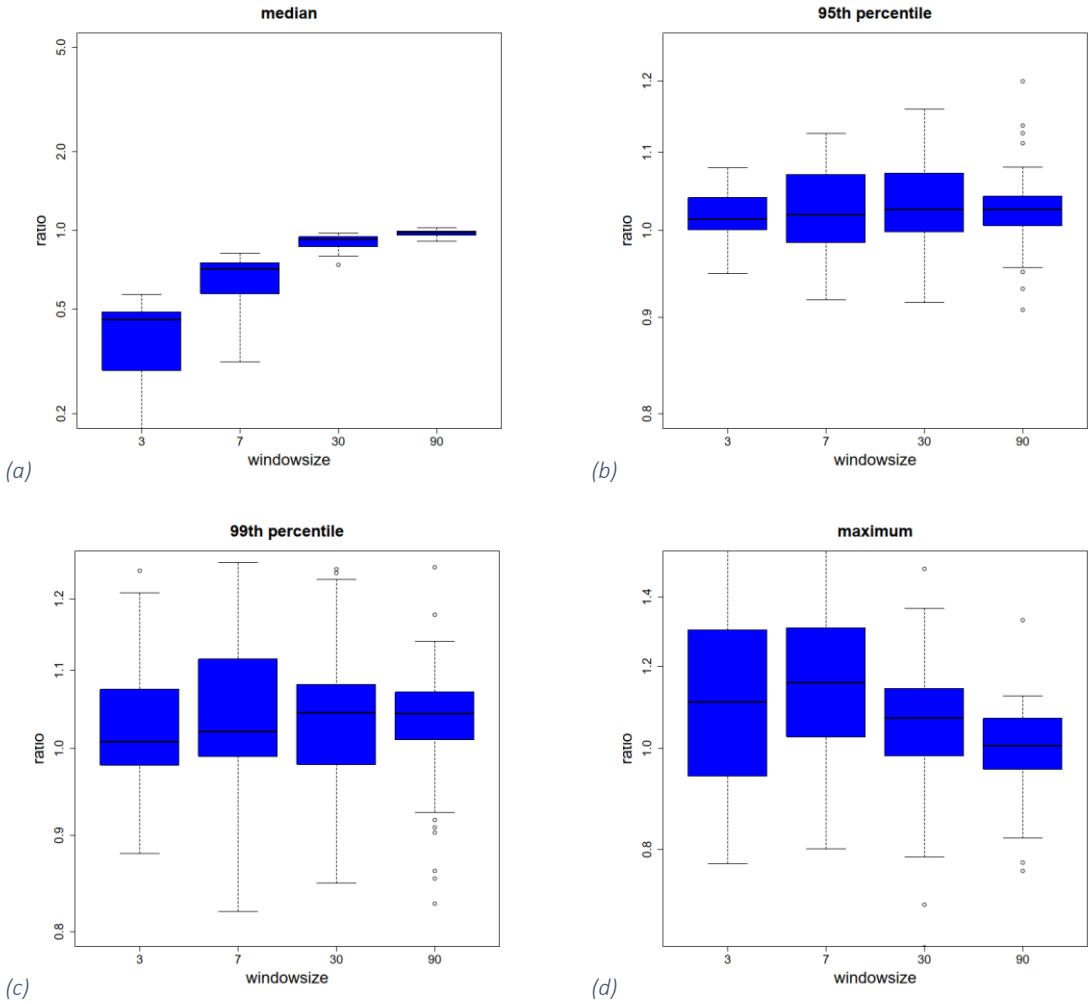

Figure 9 - Boxplots of the ratio of the median (a), 95th percentile (b), 99th percentile (c) and maximum (d) every box represents each one of the time period analyzed for the observation and the mean of the ten chain models outputs for the period between 1981 and 2020. A value of 1 indicates that the statistic is the same for the observed and model data, values below 1 indicate that the CH2018 simulations underestimate the data, while the values above 1 indicate an overestimation.

The median (or 50th percentile) differs significantly for the SMN data and CH2018 simulations. However, this ratio improves as the time interval increases: for the 90-day time window, of the ratio is closer to 1 for most station (average value of 1.01). The correspondence between the model and observations is much better for the 95th and 99th percentiles, although most of the values are above 1, i.e., the CH2018 simulations overestimate the extreme rainfall compared to the SMN data.

The median 3 and 7 day precipitation are underestimated for all Swiss stations analyzed but the median 30 and 90 day precipitation are less underestimation in the north, northwest of Switzerland and the median 90 day precipitation is almost close to that observed for these regions (see Figure 50.d in the Appendix).

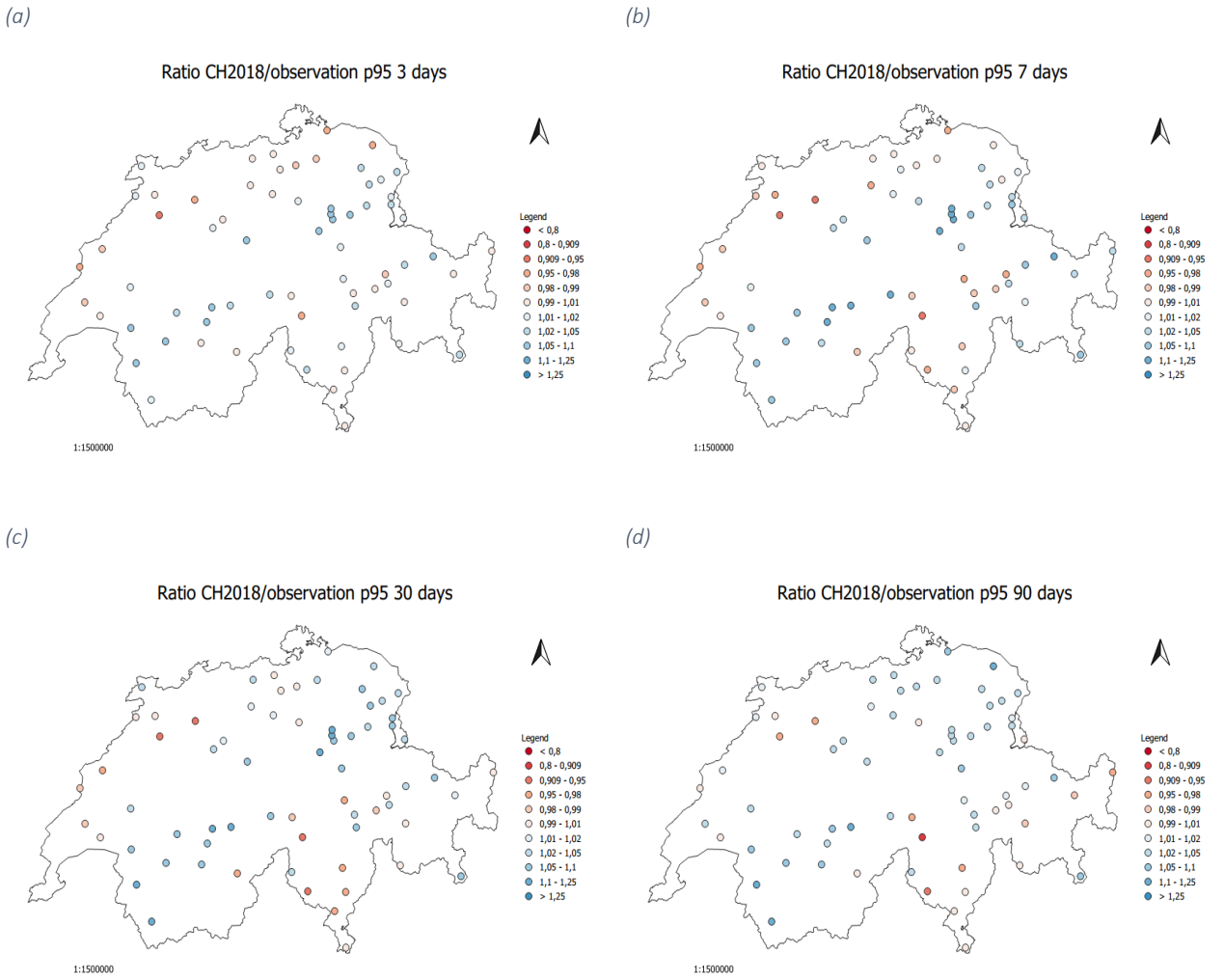

Figure 10 – Maps showing the ratio of the 95th percentile of the 3 (a), 7 (b), 30 (c) and 90 day precipitation (d) for the CH2018 simulations (mean of all ten chain models) and the observations for the period between 1981 and 2020. Values larger than 1 indicate an overestimation (blue) and values less than 1 an underestimation (red).

The 95th percentile of the 3 day precipitation is slightly overestimated across the Alps line but slightly underestimated across the southwest-northeast line near Neuchâtel and the Nüfenen pass. The results for the 7 day precipitation similar but there are more stations for which the model results are overestimated. This trend is attenuated even more looking at the 90 precipitation. In general, the areas most affected by an overestimation are located in the Alps and north of the Alps, while for Ticino and in the northeastern part of Switzerland the 95th percentile of the precipitation is underestimated (Figure 10).

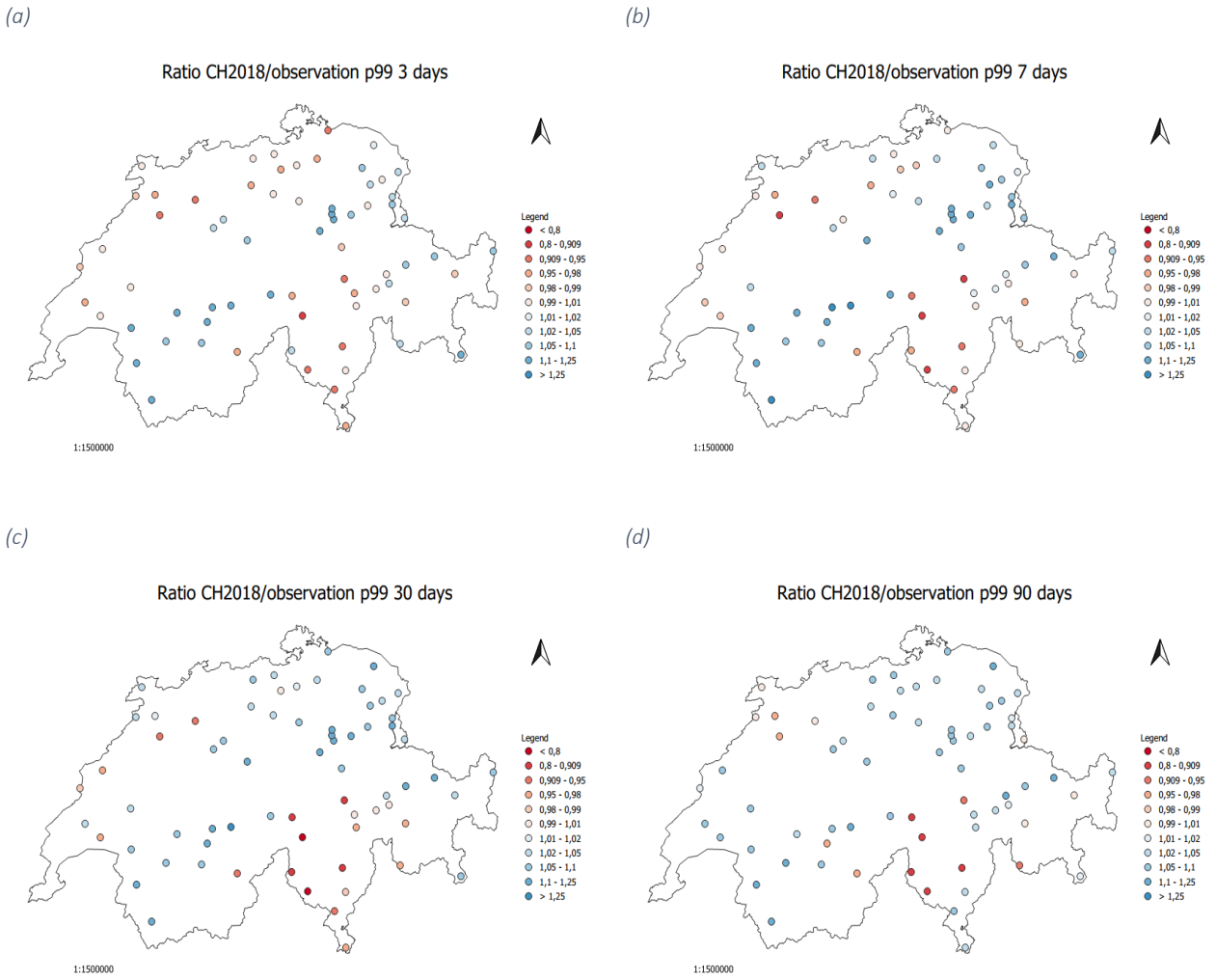

Figure 11 – Maps showing the ratio of the 99th percentile of the 3 (a), 7 (b), 30 (c) and 90 day precipitation (d) for the CH2018 simulations (mean of all ten chain models) and the observations for the period between 1981 and 2020. Values larger than 1 indicate an overestimation (blue) and values less than 1 an underestimation (red).

The results for the 99th percentile show a similar pattern of underestimation and overestimation: an overestimation in the mountains that changes to an underestimation as one moves away from them. The most stations for which this statistic are underestimated are even more evident and are mainly located in Ticino and on the southwest-northeast line starting from Neuchâtel (Figure 11).

The spatial pattern for the maximum 3 and 7-day precipitation is not very strong with stations for which the models over- and underestimate the precipitation, except for a slight tendency for overestimation for northeastern Switzerland. The 30 day maxima are mainly overestimated in the north of the Alps and underestimated in the south, while for the 90 day window the results are more mixed. The stations with the greatest underestimation are located in Ticino, as well as in the Valais on the Alps line (see Figure 51 in the Appendix).

4.2 Future

For the future analysis the dataset has been divided into two parts: the first one goes from 2021 to 2060 and the second one from 2061 until 2099. In this way the number of years is kept as close as possible to that of the historical data, with an average of 40 years.

To make the reading more agile from this point on, the period where SMN precipitation historic record are available (1981-2020) will be indicated with PC: control period. Moreover, the first future period (2021-2061) will be referred to as F1, and the second future period (2061-2099) as F2.

4.3 First future period (2021 – 2060)

The analysis for the simulations of F1 have been carried out with the same method of the past with the difference that every output has been put to comparison with the correspondent scenario in PC. Moreover, all scenarios were analyzed.

4.3.1 Comparison of the frequency distributions for two selected stations

Below is the cumulative frequency per Coldrerio for the RCP2.6 scenario (Figure 12), for the 3 and 7 day time windows the simulation for the past period simulate more rainy days with little precipitation and with the increasing of daily precipitation reverse the situation and future simulations predict more days with high rate of precipitation. However, for a range of average precipitation the simulated in the control period exceeds the prediction of the simulation

These data are consistent with the prediction that in the future the trend of extreme precipitation will increase and even if the scenario predicts a decrease in emissions following a contained global temperature rise and so neither precipitation should rise much. Nevertheless, for these changes to be noticeable probably more time is needed. Regarding the time windows of 30 and 90 days we can see a range of days with little precipitation where the model predicts more rainy days than the control period ones, but for the days with important precipitation also here the forecast is higher than the simulated in the PC.

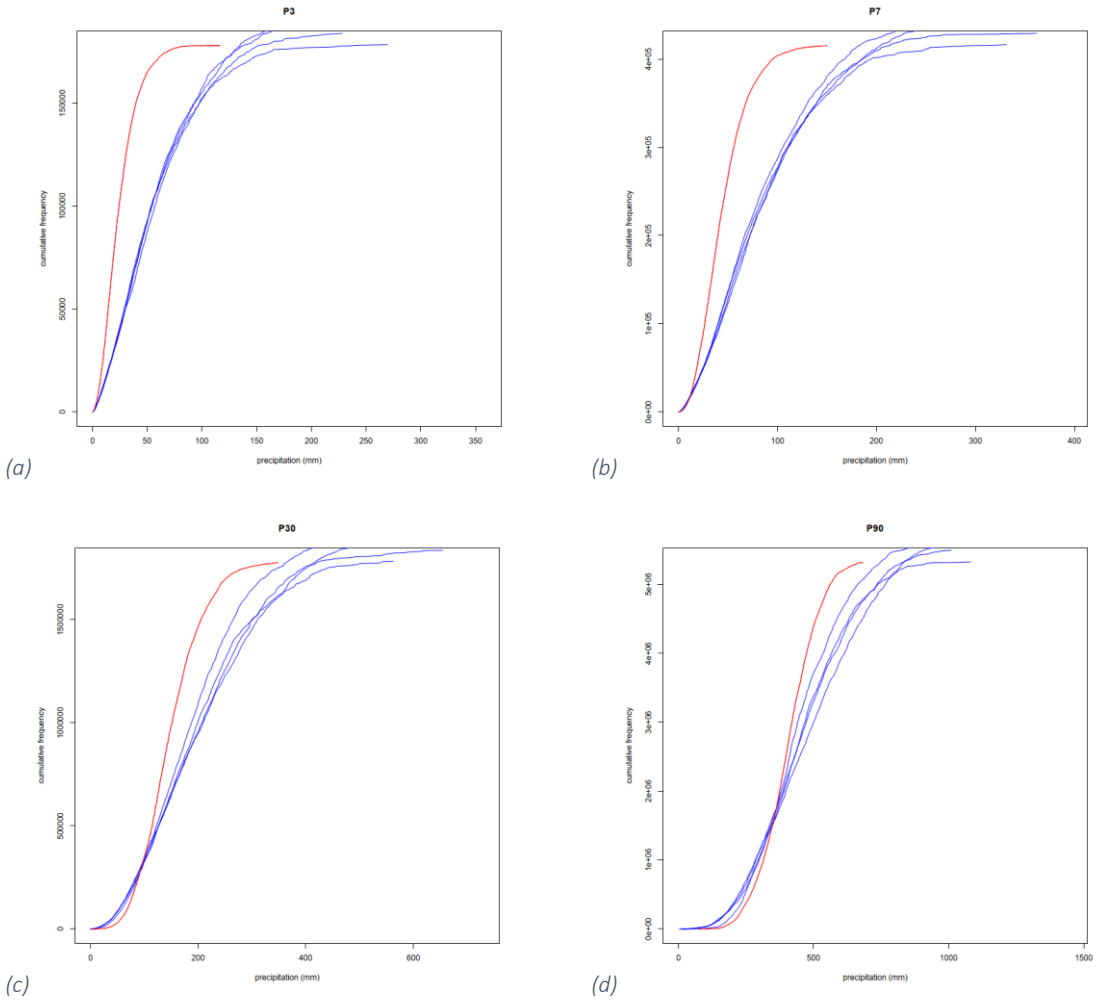

Figure 12 - Cumulative frequency of the 3 (a), 7 (b), 30 (c) and 90 days total precipitation (d) in millimeter for the Coldrerio (COL) station during the period between 2021 and 2060. The red line indicates mean of the RCP2.6 for 1981 – 2020, while the blue ones represent the result of the ten chain model simulations for the RCP2.6 scenario for 2021-2060.

Analyzing the results of the simulations for the RCP4.5 scenario (Figure 13) we see the same trend as for the RCP2.6 scenario: the more consistent the rainfall, the more days with high precipitation are simulated relative to the simulated for the PC, plus a middle range of precipitation the simulated in the PC exceeds the prediction of the simulation. For the 30- and 90-day time windows the days with little rainfall are overestimated relative to the simulated for PC.

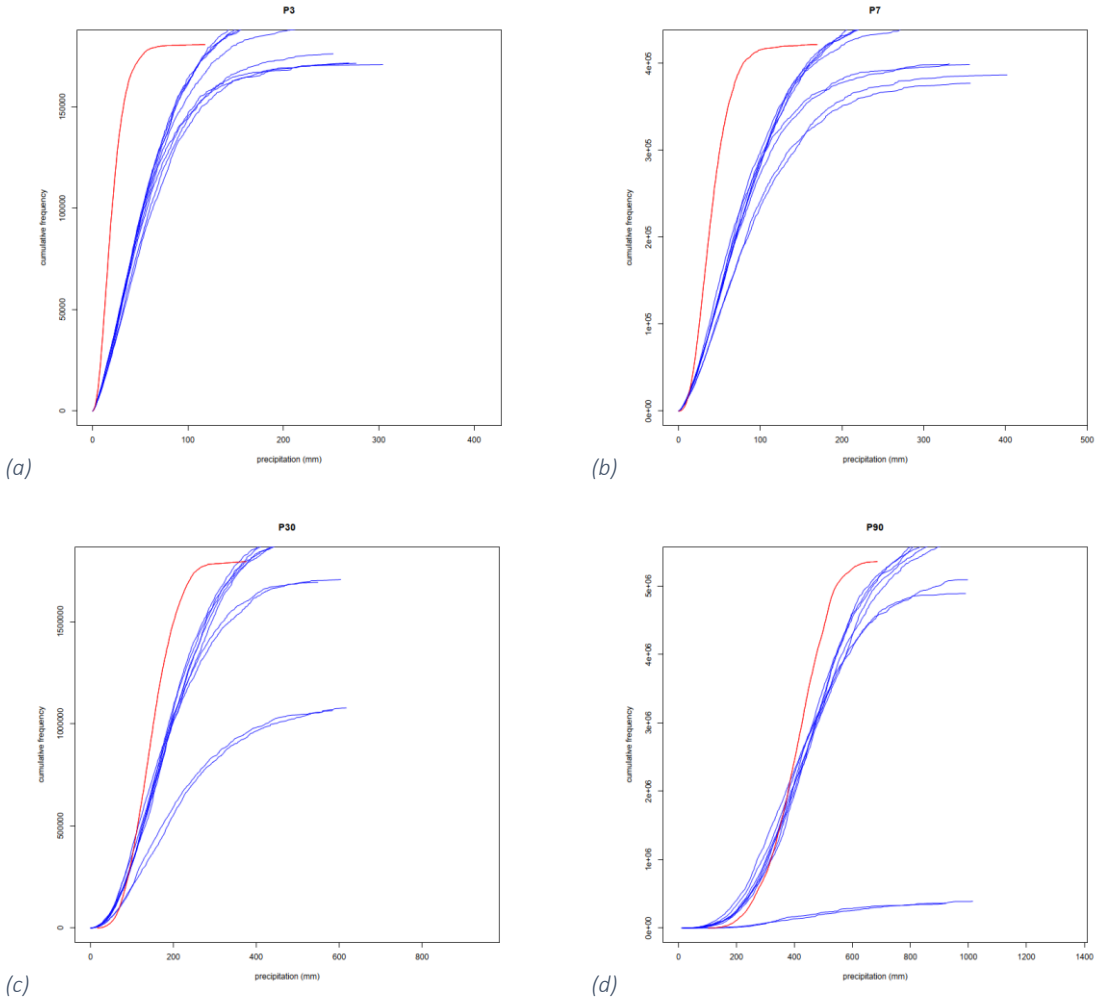

Figure 13 - Cumulative frequency of the 3 (a), 7 (b), 30 (c) and 90 days total precipitation (d) in millimeter for the Coldrerio (COL) station during the period between 2021 and 2060. The red line indicates mean of the RCP4.5 for 1981 – 2020, while the blue ones represent the result of the ten chain model simulations for the RCP4.5 scenario for 2021-2060.

The trend noted for the two previous scenarios is repeated for scenario RCP8.5 (Figure 14), the more intense the rainfall the more the model simulates its frequency compared to the simulated PC. Nevertheless, for a range of average precipitation the PC exceeds the prediction of the simulation. Moreover, time windows of 30 and 90 days there is a portion of days with little precipitation that exceeds the simulated PC one.

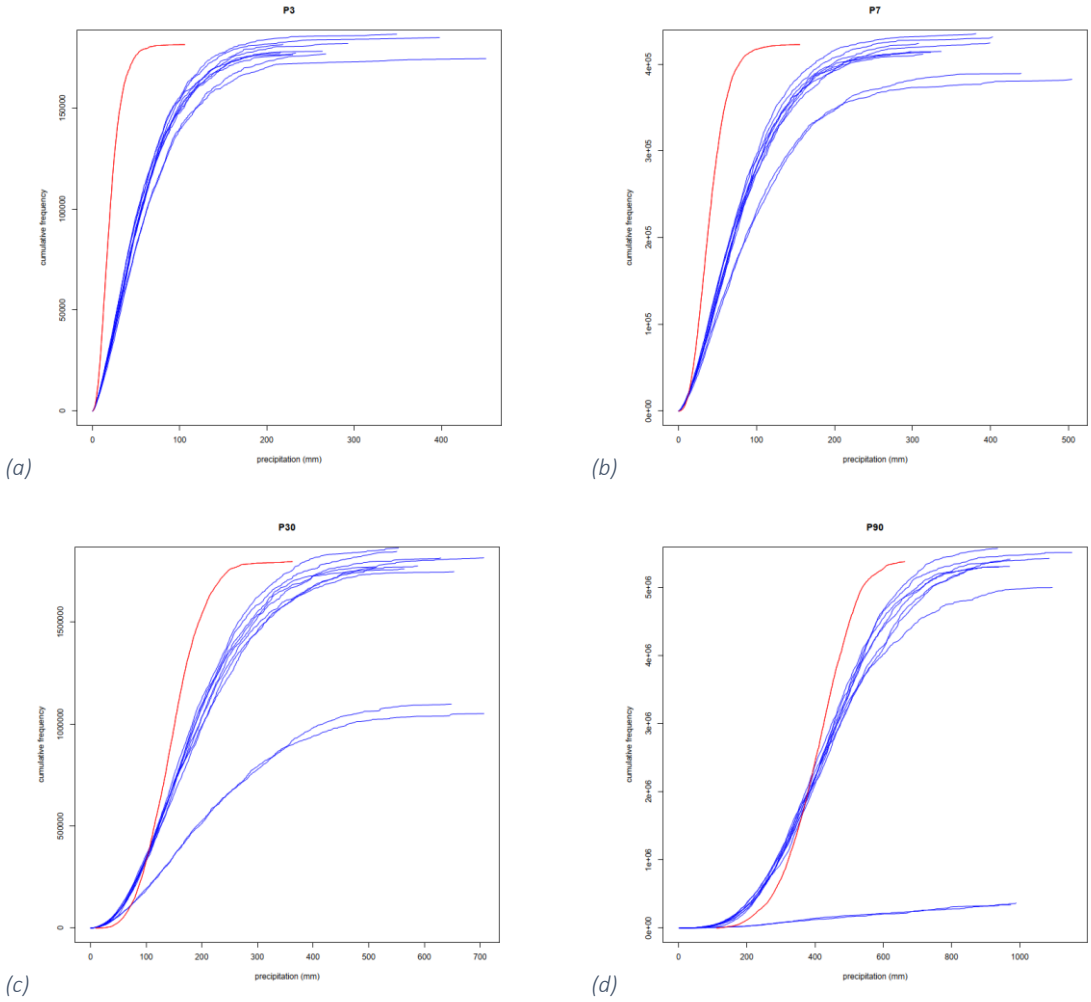

Figure 14 - Cumulative frequency of the 3 (a), 7 (b), 30 (c) and 90 days total precipitation (d) in millimeter for the Coldrerio (COL) station during the period between 2021 and 2060. The red line indicates mean of the RCP8.5 for 1981 – 2020, while the blue ones represent the result of the ten chain model simulations for the RCP8.5 scenario for 2021-2060.

Since it is not easy to see the extent of the difference between future simulation of the three scenarios data between 2021 and 2060 and the correspondent scenario in the PC, below is a table with the exact numbers of the average difference between the model and the PC data for Coldrerio over the three different scenarios (Table 4).

Difference COL (mm)	P3	P7	P30	P90
RCP2.6	6.75	11.25	33.03	89.51
RCP4.5	4.79	8.77	19.38	36.56
RCP8.5	2.62	2.27	2.48	-8.28

Table 4 - Average difference between the ten CH2018 simulations for the three scenarios during the period 2021-2060 and the ten CH2018 simulations for the correspondent scenarios during the period 1981-2020 in millimeters of the multi-day precipitation for Coldrerio (COL).

Overall the fact that future simulations are higher than those during the control period show that a general increase for extreme precipitation is expected over the next 40 years despite the precautions that can be taken, this may also mean that 40 years is too few years to see effects that would bring precipitation back to more consistent and predictable levels. In spite of the general tendency of the future forecasts the differences between the PC and F1 agrees with the constraints of the scenarios, the highest differences are noticed in the scenario 2.6, the medium ones for RCP4.5 while the minor ones for RCP8.5

As for Coldrerio station the trend where the more the rainfall is consistent and the more the rainy days are simulated compared to the simulations in the PC is also repeated for Opfikon station for all 3 scenarios (RCP2.6 Figure 15, RCP4.5 Figure 16, and RCP8.5 Figure 17). Moreover, in Table 5 the results of the average difference between the simulation of each scenario during the period between 2021 and 2060 and the simulation of the corresponding scenario for the PC.

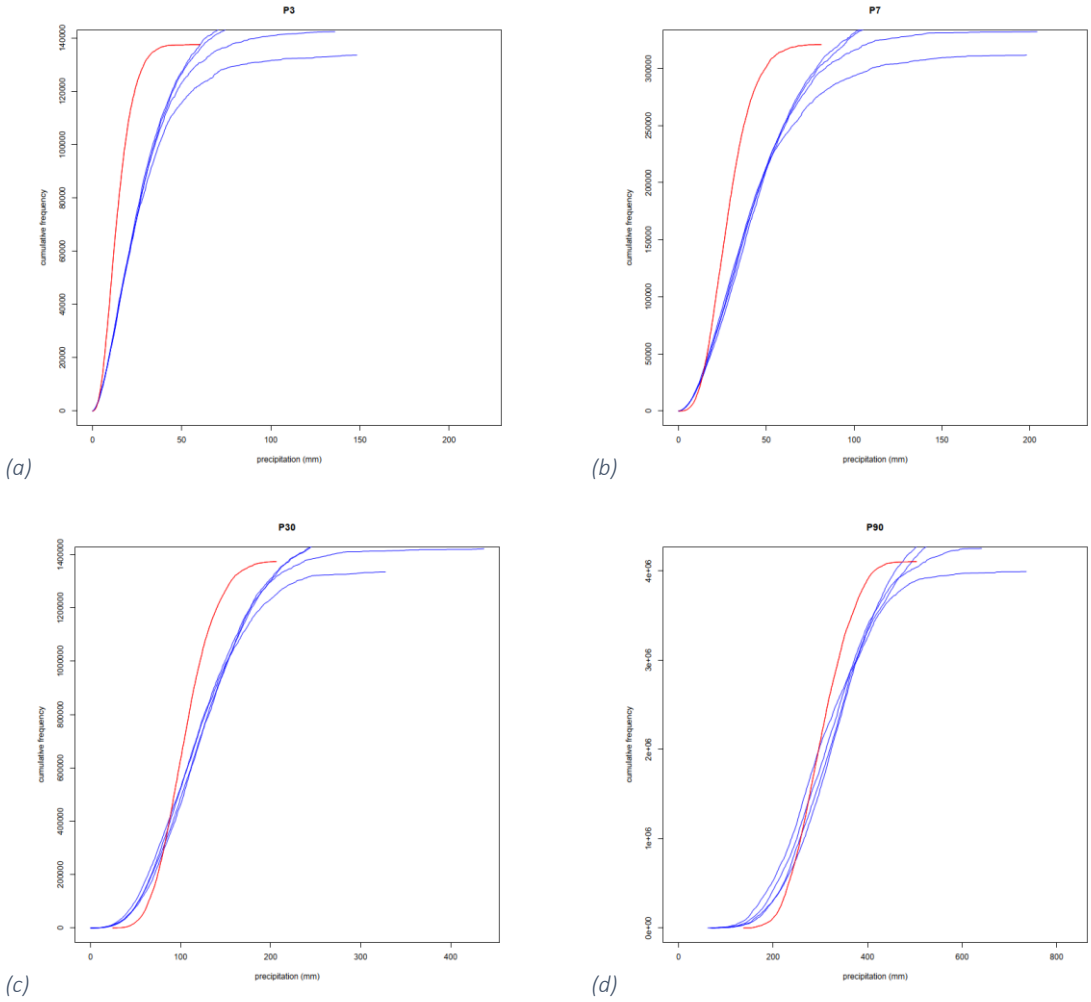

Figure 15 - Cumulative frequency of the 3 (a), 7 (b), 30 (c) and 90 days total precipitation (d) in millimeter for the Opfikon (OPF) station during the period between 2021 and 2060. The red line indicates mean of the RCP2.6 for 1981 – 2020, while the blue ones represent the result of the ten chain model simulations for the RCP2.6 scenario for 2021-2060.

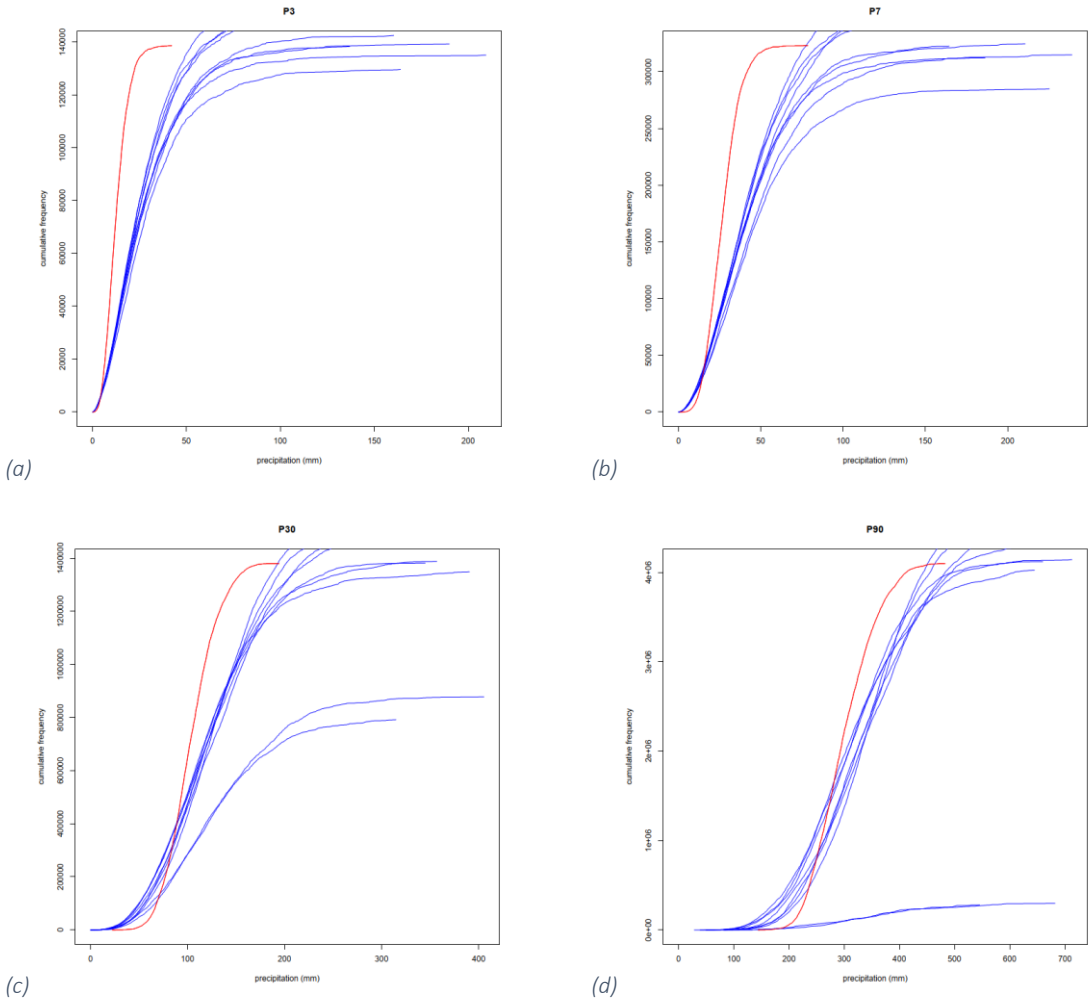

Figure 16 - Cumulative frequency of the 3 (a), 7 (b), 30 (c) and 90 days total precipitation (d) in millimeter for the Opfikon (OPF) station during the period between 2021 and 2060. The red line indicates mean of the RCP4.5 for 1981 – 2020, while the blue ones represent the result of the ten chain model simulations for the RCP4.5 scenario for 2021-2060.

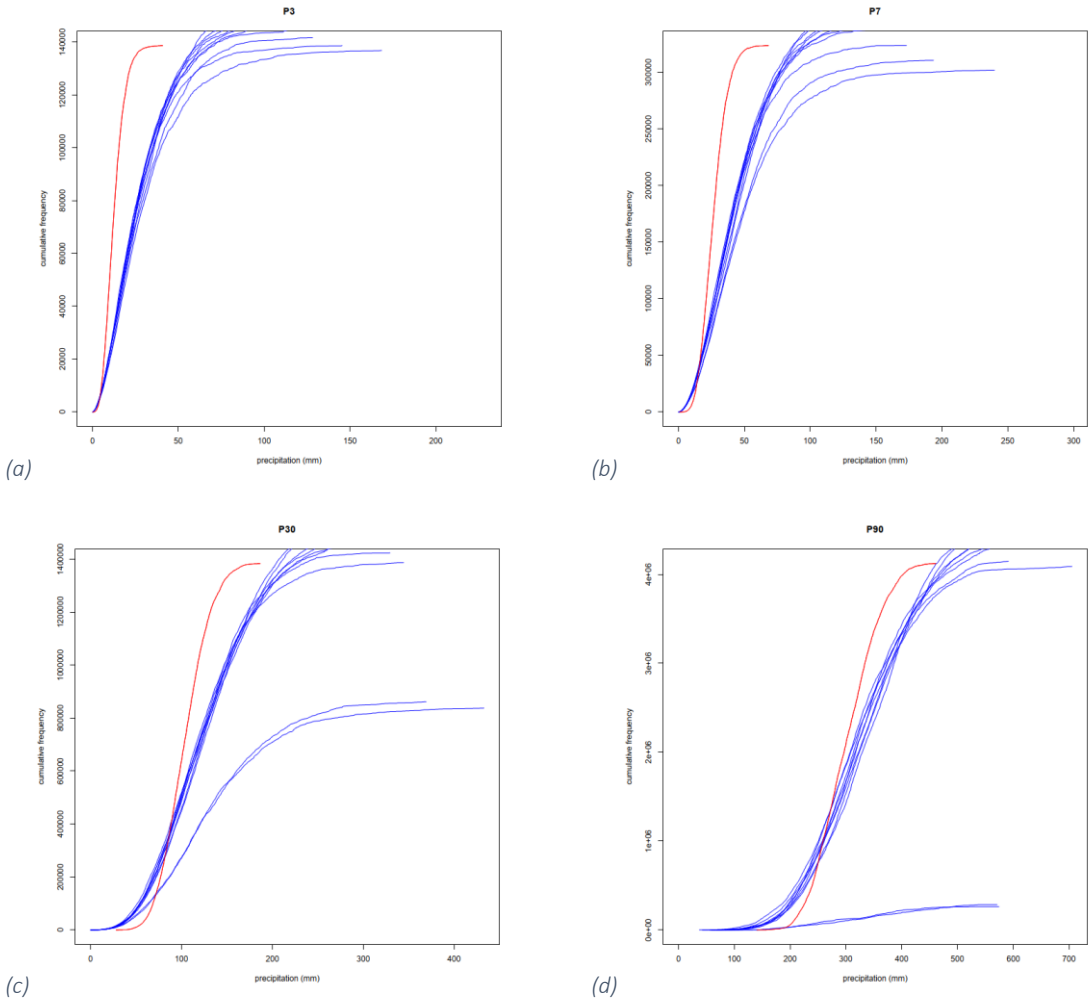

Figure 17 - Cumulative frequency of the 3 (a), 7 (b), 30 (c) and 90 days total precipitation (d) in millimeter for the Opfikon (OPF) station during the period between 2021 and 2060. The red line indicates mean of the RCP8.5 for 1981 – 2020, while the blue ones represent the result of the ten chain model simulations for the RCP8.5 scenario for 2021-2060.

To make clearer the extent of the difference between the simulated scenario in F1 and the correspondent scenario in the PC below is a table with the exact numbers of the average difference between the two datasets for Opfikon (Table 5).

Difference OPF (mm)	P3	P7	P30	P90
RCP2.6	1.92	3.36	-7.78	-0.83
RCP4.5	2.83	3.16	3.32	3.64
RCP8.5	3.02	4.6	4.67	-0.96

Table 5 - Average difference between the ten CH2018 simulations for the three scenarios during the period 2021-2060 and the ten CH2018 simulations for the correspondent scenarios during the period 1981-2020 in millimeters of the multi-day precipitation for Opfikon (OPF).

Even if both stations present the same trend, it can be seen from the analysis of the differences presented in Table 4 and 5 that the simulations are less accurate for the station of Coldrerio. With comparison to the Coldrerio station, the differences between the PC and F1 simulations do not agree with the scenario constraints. In the 3 days time window, the largest differences are found in the future simulations for the 8.5 scenario, as well as in the 7 days although the difference for RCP2.6 is slightly higher than for RCP4.5. Analyzing the 30 days it can be seen that the RCP2.6 simulations are lower than the control period, consistent with the constraints, but RCP4.5 has a lower difference than RCP8.5 when for how the scenarios are thought should be the opposite situation, namely the difference of RCP8.5 should be the least, as it is the scenario that does have unabated conditions.

4.3.2 Comparison of the percentiles for all stations

Below are presented the correlation results for each scenario (RCP2.6 Figure 18, RCP4.5 Figure 19 and RCP8.5 Figure 20) between the statistic for the ten chain model outputs in millimeter per scenario simulated for the control period (1981 -2020), plotted on the x-axis, while the chain model outputs for the period in analysis (2021 – 2060) are shown on the y-axis. Each scenario is compared with its correspondent in the past. Moreover, the error bar length is equal to the standard deviation of the ten different chain model outputs.

The error bars correspond to the standard deviation while the blue line indicates the perfect 1 to 1 correlation between the simulation of each scenario during the analyzed period (2021-2060) and the simulation of its corresponding scenario during the control period. For the median and the maximum correlation results refer to the appendix Figure 54 for the median of RCP2.6, 55 for RCP4.5 and 56 for RCP8.5, whereas refer to Figure 57, 58, 59 for the maxima of RCP2.6, RCP4.5, RCP8.5 respectively.

Correlations for the median show very good correlations for all scenarios for all time windows with few significant differences.

When considering the 95th percentile all three scenarios show good correlation between the PC and F1 simulations. The subdivision of the stations with respect to precipitation in millimeters does not show particular trends but analyzing the error bars reveals how they vary by scenario and time window. The results for the analysis of the 95th percentile can be seen in Figure 18 for RCP2.6, Figure 19 for RCP4.5 and Figure 20 for RCP8.5.

Regarding the time window of 3 and 7 days, the tendency of the error bars is to be contained for RCP2.6 compared to the other two scenarios, the scenario RCP8.5 presents somewhat higher standard deviations while it is the scenario RCP4.5 that has the highest values for the standard deviation. Regarding the longer time windows (i.e., 30 and 90 days) it is RCP8.5 to present the highest standard deviations, RCP2.6 has values very close to those of the station (i.e., close to the simulations during the PC) while RCP4.5 presents intermediate values.

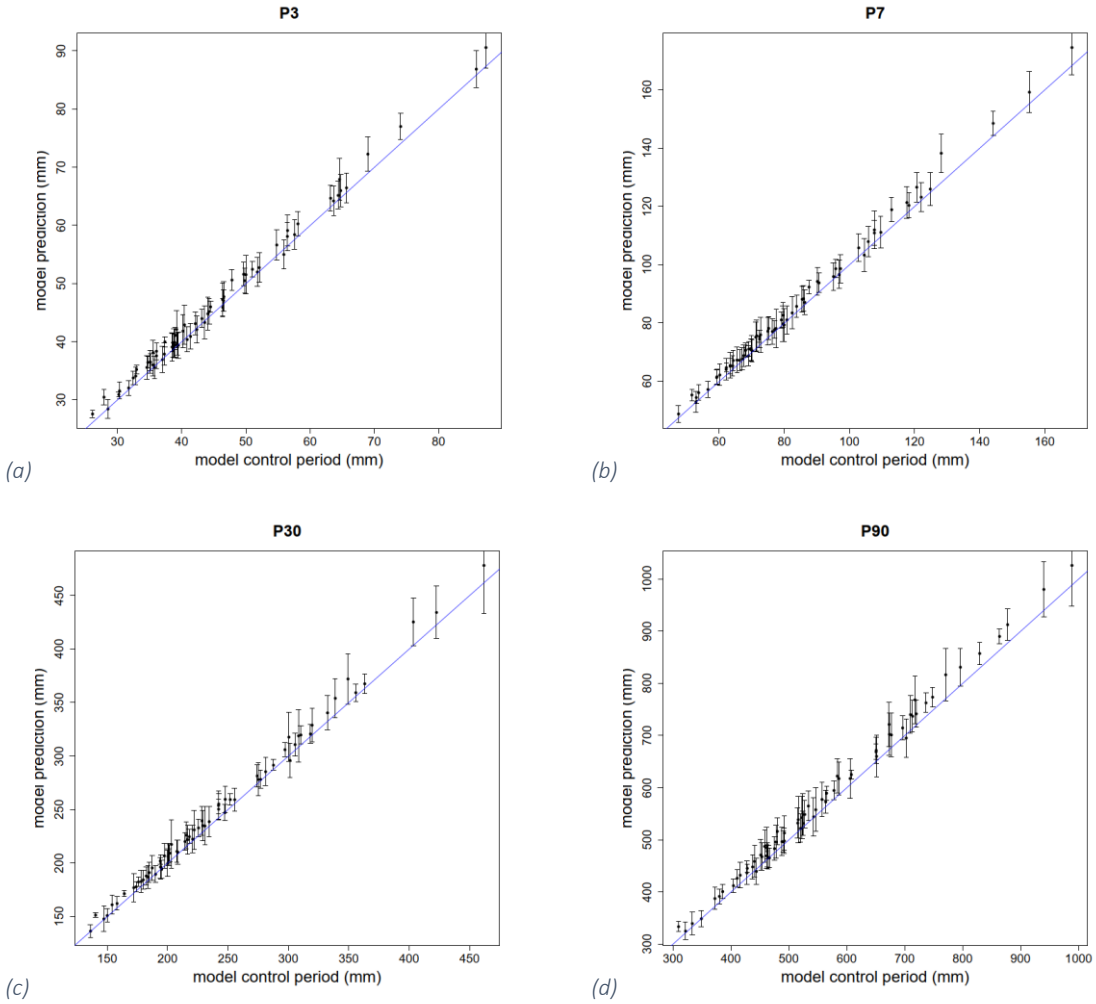

Figure 18 - Correlation between the 95th percentile of RCP2.6 (2021 – 2060) and RCP2.6 (1981 – 2020) of the 3 (a), 7 (b), 30 (c) and 90 day precipitation (d) in millimeters for the 69 stations analyzed. The blue line displays the 1:1 line while the error bars indicate the standard deviation of CH2018 model results

Scenario 2.6 (Figure 18) presents slightly overestimation of the PC data and a minimum standard deviation. Moreover the correlation for every station are fairly good, being close to the 1 to 1 correlation line.

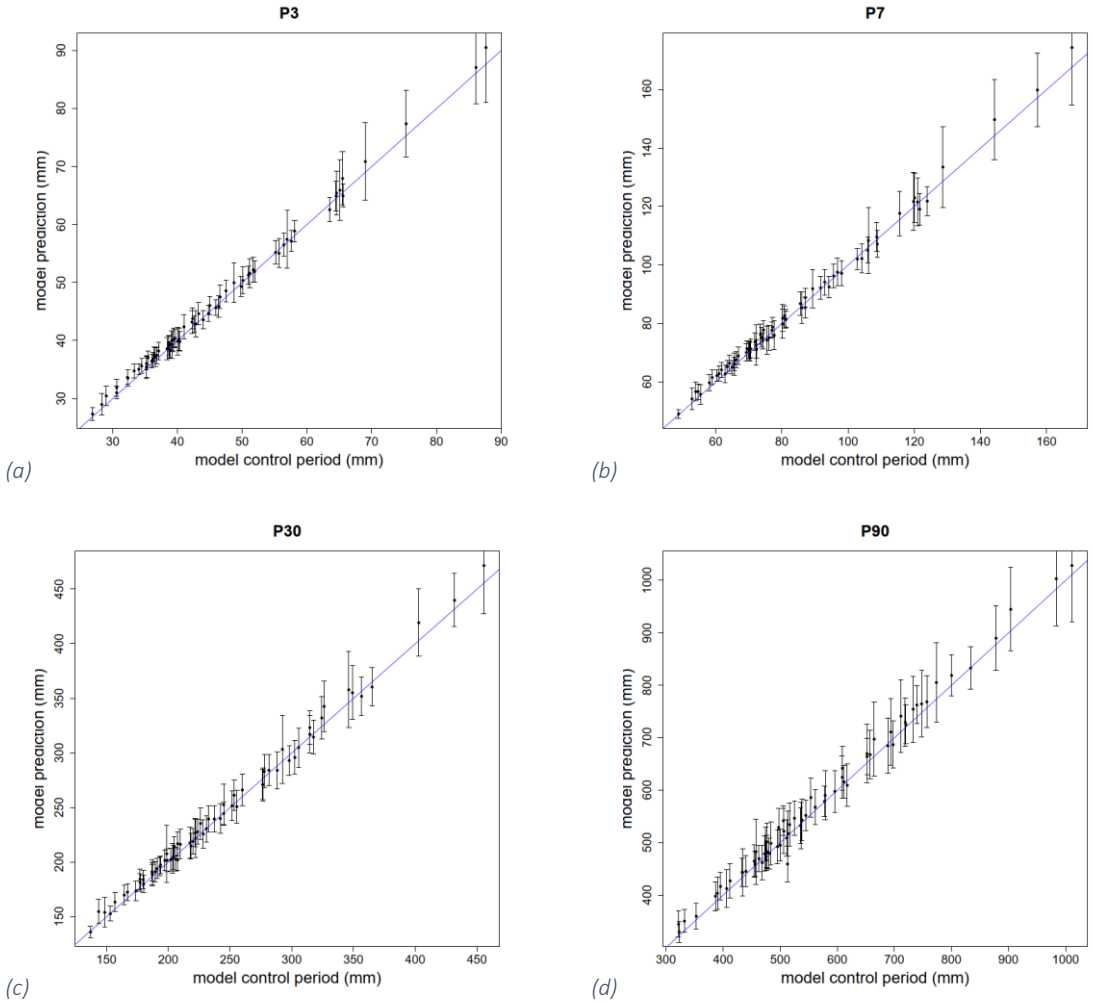

Figure 19 - Correlation between the 95th percentile of RCP4.5 (2021 – 2060) and RCP4.5 (1981 – 2020) of the 3 (a), 7 (b), 30 (c) and 90 day precipitation (d) in millimeters for the 69 stations analyzed. The blue line displays the 1:1 line while the error bars indicate the standard deviation of CH2018 model results

Scenario 4.5 (Figure 19) has unexpected values for the 3 and 7 day time windows, in fact it has the highest standard deviations compared to the other two scenarios, while it should have a middle course between scenario 2.6 and 8.5. Correlation for every station is close to the 1 to 1 correlation line as for scenario 2.6, with a slight tendency of overestimation for higher millimeter amount.

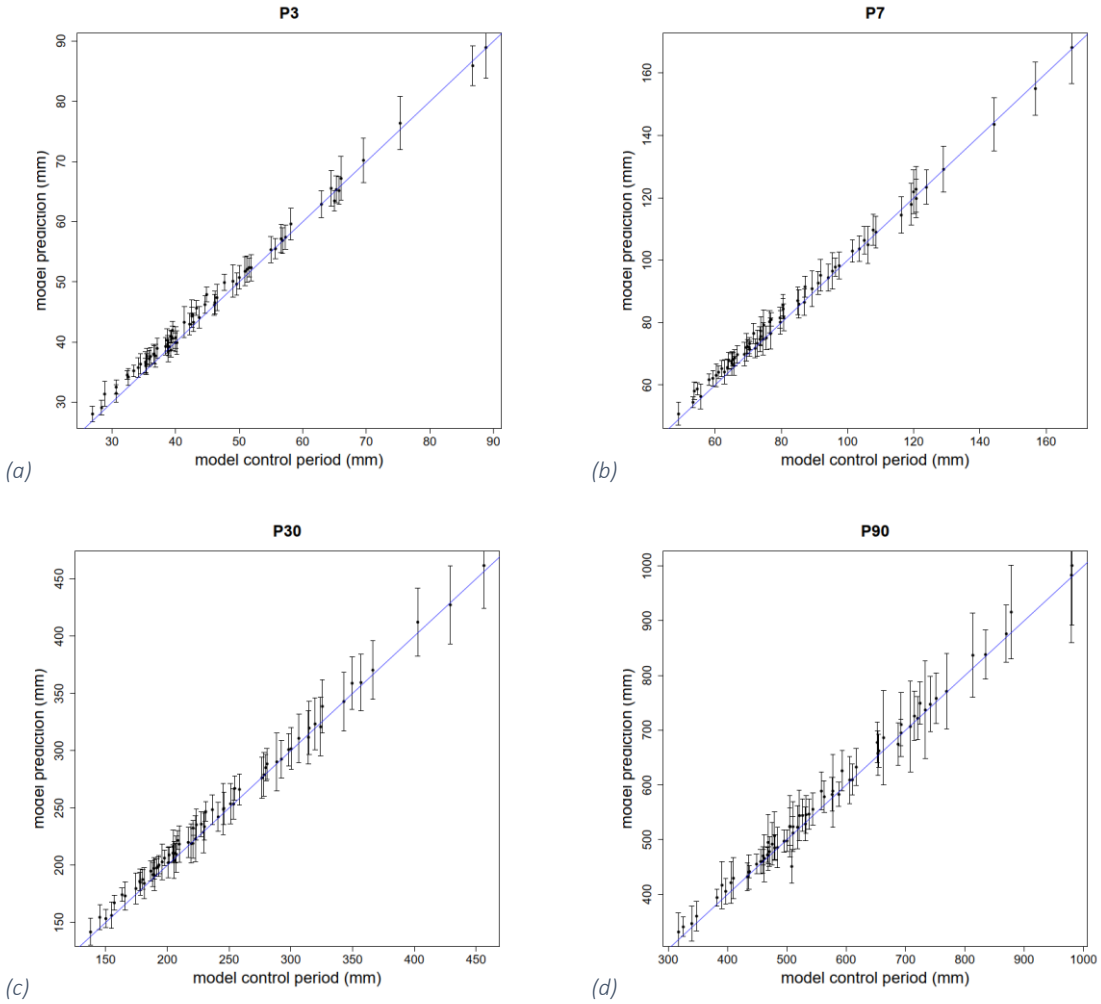

Figure 20 - Correlation between the 95th percentile of RCP8.5 (2021 – 2060) and RCP8.5 (1981 – 2020) of the 3 (a), 7 (b), 30 (c) and 90 day precipitation (d) in millimeters for the 69 stations analyzed. The blue line displays the 1:1 line while the error bars indicate the standard deviation of CH2018 model results

Finally scenario 8.5 (Figure 20), except for the short time windows just mentioned, follows expectations in that without intervention an increase over the control period is expected, i.e. F1 simulations overestimate those of the PC.

For the most part the results of the correlations follow the expectations, the correlation is mostly close to 1 to 1, in 40 years the effects are not strongly visible even with precautions and the standard deviation increase with increasing amount of precipitation in millimeters, which is not surprising because the extreme events are not fully expressed in the PC.

Below are the results of the 99th percentile correlations by station (Figure 21 for RCP2.6, 22 for RCP4.5 and RCP8.5 in Figure 23), it can be seen that the 3-day time windows have good correlations with small standard deviations for all three scenarios, followed by the 7-day time window with a similar trend even if the standard deviations are slightly larger. The 30-day time window has good correlations on the three scenarios. Moreover, the standard deviations are small for RCP2.6 and are slightly higher for RCP4.5 and even higher for RCP8.5. Finally, the 90-day time window has a good correlation with small standard deviations while RCP4.5 and RCP8.5 have good correlations but slightly higher standard deviations.

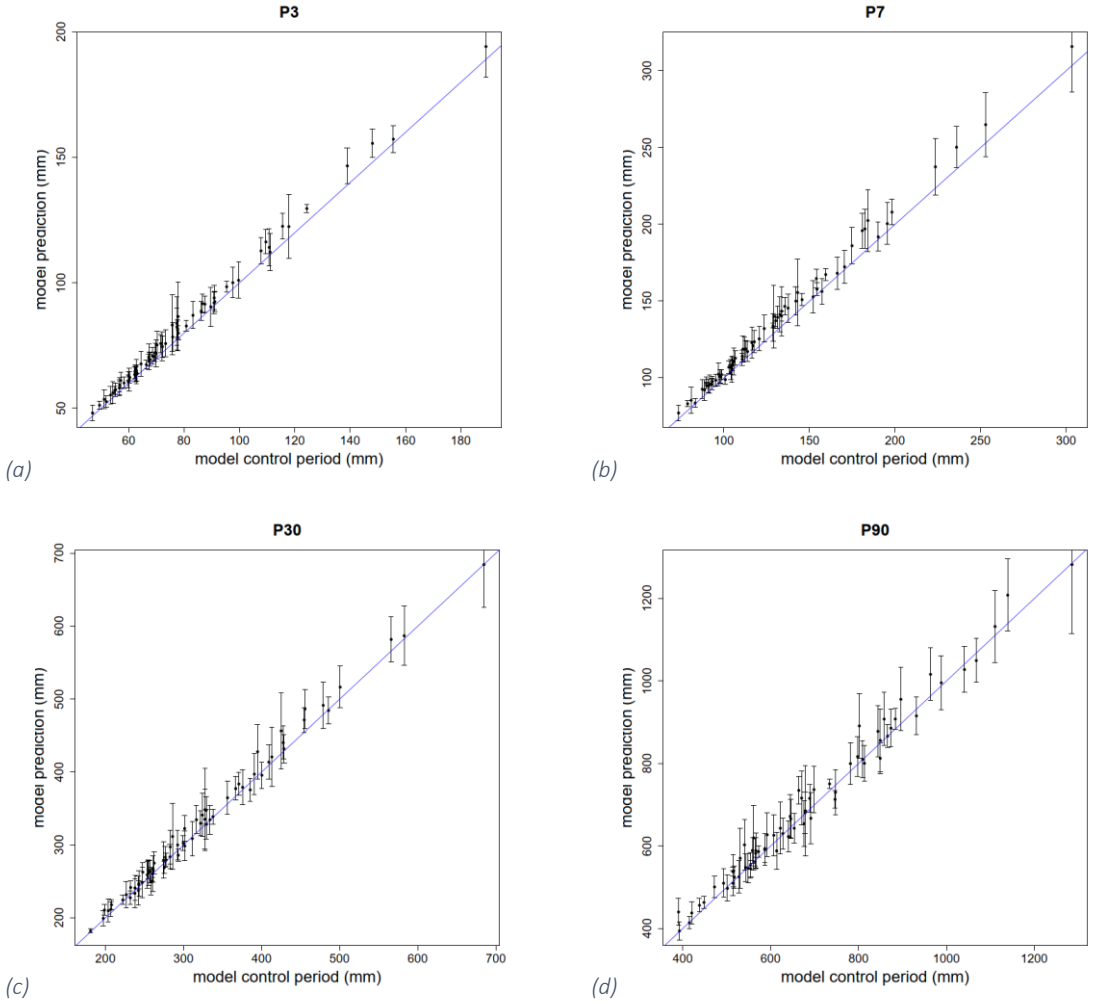

Figure 21 - Correlation between the 99th percentile of RCP2.6 (2021 – 2060) and RCP2.6 (1981 – 2020) of the 3 (a), 7 (b), 30 (c) and 90 day precipitation (d) in millimeters for the 69 stations analyzed. The blue line displays the 1:1 line while the error bars indicate the standard deviation of CH2018 model results

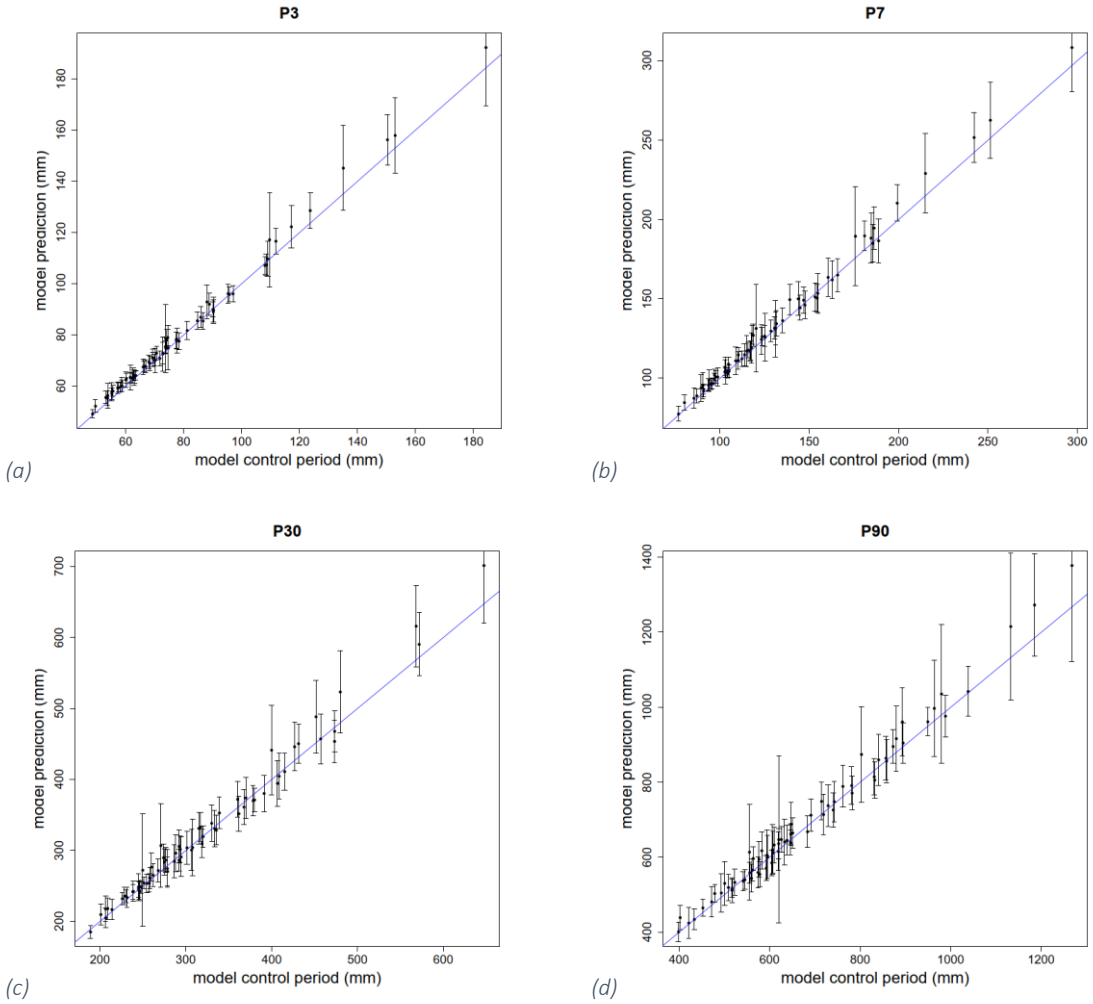

Figure 22 - Correlation between the 99th percentile of RCP4.5 (2021 – 2060) and RCP4.5 (1981 – 2020) of the 3 (a), 7 (b), 30 (c) and 90 day precipitation (d) in millimeters for the 69 stations analyzed. The blue line displays the 1:1 line while the error bars indicate the standard deviation of CH2018 model results

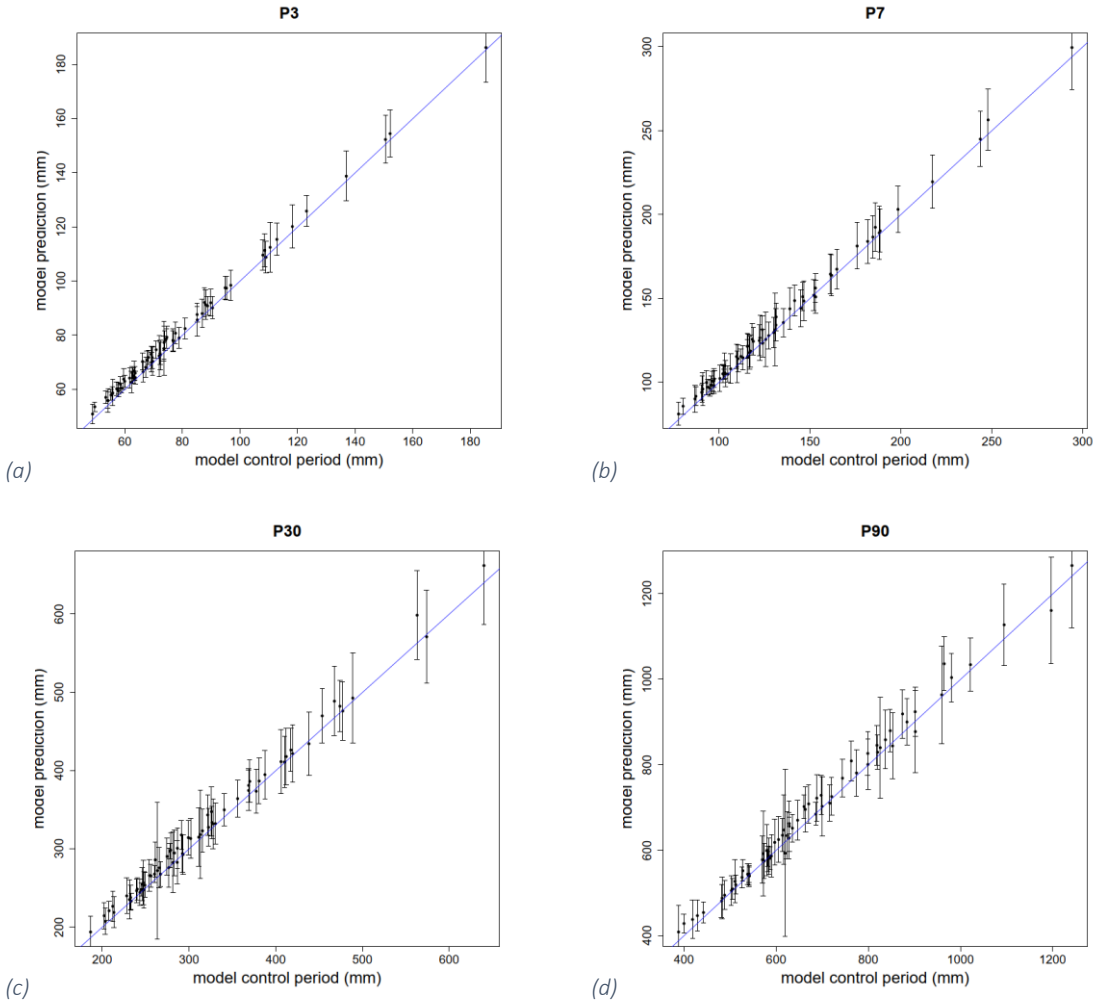

Figure 23 - Correlation between the 99th percentile of RCP8.5 (2021 – 2060) and RCP8.5 (1981 – 2020) of the 3 (a), 7 (b), 30 (c) and 90 day precipitation (d) in millimeters for the 69 stations analyzed. The blue line displays the 1:1 line while the error bars indicate the standard deviation of CH2018 model results

Even if the standard deviations are higher than the 95th percentile analysis, overall looking at the 99th percentile does suggest that the trend seen for the 95th percentile is for the most past the same: correlations close to 1 to 1, standard deviation increase with increasing amount of precipitation in millimeter.

Contrary to expectations the maximums (Figure 57, 58, 59 for RCP2.6, RCP4.5 and RCP8.5 respectively) RCP2.6 the PC results are generally overestimated with some exceptions for the 3 and 7 days where the high precipitation is underestimated instead, as regards of the standard deviations there are higher for the 3 and 30 days while for the 7 and 90 days are always high but more contained. RCP4.5 time windows of 3 and 7 days underestimate the past while the 30 and 90 days overestimate it in general the more the time window increases the better are the correlations between PC and F1 simulation data. Finally the scenario 8.5 on the other hand the 3 days underestimate PC with large standard deviations, the 7 days time window underestimate PC but the standard deviations are more contained than the 3 days, whereas 30 and 90 days

have standard deviations similar to the 7 days but moreover, the distribution in terms of millimeters is more homogeneous and a slight tendency to overestimate the PC data.

The boxplots that follow (Figure 24) present the ratio between the chain model mean value of the statistic and the same chain model mean value in the PC. They are organized for the four statistics and scenarios and to have a better view of the different impact of the scenarios regarding the statistics analyzed. RCP2.6 is represented in blue, the green stands for RCP4.5 and red is for RCP8.5.

Altogether the boxplots are very close to a one-to-one correlation with the PC simulations although in general they show a tendency to overestimate the simulations for the corresponding scenario in the PC. The median and 95th percentile show overestimations for all scenarios and time windows. The 99th percentile approaches the 1-to-1 correlation for the 30- and 90-day time windows, while the maxima are underestimated with the RCP4.5 and RCP8.5 scenarios while the RCP2.6 scenario is very close to the 1 value.

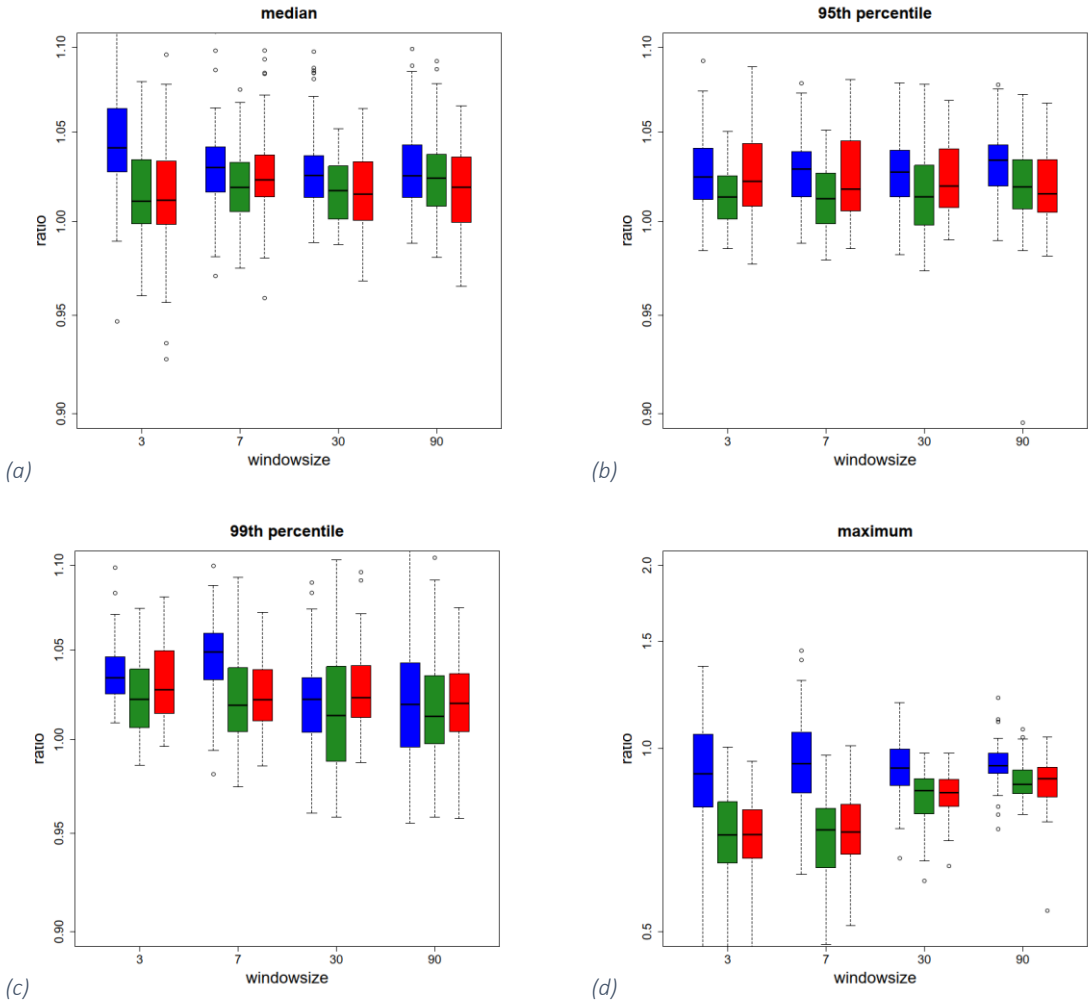

Figure 24 - Boxplots of the ratio of the median (a), 95th percentile (b), 99th percentile (c) and maximum (d) every box represents each one of the time period analyzed for the mean of the ten CH2018 simulation for each scenario for the period 2021-2060 and the mean of the ten CH2018 simulation for the same scenario for the period 2021-2060 between 1981 and 2020 (i.e. mean of RCP2.6 simulations in 2021-2060 over the mean of RCP2.6 simulation in 1981-2020 and so on). The results for the RCP2.6 are presented in blue, green for RCP4.5 and red for RCP8.5. A value of 1 indicates that the statistic is the same for the observed and model data, values below 1 indicate that the CH2018 simulations underestimate the data, while the values above 1 indicate an overestimation.

The median suggests that there would be an overestimation by scenario 2.6 indicating an increase in mean, 95th and 99th percentile precipitation while keeping the maxima like the PC, thus with a general trend towards an increase in extreme precipitation but with moderation. Scenario 4.5 overestimates the mean and 95th percentile, while for the 99th it remains in line with the control period, for the maxima the trend is of underestimation, which is contrary to expectations of a moderate increase. Regarding scenario 8.5, it follows the trend of RCP4.5 although in a more pronounced way, meaning that, except for the maximums, its trend it is in line with constraints expectations.

Spatial analysis of the data for the median, the RCP2.6 (Figure 60 in the appendix) present a general overestimate with exceptions visible in Ticino for the time windows of 7 30 and 90 days. RCP4.5 (Figure 61 in the appendix) shows an underestimation in the Alps while the rest of the territory is slightly overestimated, this trend improves with increasing time window. As for the RCP8.5 (Figure 62 in the appendix), Ticino and the west of Switzerland are underestimated, the estimate for the Swiss plateau is fairly good for the time window of three days, the 7 days present a general overestimation except for Ticino which is underestimated while the 30 days underestimate the Alps and Ticino compared to the rest of Switzerland which has overestimated. Finally for the 90 days the underestimation tends to the south of the Alps.

The spatial analysis of the 95th percentile shows that the correlations for the RCP2.6 scenario (Figure 25) overestimate the data for all time windows in the west area of Switzerland and has a slight underestimation in the Valais area. Scenarios 4.5 (Figure 26) shows that the prediction will tend to underestimate the alps area and overestimate the rest of the area. While the predictions for scenario 8.5 (Figure 27) are in line with the simulations for the Alps, under the pre-Alps in Ticino and lower Grisons are slightly underestimated while in the rest of the territory overestimated.

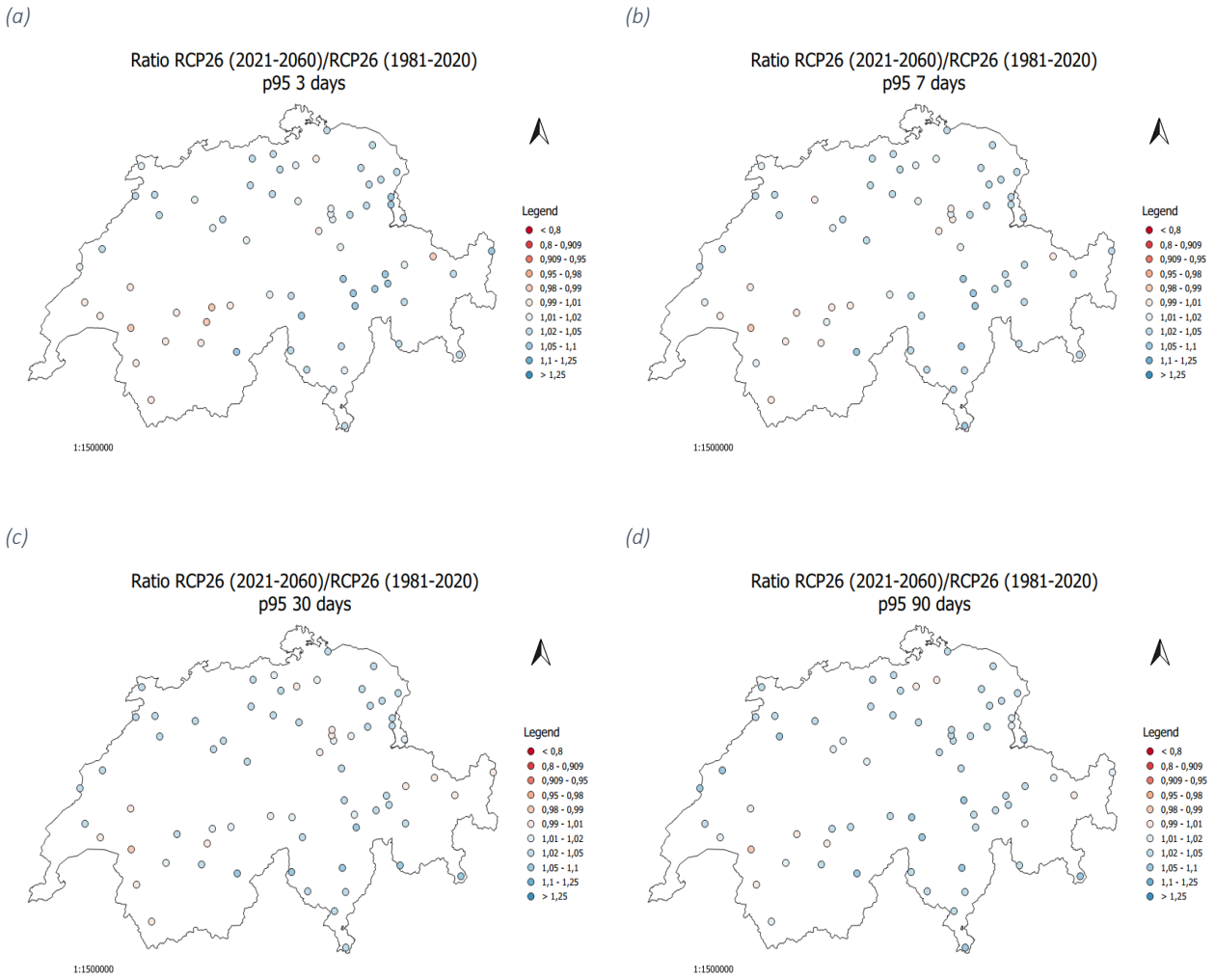

Figure 25 - Maps showing the ratio of the 95th percentile of the 3 (a), 7 (b), 30 (c) and 90 day precipitation (d) for the RCP2.6 scenario of the CH2018 simulations (mean of all ten models) for the period between 2021 and 2060 and the RCP2.6 scenario of the CH2018 simulation (mean of all ten models) for the control period (1981 – 2020). Values larger than 1 indicate an overestimation (blue) and values less than 1 an underestimation (red).

(a)

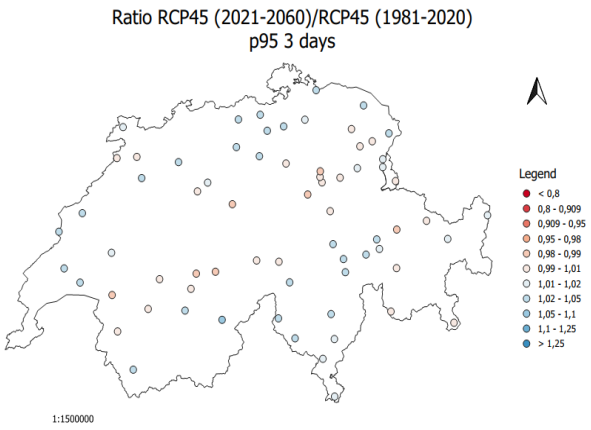

(b)

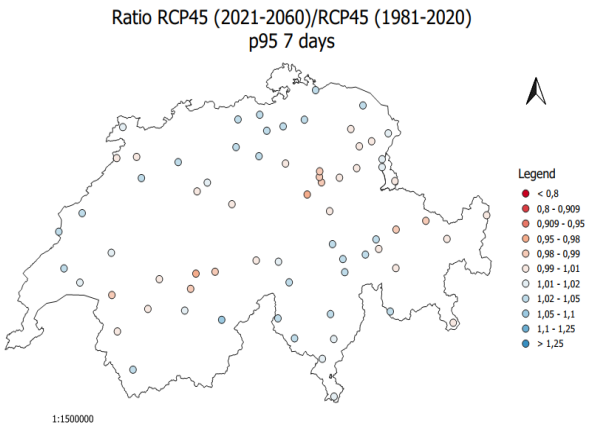

(c)

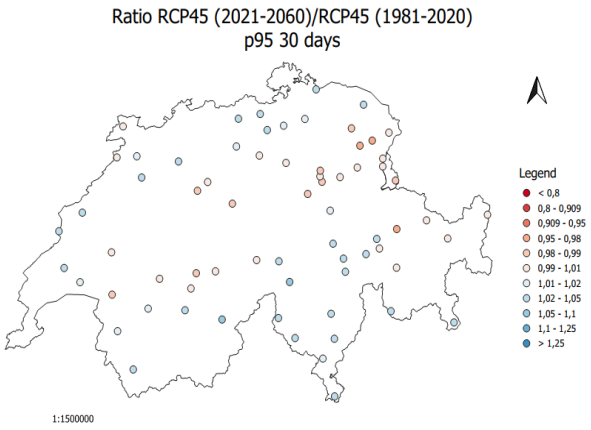

(d)

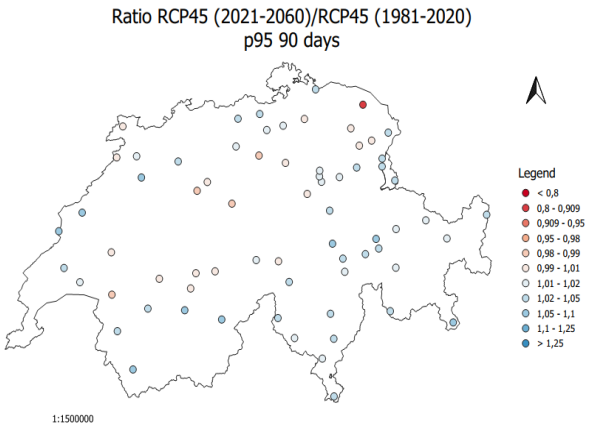

Figure 26 - Maps showing the ratio of the 95th percentile of the 3 (a), 7 (b), 30 (c) and 90 day precipitation (d) for the RCP4.5 scenario of the CH2018 simulations (mean of all ten models) for the period between 2021 and 2060 and the RCP4.5 scenario of the CH2018 simulation (mean of all ten models) for the control period (1981 – 2020). Values larger than 1 indicate an overestimation (blue) and values less than 1 an underestimation (red).

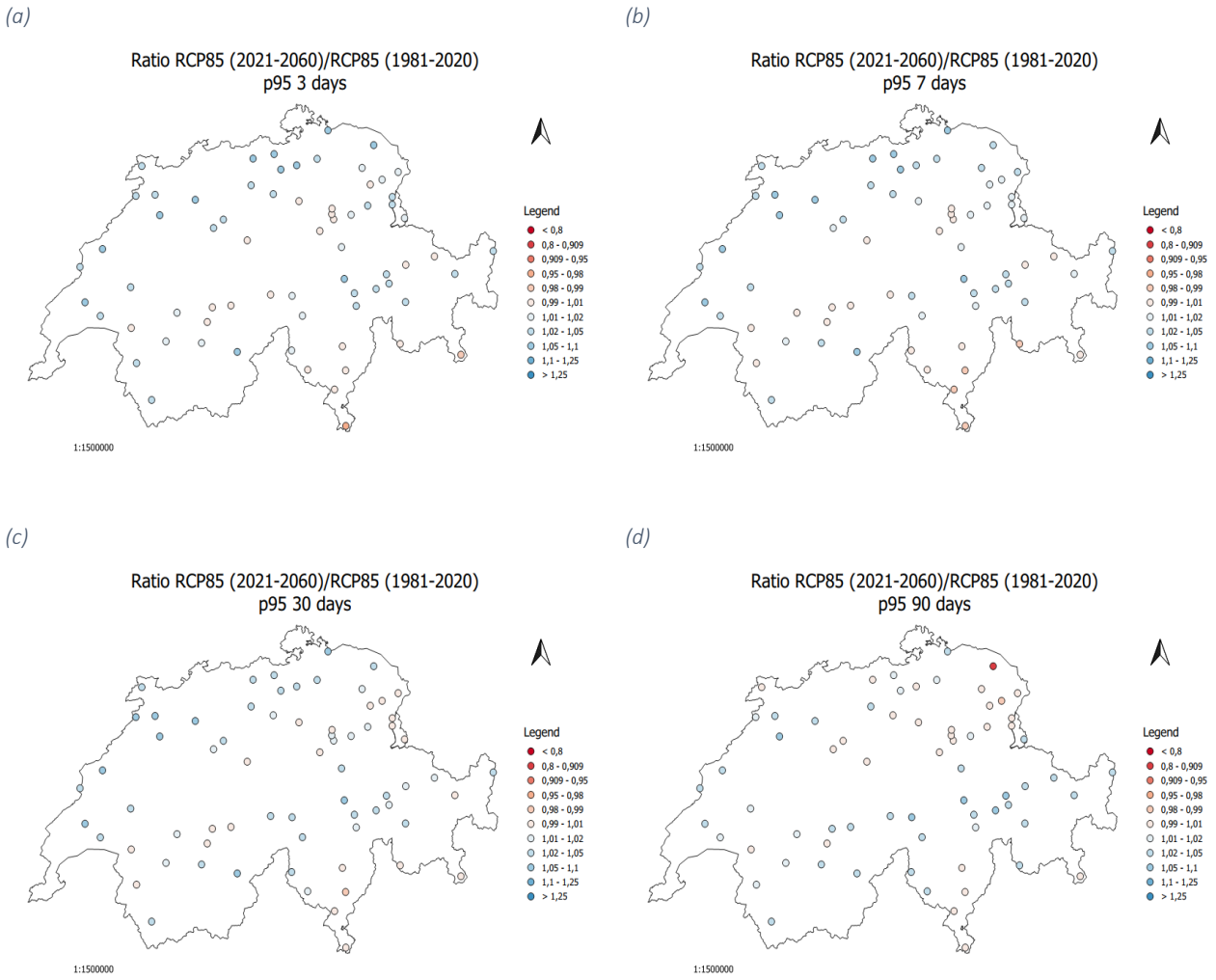

Figure 27 – Maps showing the ratio of the 95th percentile of the 3 (a), 7 (b), 30 (c) and 90 day precipitation (d) for the RCP8.5 scenario of the CH2018 simulations (mean of all ten models) for the period between 2021 and 2060 and the RCP8.5 scenario of the CH2018 simulation (mean of all ten models) for the control period (1981 – 2020). Values larger than 1 indicate an overestimation (blue) and values less than 1 an underestimation (red).

Spatial analysis for the 95th percentile shows that a spatial correlation is most evident for scenarios 4.5 and 8.5. The effect of the alps is evident from the disposition of the over- and underestimates. It therefore suggests that a decrease in greenhouse gas would have an underestimate over the entire territory without taking topography into account (RCP2.6) while if greenhouse gases are not or only partially monitored (RCP8.5, RCP4.5) the alps would have an underestimate while the rest of the territory would have an overestimate, i.e. there would be more rainfall in the alps and less in the rest of Switzerland.

Regarding the 99th percentile, scenario 2.6 (Figure 28) has no significant spatial correlations for the 3 and 7 days while for the 30 and 90 days there is a slight trend on the Swiss plateau of an underestimation. Scenario 4.5 (Figure 29) has a good estimation for the north of the Alps for the 3 and 7 days while for the 30 days there is an underestimation in the area east of Switzerland, an overestimation in the south and northwest, while for the 90 days the trend is an underestimation on the arc north of the Alps from Lausanne to Schaffhausen; for the rest of Switzerland the trend is towards overestimation. Scenario 8.5 (Figure 30), however, does not present significant spatial correlations in addition to a general overestimation on the territory.

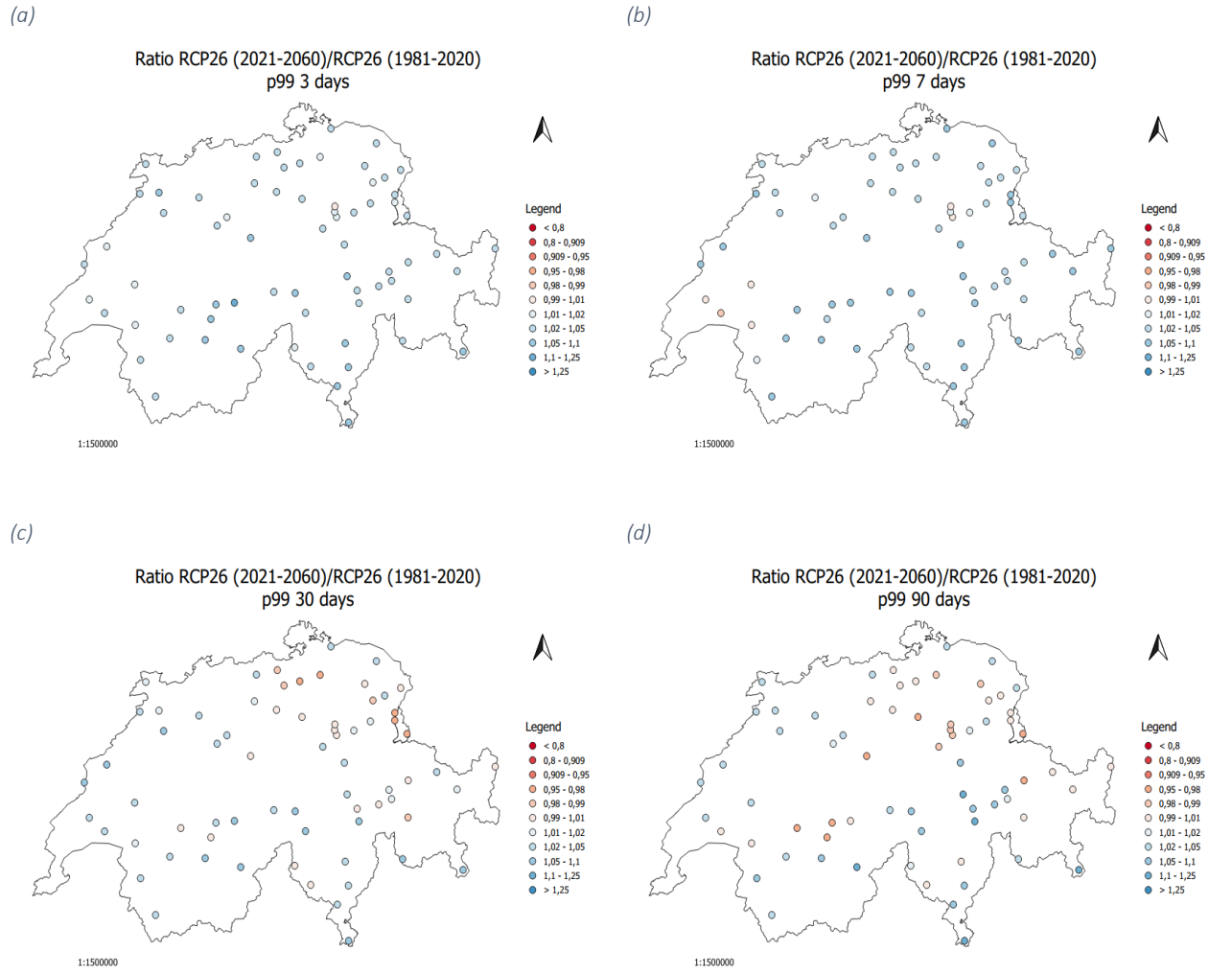

Figure 28 - Maps showing the ratio of the 99th percentile of the 3 (a), 7 (b), 30 (c) and 90 day precipitation (d) for the RCP2.6 scenario of the CH2018 simulations (mean of all ten models) for the period between 2021 and 2060 and the RCP2.6 scenario of the CH2018 simulation (mean of all ten models) for the control period (1981 – 2020). Values larger than 1 indicate an overestimation (blue) and values less than 1 an underestimation (red).

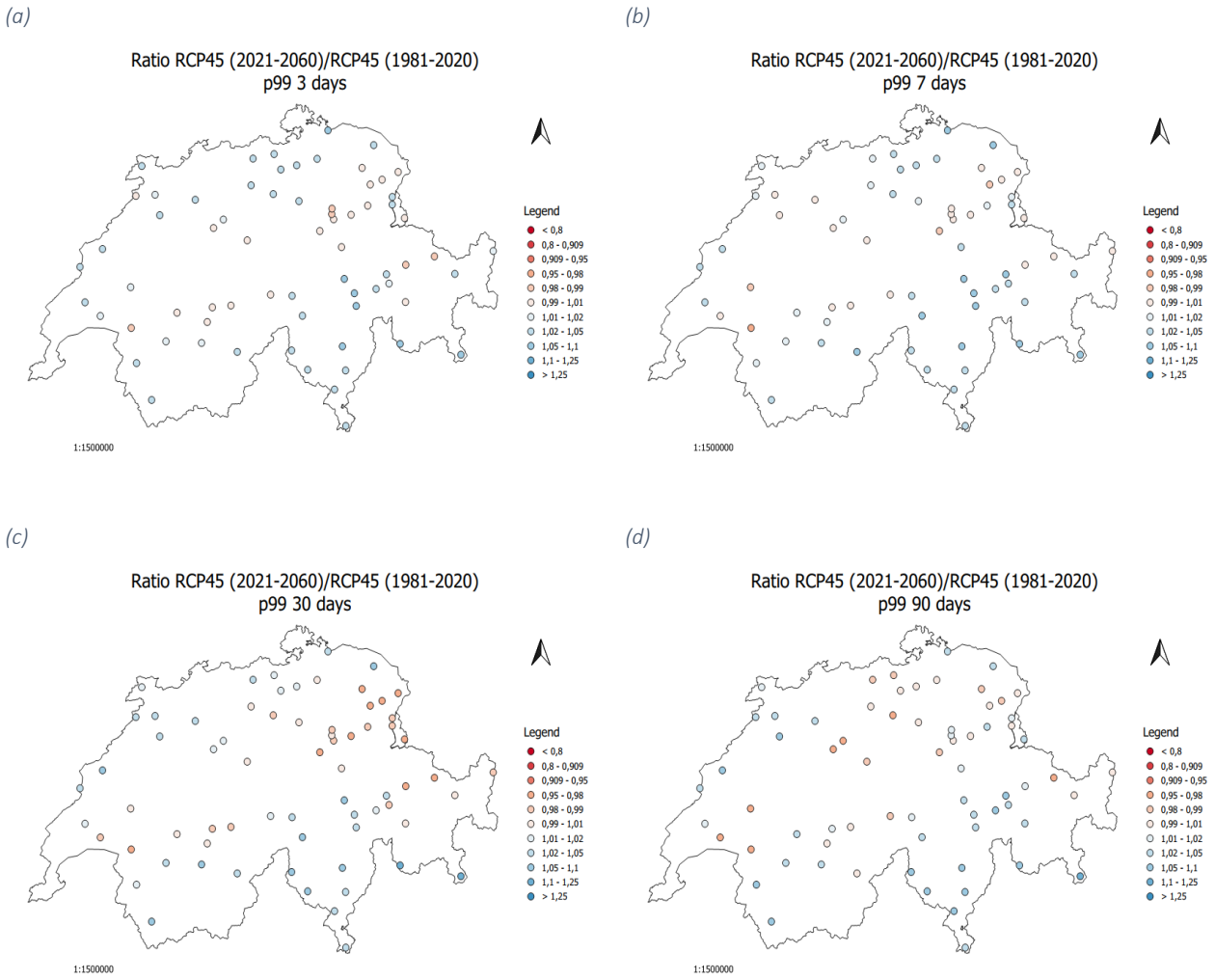

Figure 29 - Maps showing the ratio of the 99th percentile of the 3 (a), 7 (b), 30 (c) and 90 day precipitation (d) for the RCP4.5 scenario of the CH2018 simulations (mean of all ten models) for the period between 2021 and 2060 and the RCP4.5 scenario of the CH2018 simulation (mean of all ten models) for the control period (1981 – 2020). Values larger than 1 indicate an overestimation (blue) and values less than 1 an underestimation (red).

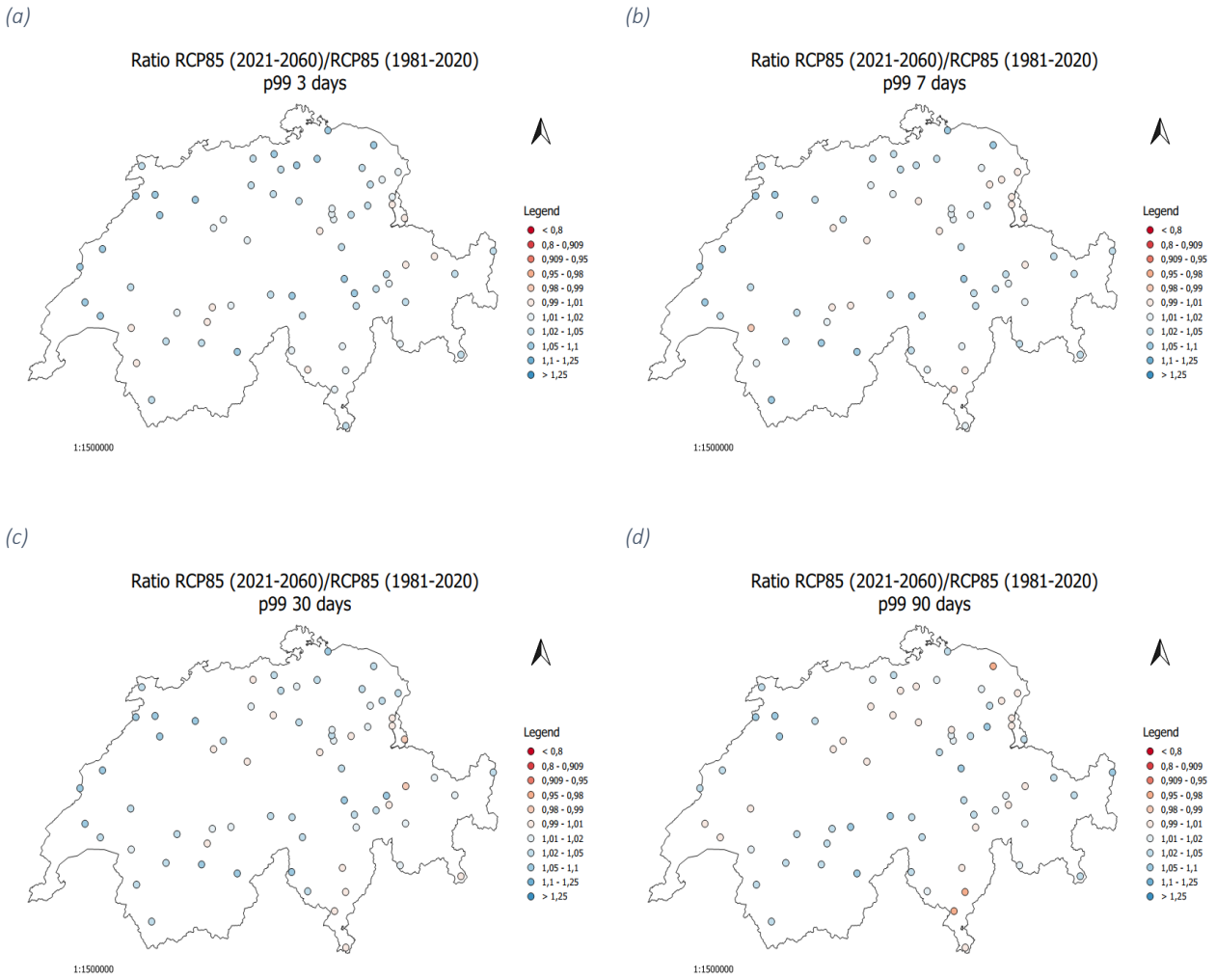

Figure 30 - Maps showing the ratio of the 99th percentile of the 3 (a), 7 (b), 30 (c) and 90 day precipitation (d) for the RCP8.5 scenario of the CH2018 simulations (mean of all ten models) for the period between 2021 and 2060 and the RCP8.5 scenario of the CH2018 simulation (mean of all ten models) for the control period (1981 – 2020). Values larger than 1 indicate an overestimation (blue) and values less than 1 an underestimation (red).

Overall, a general spatial underestimation for the 99th percentile with visible but unremarkable trends for the 3- and 7-day in all three scenarios. The 30 and 90 days show some spatial trends for scenarios 4.5 and 8.5.

Regarding the maximums (Appendix Figure 63, 64, 65 for RCP2.6, 4.5, and 8.5 respectively), the general underestimation presented in the box plots does not find particular spatial dispositions on Switzerland even the scenario 2.6 that should have been closer to the correlation one to one does not present particular spatial dispositions for the three days there are some slight exceptions of overestimation in Valais, Ticino in the south of Graubünden.

4.4 Second future period (2061 – 2099)

All the considerations made for the F1 apply also for the analyses of this F2 period. However, we expect that the difference between the analyzed period (2061-2099) and the PC (1981-2020) will be a bit more pronounced, since the effect of the constraints of the simulations for each scenario had more time for which a difference can be more noticeable, even though where was already visible in the F1 period analysis.

4.4.1 Comparison of the frequency distributions for two selected stations

As for F1, the first analysis presented is the cumulative frequency for Coldrerio and Opfikon station. The results are presented by scenario and each figure presents the four time windows analyzed for that scenario. Figures 31, 32, and 33 are the results of each RCPs for Coldrerio while Figures 34, 35, and 36 present each RCPs results for Opfikon. Furthermore, as indicated in the Figure caption, the red line indicates the average of the scenario analyzed for PC while the blue lines are the result of the CH2018 ten chain model simulations for F2.

To the naked eye the differences between F1 and F2 are hardly visible, to facilitate reading therefore in Table 6 the average differences between the ten CH2018 chain model simulations for each scenario during F2 and the results of the respective scenario during PC are summarized.

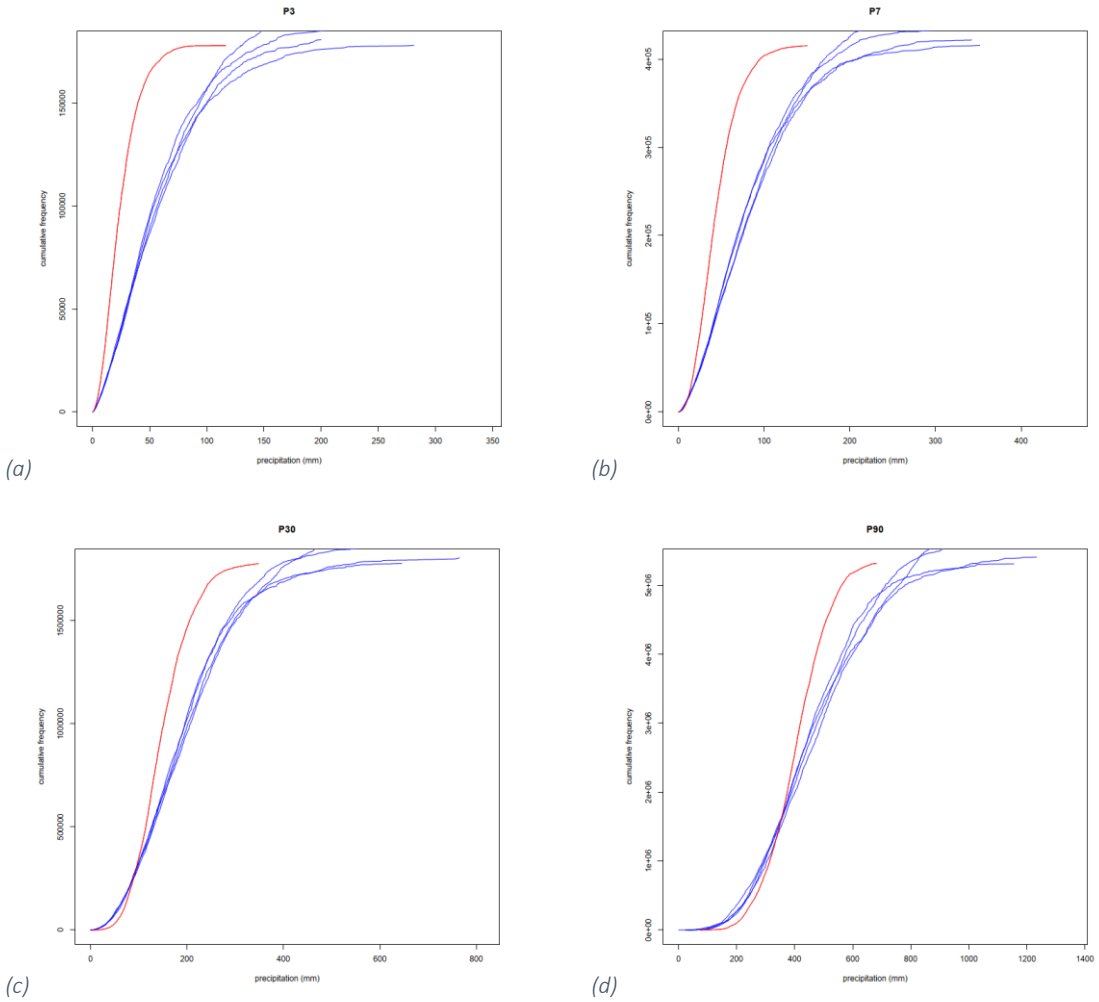

Figure 31 – Cumulative frequency of the 3 (a), 7 (b), 30 (c) and 90 days total precipitation (d) in millimeter for the Coldrerio (COL) station during the period between 2061 and 2099. The red line indicates mean of the RCP2.6 for 1981 – 2020, while the blue ones represent the result of the ten chain model simulations for the RCP2.6 scenario for 2061-2099.

As anticipated Figure 31 presents the results of the cumulative frequency for Coldrerio and more precisely for RCP2.6. As stated before the difference to F1 is not easy to perceive. For the 3 and 7 days more than the 30 and 90 days, where a decrease in the slope of the curve is noticeable, indicating that more days are needed to reach the maximum millimeters simulated in F1. It follows that the simulation for F2 does not predict heavy rain as much as F1, consistent with the constraints of RCP2.6.

From the overlay of the F1 and F2 results, a shift to the right of the curves can be seen, indicating that the total simulated millimeters are higher than in the first future period. Thus, the simulation indicates less heavy rain but over more rainy days.

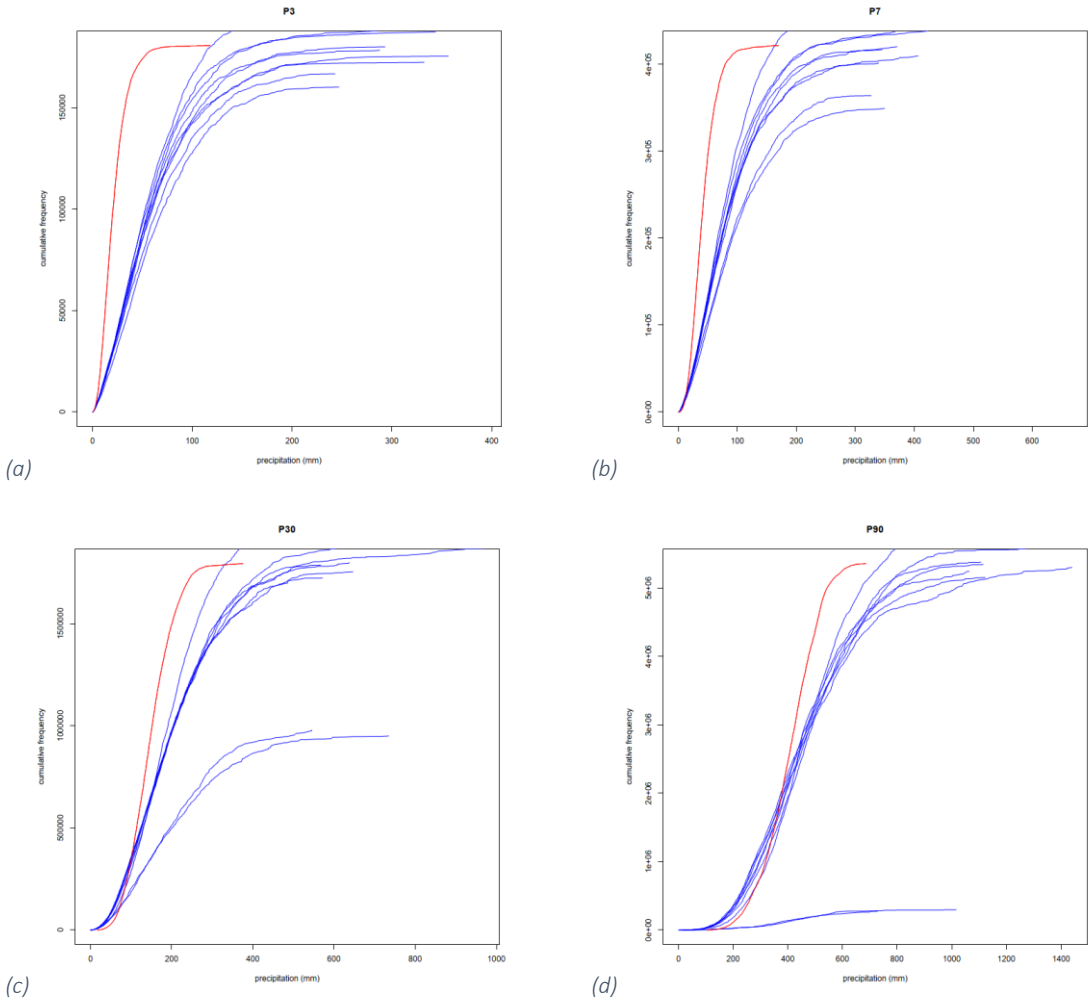

Figure 32 – Cumulative frequency of the 3 (a), 7 (b), 30 (c) and 90 days total precipitation (d) in millimeter for the Coldrerio (COL) station during the period between 2061 and 2099. The red line indicates mean of the RCP4.5 for 1981 – 2020, while the blue ones represent the result of the ten chain model simulations for the RCP4.5 scenario for 2061-2099.

Figure 32 presents the cumulative frequency results for Coldrerio for the RCP4.5 scenario. The trend in each time window mirrors those already noted for F1. In addition, the considerations made for Figure 31 also apply to this scenario: the total millimeters are higher and the slope slightly smaller than the results in F1. RCP4.5 constraints predict a less dramatic decrease in emissions than RCP2.6, but in each case is consistent with expectations.

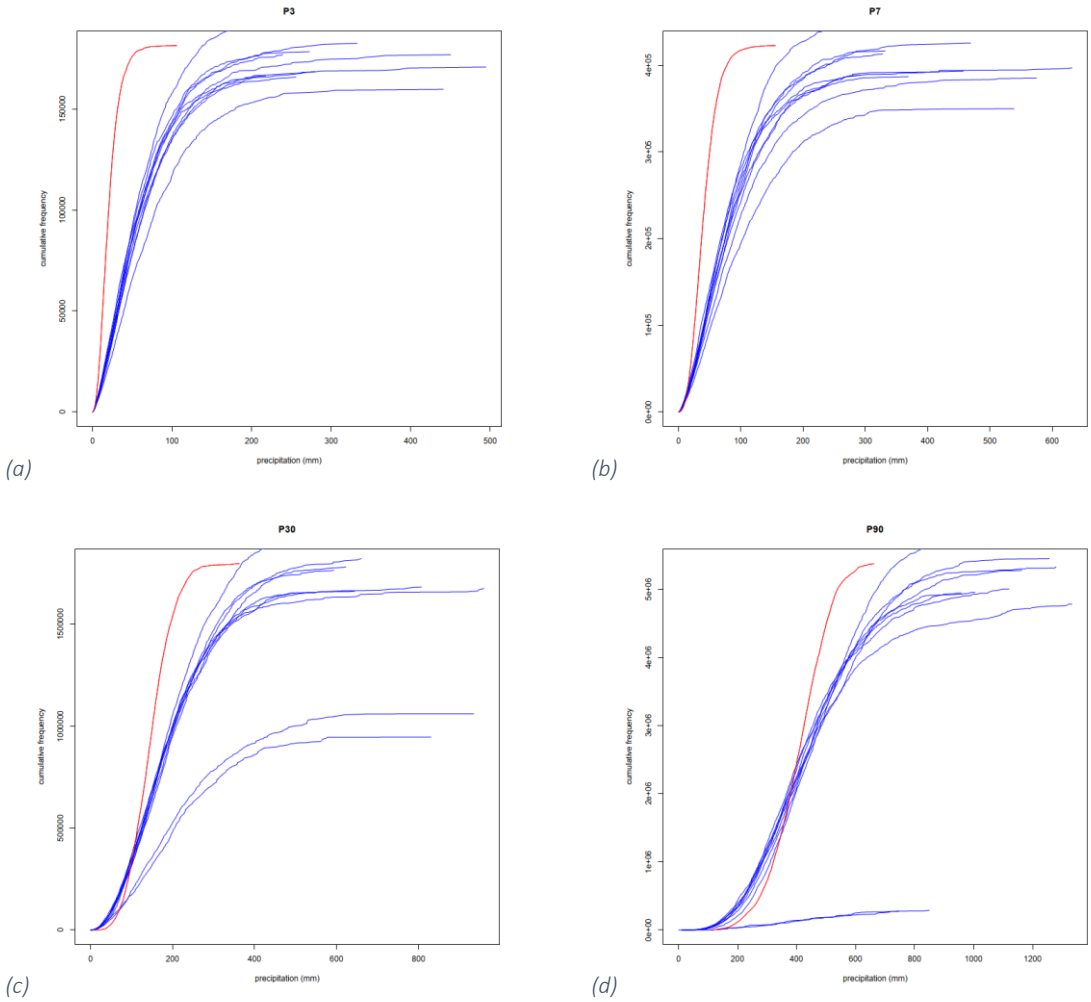

Figure 33 – Cumulative frequency of the 3 (a), 7 (b), 30 (c) and 90 days total precipitation (d) in millimeter for the Coldrerio (COL) station during the period between 2061 and 2099. The red line indicates mean of the RCP8.5 for 1981 – 2020, while the blue ones represent the result of the ten chain model simulations for the RCP8.5 scenario for 2061-2099.

The same considerations with respect to F1 also apply to the RCP8.5 scenario in Figure 33. Higher total millimeters and less strong tilt for longer time windows.

Difference COL (mm)	P3	P7	P30	P90
RCP2.6	5.88	9.61	50.35	100.23
RCP4.5	5.27	8.50	18.61	27.61
RCP8.5	5.80	9.99	18.08	20.23

Table 6 - Average difference between the ten CH2018 simulations for the three scenarios during the period 2061-2099 and the ten CH2018 simulations for the correspondent scenarios during the period 1981-2020 in millimeters of the multi-day precipitation for Coldrerio (COL).

In general, comparing the two tables for the difference between the period under analysis and PC (Table 4 summarizing the average differences between the ten chain model outputs for F1 and the mean of

the simulations outputs for each scenario during PC and Table 6 with the summary of the average differences between the ten chain model outputs for F2 and the mean of the simulations outputs for each scenario during PC), it can be seen that these F2 values are lower for scenarios 2.6 and 4.5 compared to Table 4, but they are significantly higher for RCP8.5.

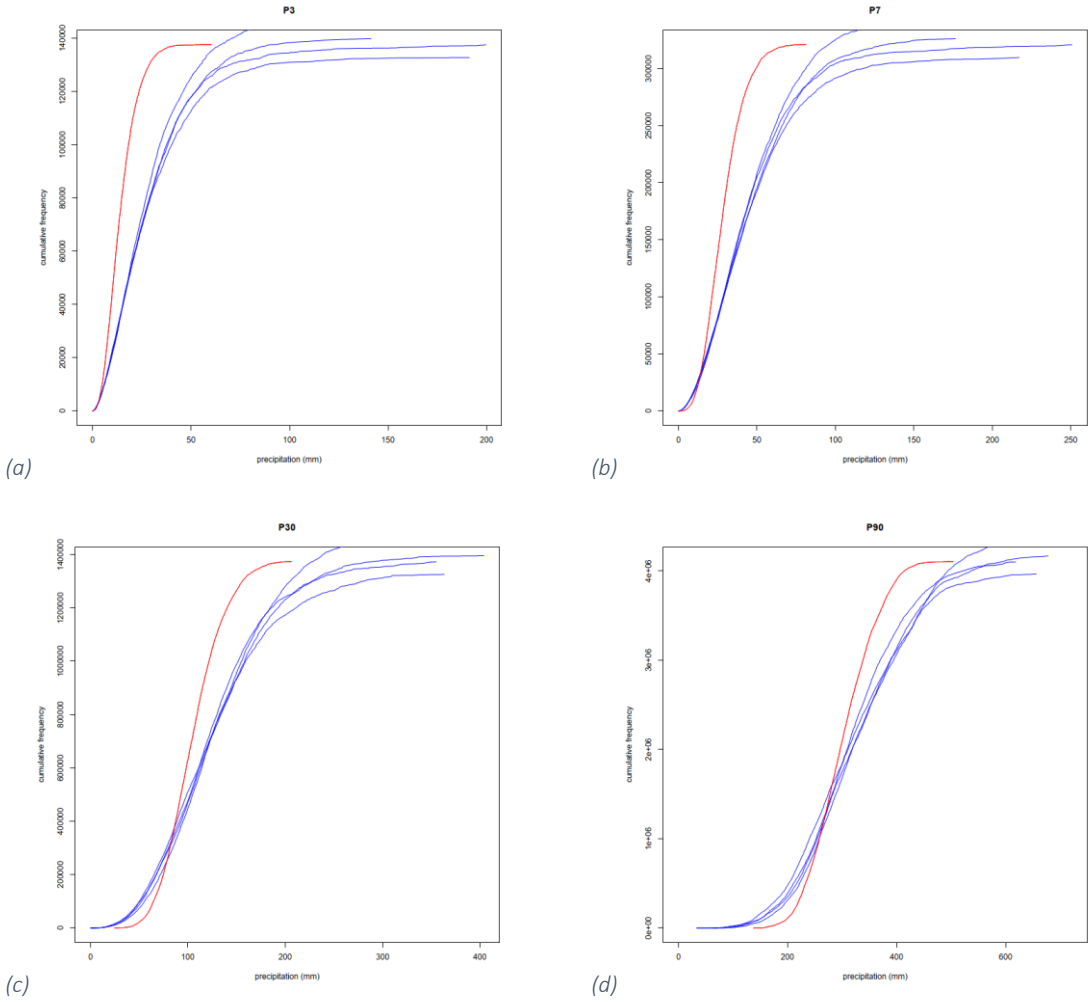

Figure 34 - Cumulative frequency of the 3 (a), 7 (b), 30 (c) and 90 days total precipitation (d) in millimeter for the Opfikon (OPF) station during the period between 2061 and 2099. The red line indicates mean of the RCP2.6 for 1981 – 2020, while the blue ones represent the result of the ten chain model simulations for the RCP2.6 scenario for 2061-2099.

Analyses of the cumulative frequencies for Opfikon show the same trend as observed for Coldrerio, higher total millimeters and for the 30 and 90 day time windows the slope is less strong for all scenarios. It can also be seen from the graphs that the total precipitation Opfikon arrives at is lower than Coldrerio in all scenarios for all time windows Since the difference between F2 and PC results by analyzing the graphs is not immediate except for observations on their trend, refer to Table 7 for specifics.

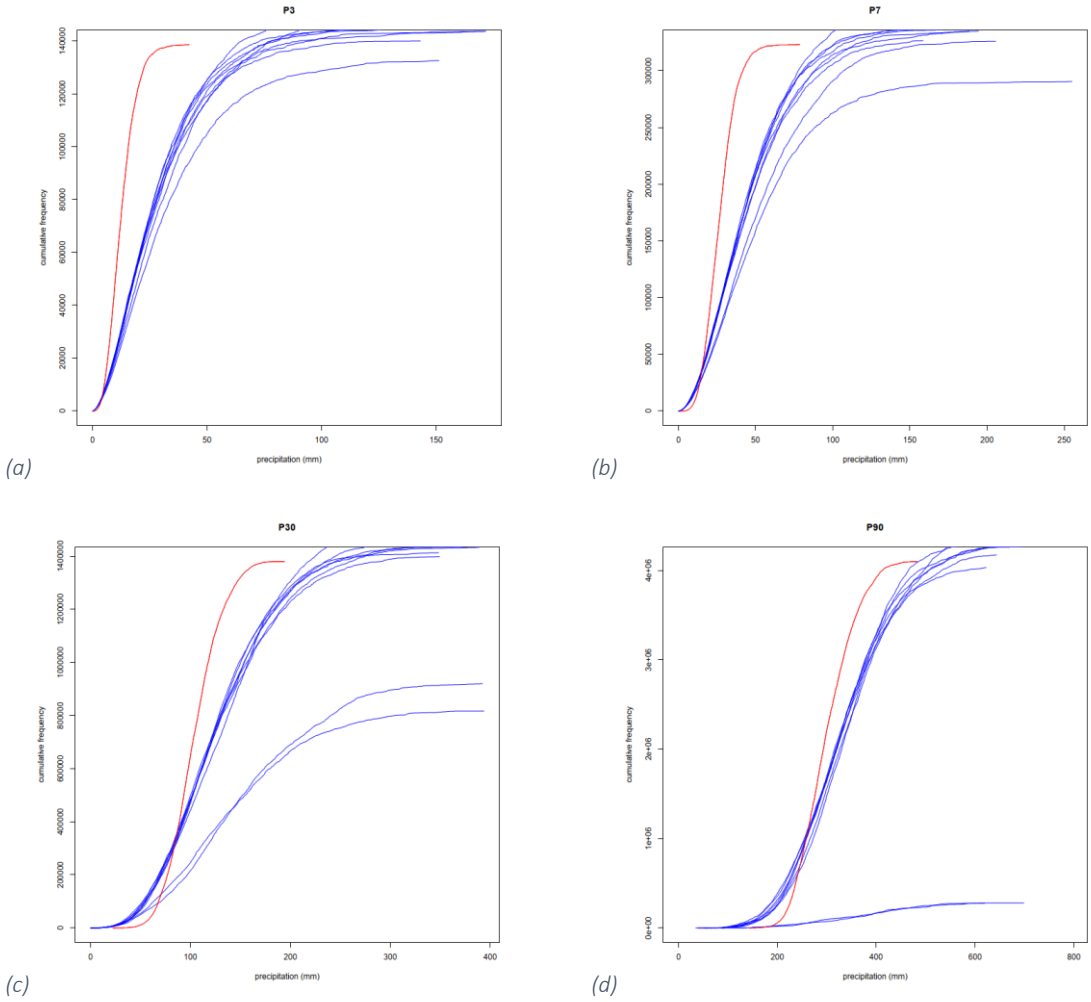

Figure 35 - Cumulative frequency of the 3 (a), 7 (b), 30 (c) and 90 days total precipitation (d) in millimeter for the Opfikon (OPF) station during the period between 2061 and 2099. The red line indicates mean of the RCP4.5 for 1981 – 2020, while the blue ones represent the result of the ten chain model simulations for the RCP4.5 scenario for 2061-2099.

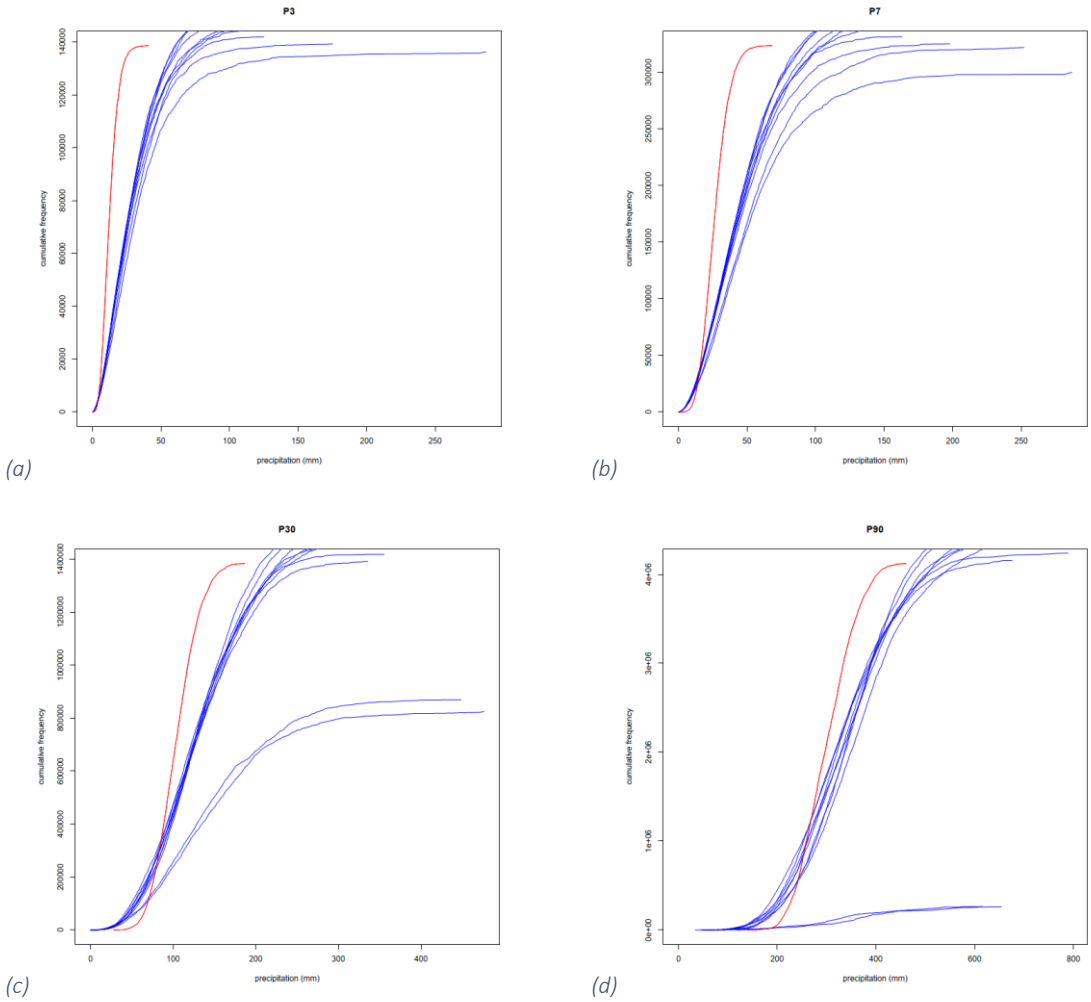

Figure 36 - Cumulative frequency of the 3 (a), 7 (b), 30 (c) and 90 days total precipitation (d) in millimeter for the Opfikon (OPF) station during the period between 2061 and 2099. The red line indicates mean of the RCP8.5 for 1981 – 2020, while the blue ones represent the result of the ten chain model simulations for the RCP8.5 scenario for 2061-2099.

Difference OPF (mm)	P3	P7	P30	P90
RCP2.6	1.01	1.12	-1.68	0.73
RCP4.5	5.23	8.05	13.89	15.64
RCP8.5	7.76	12.87	21.29	47.82

Table 7 - Average difference between the ten CH2018 simulations for the three scenarios during the period 2061-2099 and the ten CH2018 simulations for the correspondent scenarios during the period 1981-2020 in millimeters of the multi-day precipitation for Opfikon (OPF).

As with Table 6, Table 7 collects the average of the difference between the ten chain model outputs of the simulations for each scenario for the F2 period and the average of the simulations for each scenario during the PC. The differences between the data during the PC and those for F2 are lower than in Table 5 (which includes the same differences as Table 7 but for F1) for scenario 2.6, but not for scenarios 4.5 and 8.5. As with Table 6, Table 7 collects the average of the difference between the ten chain model outputs of the simulations

for each scenario for the F2 period and the average of the simulations for each scenario during the PC. The differences between the data during the PC and those for F2 are lower than in Table 5 (which includes the same differences as Table 7 but for F1) for scenario 2.6, but not for scenarios 4.5 and 8.5.

4.4.2 Comparison of the percentiles for all stations

The second analysis was done for all stations selected for the work. The results of the correlations for each scenario in the F2 dataset with the corresponding scenario dataset for the PC are presented below. As for F1 on the x-axis the PC outputs are plotted while on the y-axis the F2 outputs are plotted. The error bars correspond to the standard deviation of the tan chain model simulation outputs. The blue line, on the other hand, is an indicator of the 1-to-1 correlation between the two datasets.

In addition, the results of the median and maximum analyses can be found in the appendix section. For the median of scenario 2.6 refer to figure 66, for RCP4.5 refer to figure 67 while scenario 8.5 is presented in figure 68. For the maximums refer to figure 69, 70 and 71 which show the results of RCP2.6, RCP4.5 and RCP8.5 respectively.

Median analysis (Figure 66 for RCP2.6, Figure 67 for RCP4.5, and Figure 68 for RCP8.5) for all three scenarios show good correlation. The stations are very close to the 1-to-1 correlation line with a tendency to overestimate the PC results. The standard deviations also gradually increase from analyzing scenario 2.6 to scenario 4.5 and again when analyzing scenario 8.5.

The second statistical variable analyzed is the 95th percentile. Figures 37, 38, and 39 present the results of the correlation analyses for RCP2.6, RCP4.5, and RCP8.5, respectively. Considerations were made in a single paragraph following Figure 39 to have more clear overview of the three scenarios simulations results.

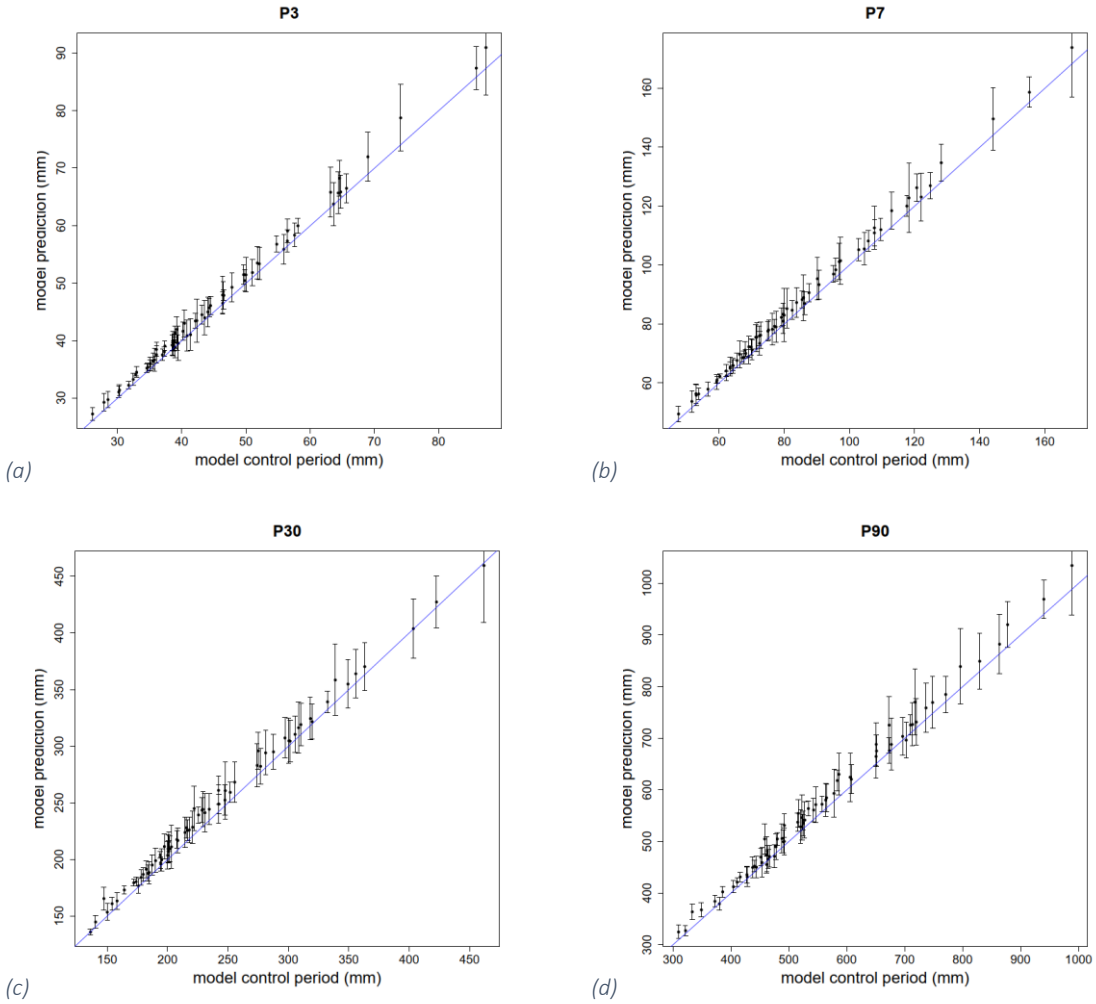

Figure 37 - Correlation between the 95th percentile of RCP2.6 (2061 – 2099) and RCP2.6 (1981 – 2020) of the 3 (a), 7 (b), 30 (c) and 90 day precipitation (d) in millimeters for the 69 stations analyzed. The blue line displays the 1:1 line while the error bars indicate the standard deviation of CH2018 model results

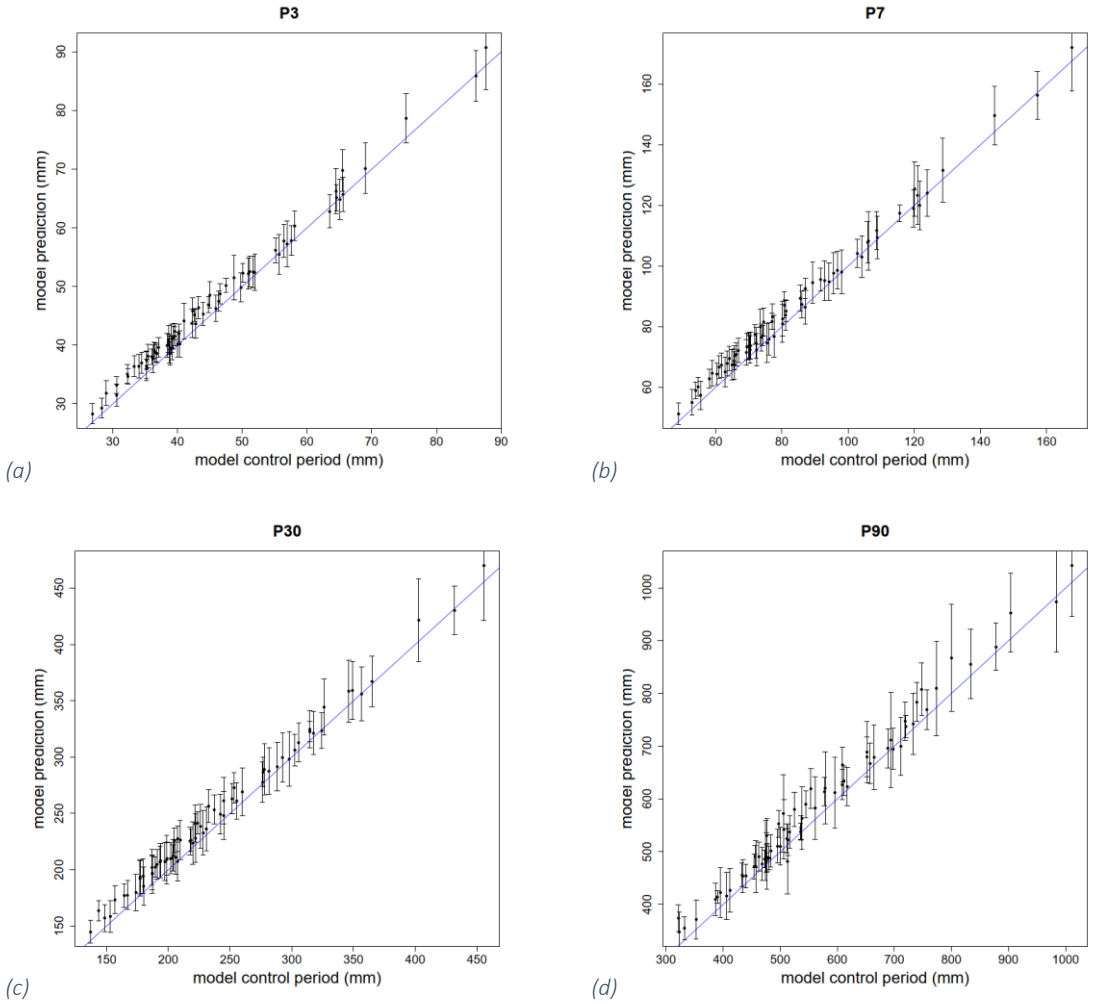

Figure 38 - Correlation between the 95th percentile of RCP4.5 (2061 – 2099) and RCP4.5 (1981 – 2020) of the 3 (a), 7 (b), 30 (c) and 90 day precipitation (d) in millimeters for the 69 stations analyzed. The blue line displays the 1:1 line while the error bars indicate the standard deviation of CH2018 model results

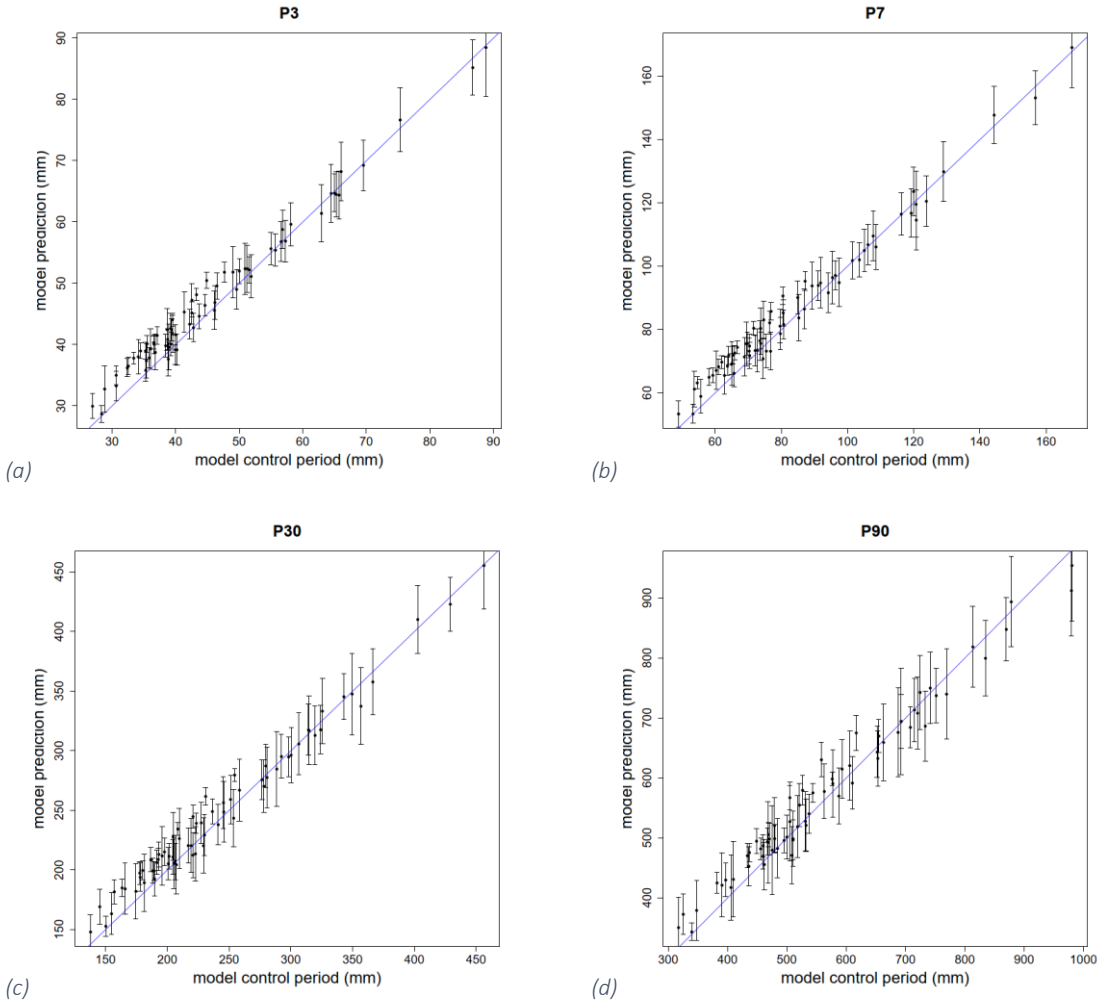

Figure 39 - Correlation between the 95th percentile of RCP8.5 (2061 – 2099) and RCP8.5 (1981 – 2020) of the 3 (a), 7 (b), 30 (c) and 90 day precipitation (d) in millimeters for the 69 stations analyzed. The blue line displays the 1:1 line while the error bars indicate the standard deviation of CH2018 model results

Figures 37, 38, 39 show the 95th percentile correlations of RCP2.6, RCP4.5, and RCP8.5, respectively, for the 69 stations analyzed. It can be seen that the stations are close to the blue line, an indicator of 1:1 correlation, with a general overestimation of the PC results. Compared to the median, the values for the standard deviations are less high and the difference between the three scenarios too small to make adequate considerations. In the longer time windows (30 and 90 days) it can be seen that the stations are more evenly distributed for high rainfall amounts (in millimeters), heavy rain therefore seems better displayed for these time windows.

The third statistical variable refers to the 99th percentile. Figures 40, 41, and 42 present the results of the correlation analyses for RCP2.6, RCP4.5, and RCP8.5, respectively. Considerations were made in a single paragraph following Figure 42 to have the clearest possible overview.

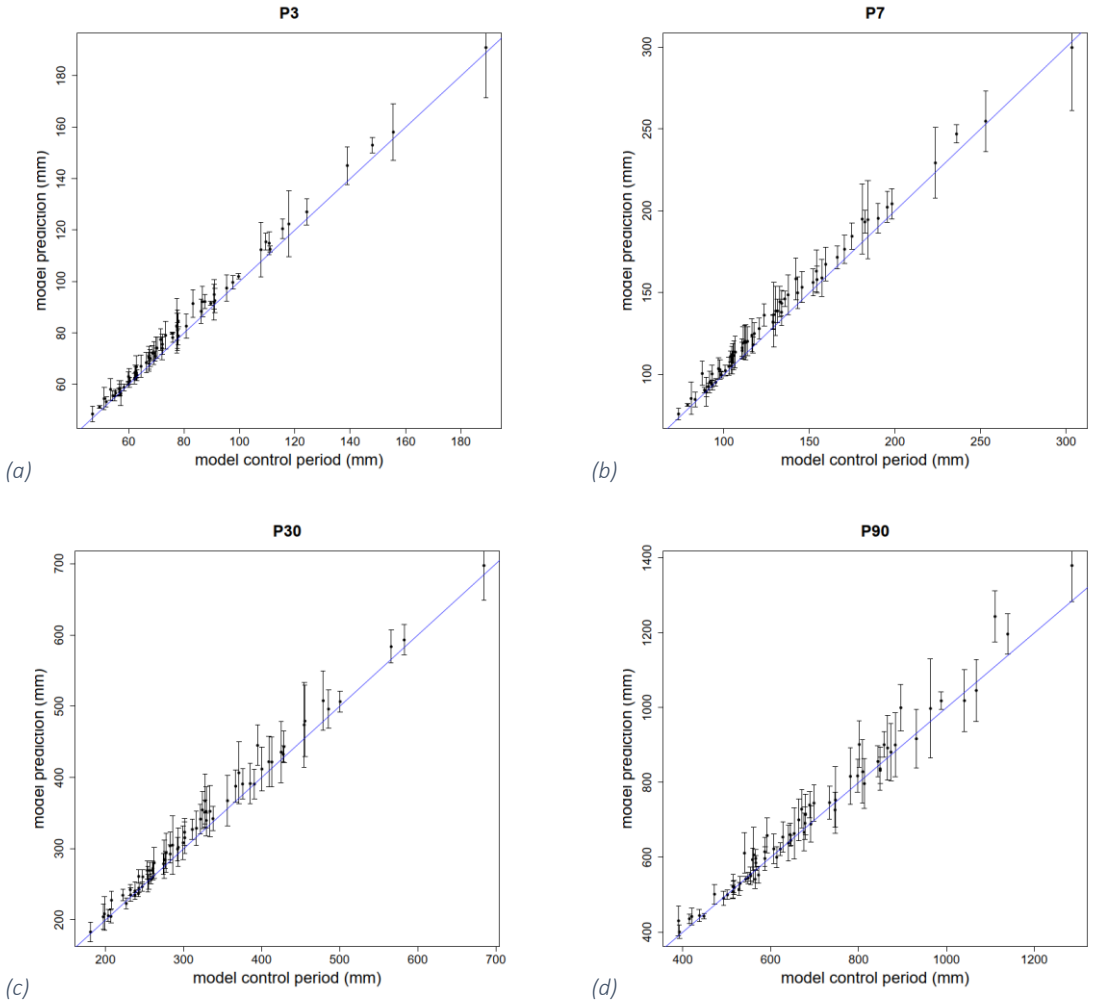

Figure 40 - Correlation between the 99th percentile of RCP2.6 (2061 – 2099) and RCP2.6 (1981 – 2020) of the 3 (a), 7 (b), 30 (c) and 90 day precipitation (d) in millimeters for the 69 stations analyzed. The blue line displays the 1:1 line while the error bars indicate the standard deviation of CH2018 model results

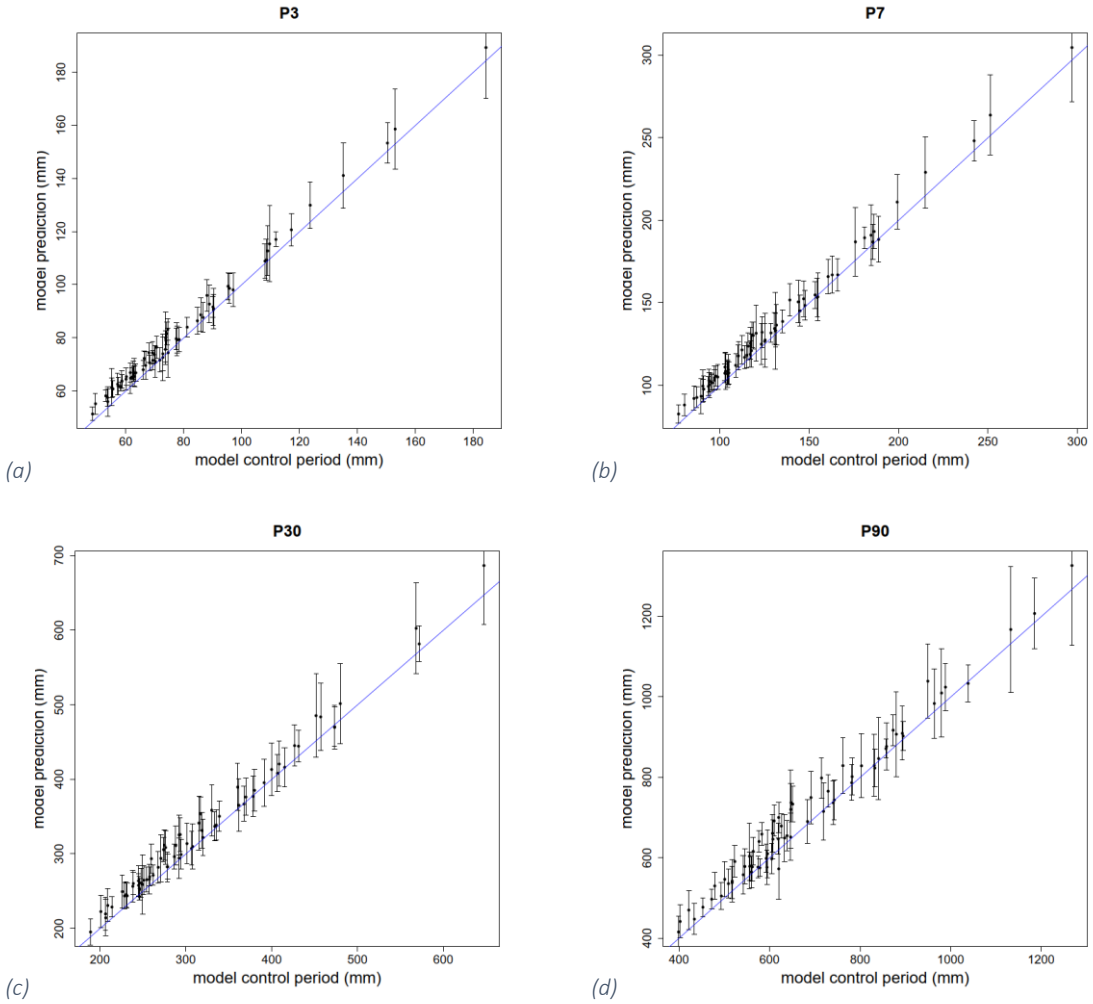

Figure 41 - Correlation between the 99th percentile of RCP4.5 (2061 – 2099) and RCP4.5 (1981 – 2020) of the 3 (a), 7 (b), 30 (c) and 90 day precipitation (d) in millimeters for the 69 stations analyzed. The blue line displays the 1:1 line while the error bars indicate the standard deviation of CH2018 model results

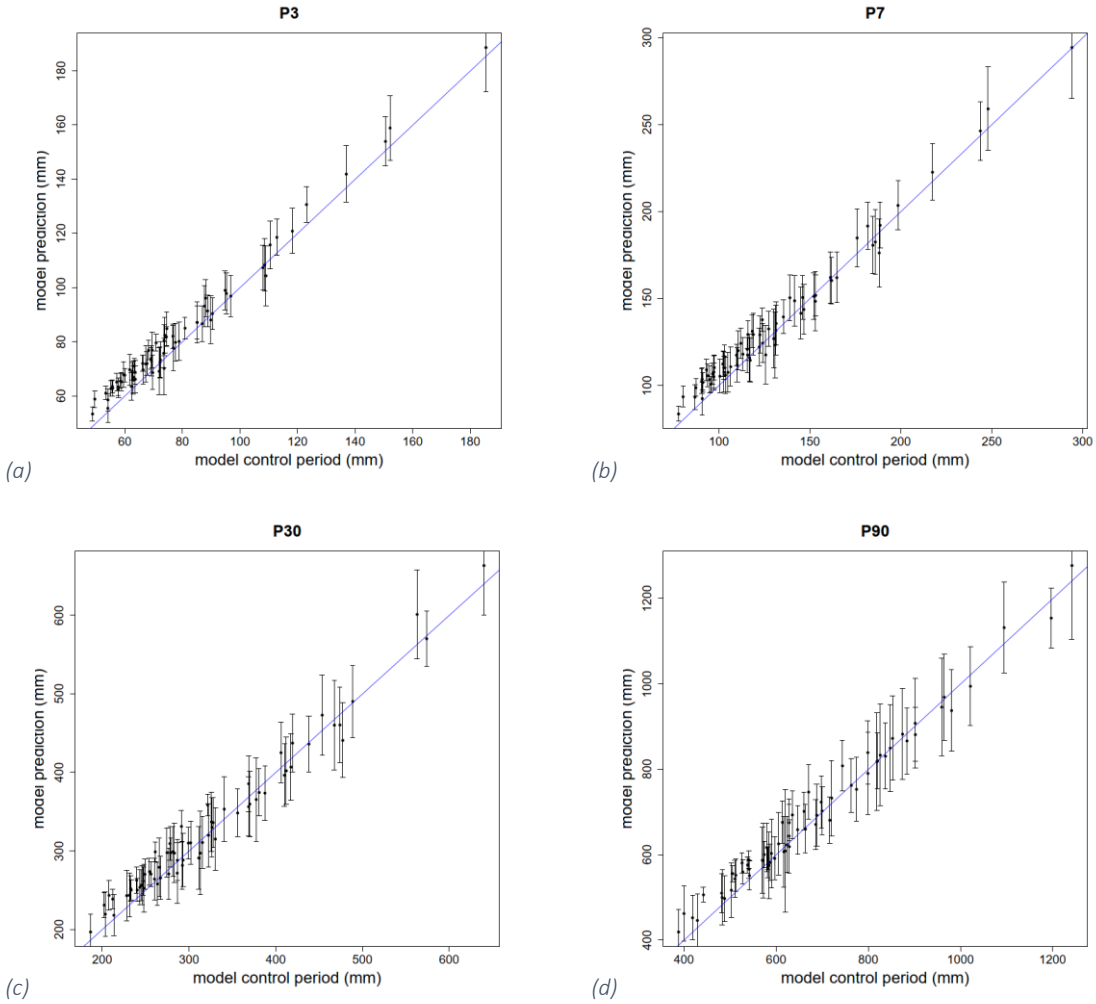

Figure 42 - Correlation between the 99th percentile of RCP8.5 (2061 – 2099) and RCP8.5 (1981 – 2020) of the 3 (a), 7 (b), 30 (c) and 90 day precipitation (d) in millimeters for the 69 stations analyzed. The blue line displays the 1:1 line while the error bars indicate the standard deviation of CH2018 model results

Also for this variable, the correlations between F2 and PC are good, the stations are close to the 1 to 1 correlation line. In contrast to the 95th percentile, the representation of the involuted stations becomes thinner and rarer for rainfall with many millimeters of rain. This inhomogeneity is an indicator that heavy rain only occurs in a few areas of Switzerland.

Regarding the analysis of the maxima (Appendix Figure 69, 70 and 71 for RCP2.6, 4.5, and 8.5 respectively), the values of the standard deviations are very high especially for the short time windows (3 and 7 days). The trend for large amounts of precipitation (in millimeters) is only perceived by a few stations. In general, the stations remain fairly close to the 1-to-1 correlation line, although less precisely than for the other variables examined. Indicator that for maxima the simulations are not in line with the PC.

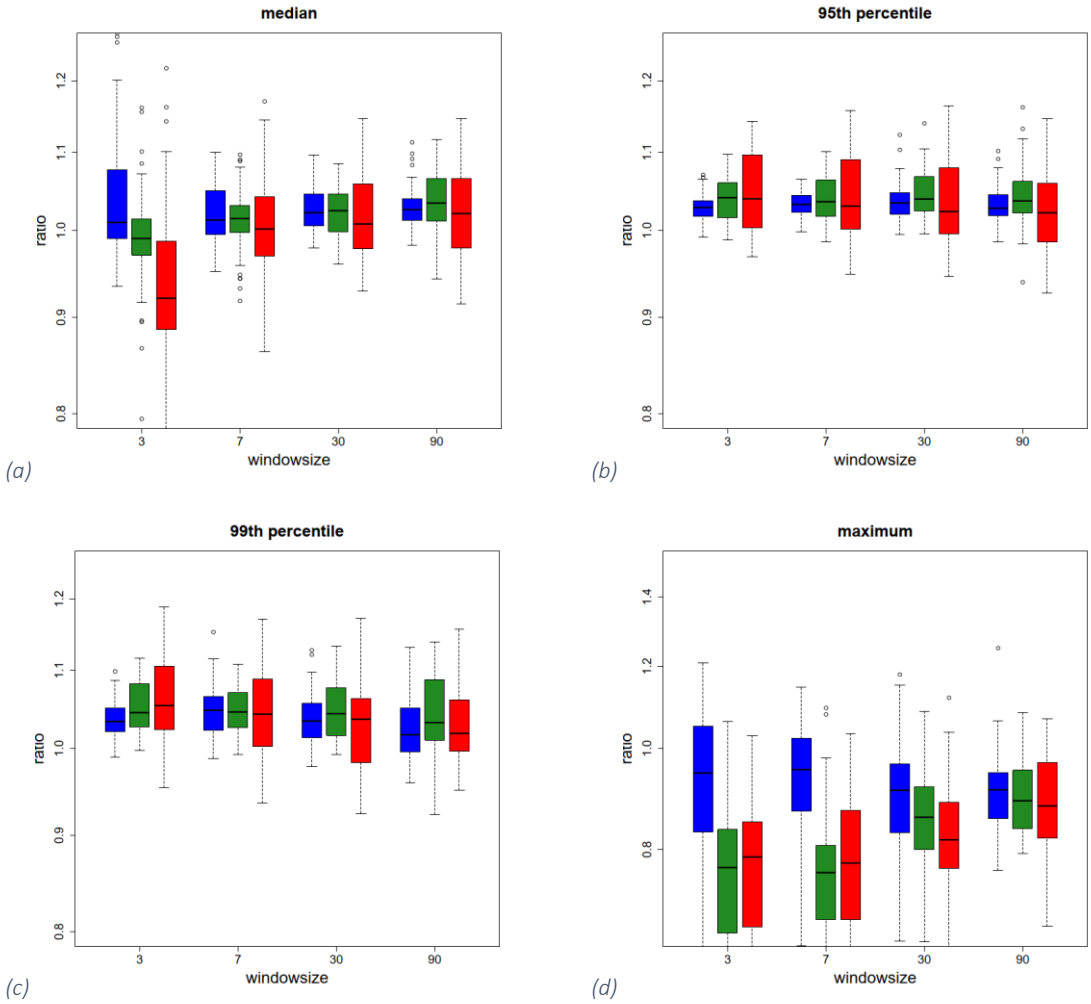

Figure 43 - Boxplots of the ratio of the median (a), 95th percentile (b), 99th percentile (c) and maximum (d) every box represents each one of the time period analyzed for the mean of the ten CH2018 simulation for each scenario for the period 2061-2099 and the mean of the ten CH2018 simulation for the same scenario for the period 2061 – 2099 between 1981 and 2020 (i.e. mean of RCP2.6 simulations in 2061 – 2099 over the mean of RCP2.6 simulation in 1981-2020 and so on). The results for the RCP2.6 are presented in blue, green for RCP4.5 and red for RCP8.5. A value of 1 indicates that the statistic is the same for the observed and model data, values below 1 indicate that the CH2018 simulations underestimate the data, while the values above 1 indicate an overestimation.

The ratio between the results of the analyzed statistical variables for F2 and PC is presented in Figure 43. The value 1indicates the perfect overlap of the results for the two periods F2 and PC. It can be seen that in general the interquartile range (IQR) for scenario 8.5 is wider than for the other two scenarios. Exceptions are the 3- and 7-day time windows of the maxima analysis.

The median (Figure 43.a) shows a slight tendency for the data to be overestimated for time windows greater than 3 days. In contrast, the 3 days are slightly overestimated for RCP2.6; they have good overlap for RCP4.5, while being underestimated by RCP8.5. IQR values are consistent with those of the standard deviations indicated by the error bars in the correlation plots.

The 95th and 99th percentiles show similar trends, with the 99th percentile being slightly more overlapping for the 30-day time window. In addition, both RCP2.6 and RCP4.5 have a higher IQR.

The maxima, on the other hand, are generally underestimated except for the 3- and 7-day time windows for RCP2.6, which has good overlap in results. In addition, the IQR of RCP8.5 is slightly higher than the other two scenarios, except for the 30-day time window.

Turning to the spatial analysis, regarding the median (Appendix Figures 72, 73, 74 for RCP2.6, 4.5 and 8.5 respetively), separate considerations must be made for each scenario since they have different trends.

Starting with RCP2.6, first, the impact of topography is evident in each time window analyzed. The estimate for the shorter time windows has a tendency to underestimate areas north of the Alps and overestimate areas to the south. The exceptions are the northeastern areas where the estimate remains around 1, indicating a perfect overlap of results. Longer time windows have good estimates for areas north of the alps, but overestimate areas to the south.

The impact of topography for RCP4.5, on the other hand, is less clear. The 3-day time window underestimates the PC results almost everywhere, except in canton Graubünden where there is a tendency to overestimate. In the 7 days window the underestimation is mainly confined to the canton Ticino. Graubünden is always overestimated but in the rest of Switzerland the overestimation is slight or even in line with the PC results. The time windows of 30 and 90 days follow the same trend as the 7 days, but in a milder way, the values are less high.

As for RCP8.5, there is little topographic impact for the 3-day time window. Except for Graubünden the whole territory is overestimated. The 7-day time window shows a hint with respect to the topographic impact. The alpine arc and Ticino are underestimated, Graubünden overestimated but in the rest of the territory the estimates are in line with the PC results. The 30 and 90 days time windows follow the trend of the 7 days time window but in a more pronounced way bringing the estimates outside the alpine arc and the canton Grisons from in line to overestimated.

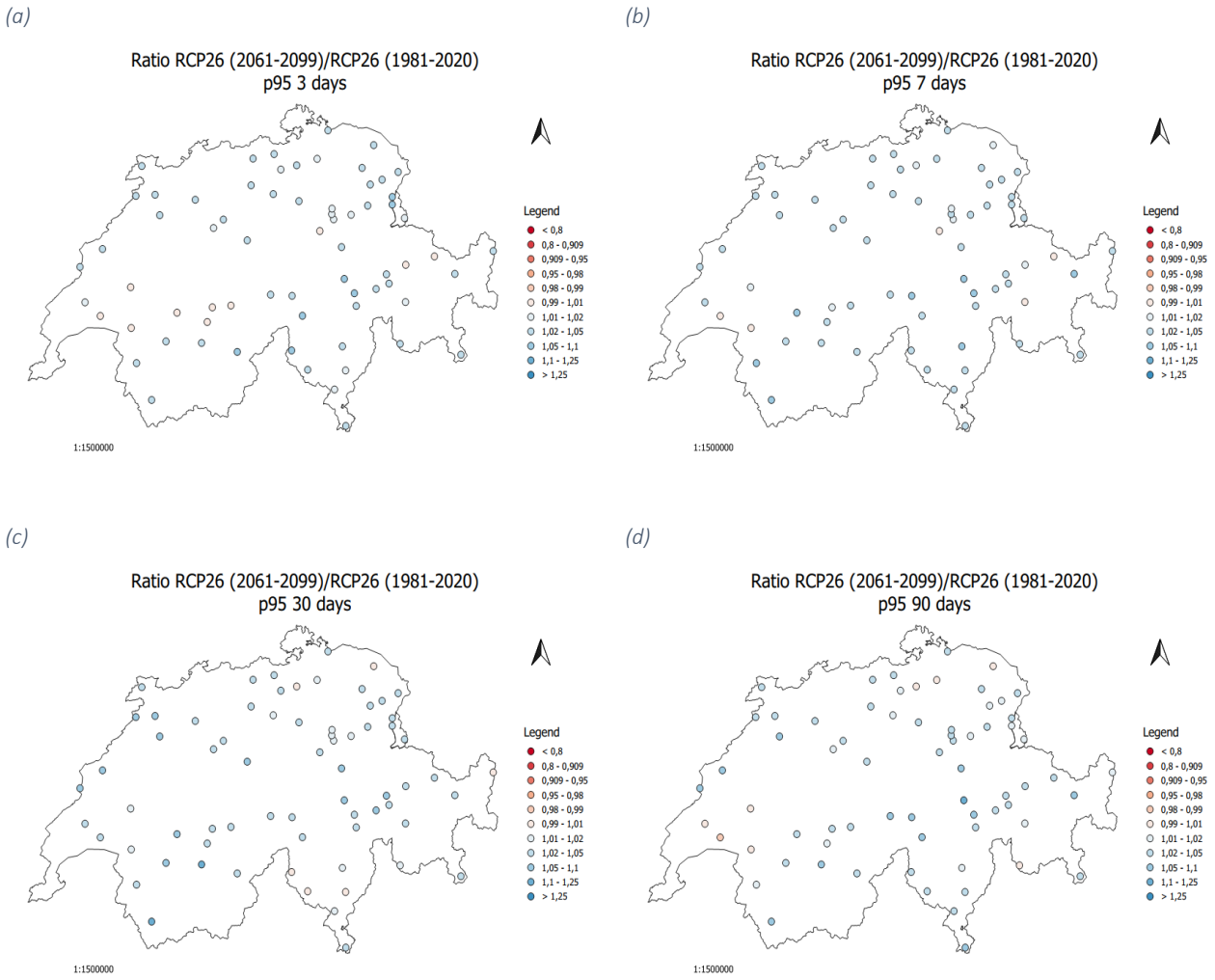

Figure 44 – Maps showing the ratio of the 95th percentile of the 3 (a), 7 (b), 30 (c) and 90 day precipitation (d) for the RCP2.6 scenario of the CH2018 simulations (mean of all ten models) for the period between 2061 and 2099 and the RCP2.6 scenario of the CH2018 simulation (mean of all ten models) for the control period (1981 – 2020). Values larger than 1 indicate an overestimation (blue) and values less than 1 an underestimation (red).

Regarding the 95th percentile RCP2.6 (Figure 44) does not show substantial differences between the various temporal windows nor spatial inclinations.

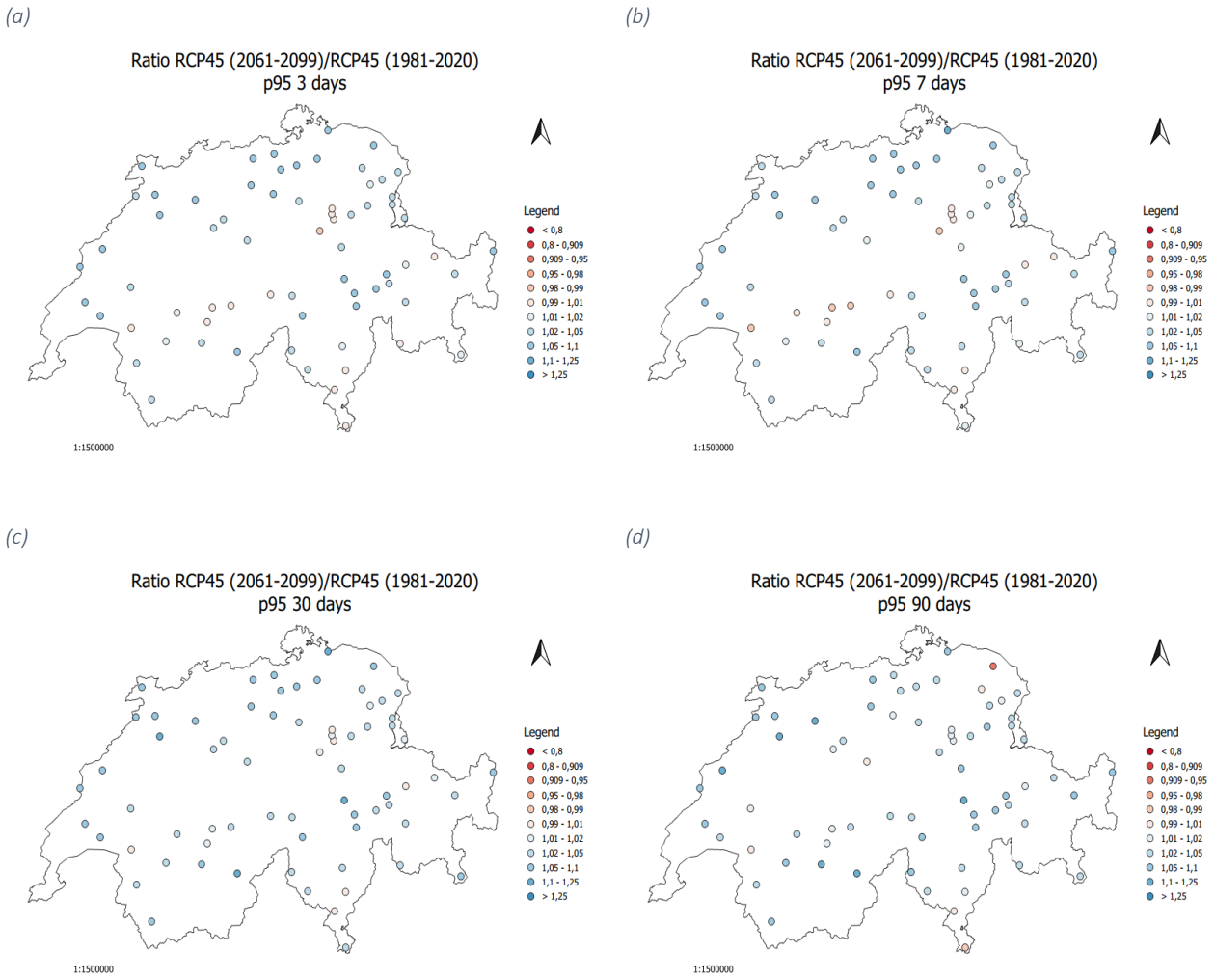

Figure 45 – Maps showing the ratio of the 95th percentile of the 3 (a), 7 (b), 30 (c) and 90 day precipitation (d) for the RCP4.5 scenario of the CH2018 simulations (mean of all ten models) for the period between 2061 and 2099 and the RCP4.5 scenario of the CH2018 simulation (mean of all ten models) for the control period (1981 – 2020). Values larger than 1 indicate an overestimation (blue) and values less than 1 an underestimation (red).

The 95th percentile for RCP 4.5 (Figure 45) shows a good estimate along the alpine arc while in the rest of the territory it presents a general overestimation. The difference for the different time windows is not substantial, the overestimation values are slightly higher for the long time windows (30 and 90 days).

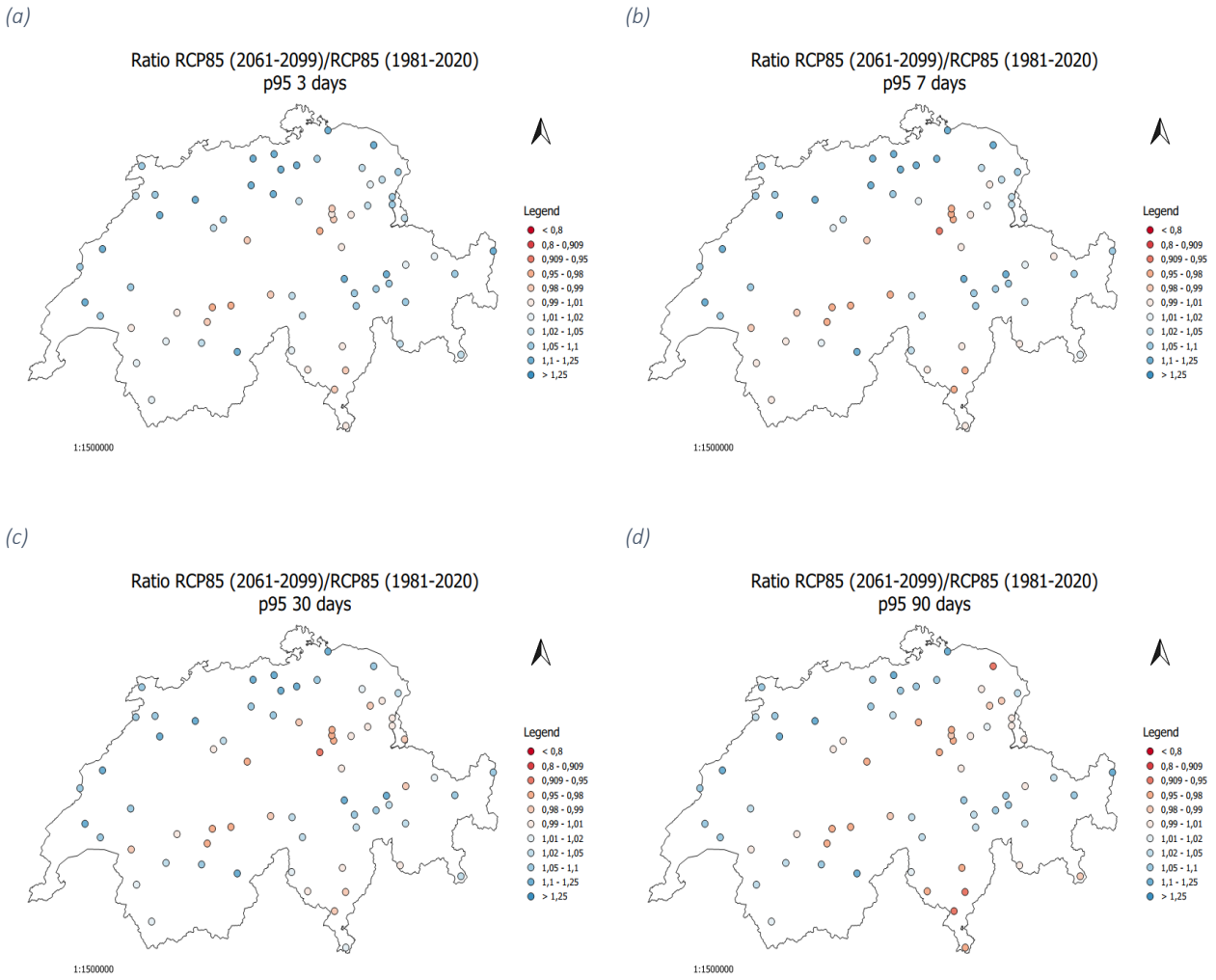

Figure 46 - Maps showing the ratio of the 95th percentile of the 3 (a), 7 (b), 30 (c) and 90 day precipitation (d) for the RCP8.5 scenario of the CH2018 simulations (mean of all ten models) for the period between 2061 and 2099 and the RCP8.5 scenario of the CH2018 simulation (mean of all ten models) for the control period (1981 – 2020). Values larger than 1 indicate an overestimation (blue) and values less than 1 an underestimation (red).

Finally, the analysis of the 95th percentile with respect to scenario 8.5 (Figure 46) shows an underestimation in the Alps and Ticino and an overestimation in the rest of the territory for all time windows. The overestimation in Ticino is more pronounced in the time windows of 7 and 90 days.

All in all, the Swiss territory analyzed for the 95th percentile shows an overestimation of the territory according to all scenarios. Exceptions are the Alps and Ticino where precipitation is in line with the PC for scenario 4.5 while scenario 8.5 underestimates it.

The next statistic in the analysis refers to the 99th percentile.

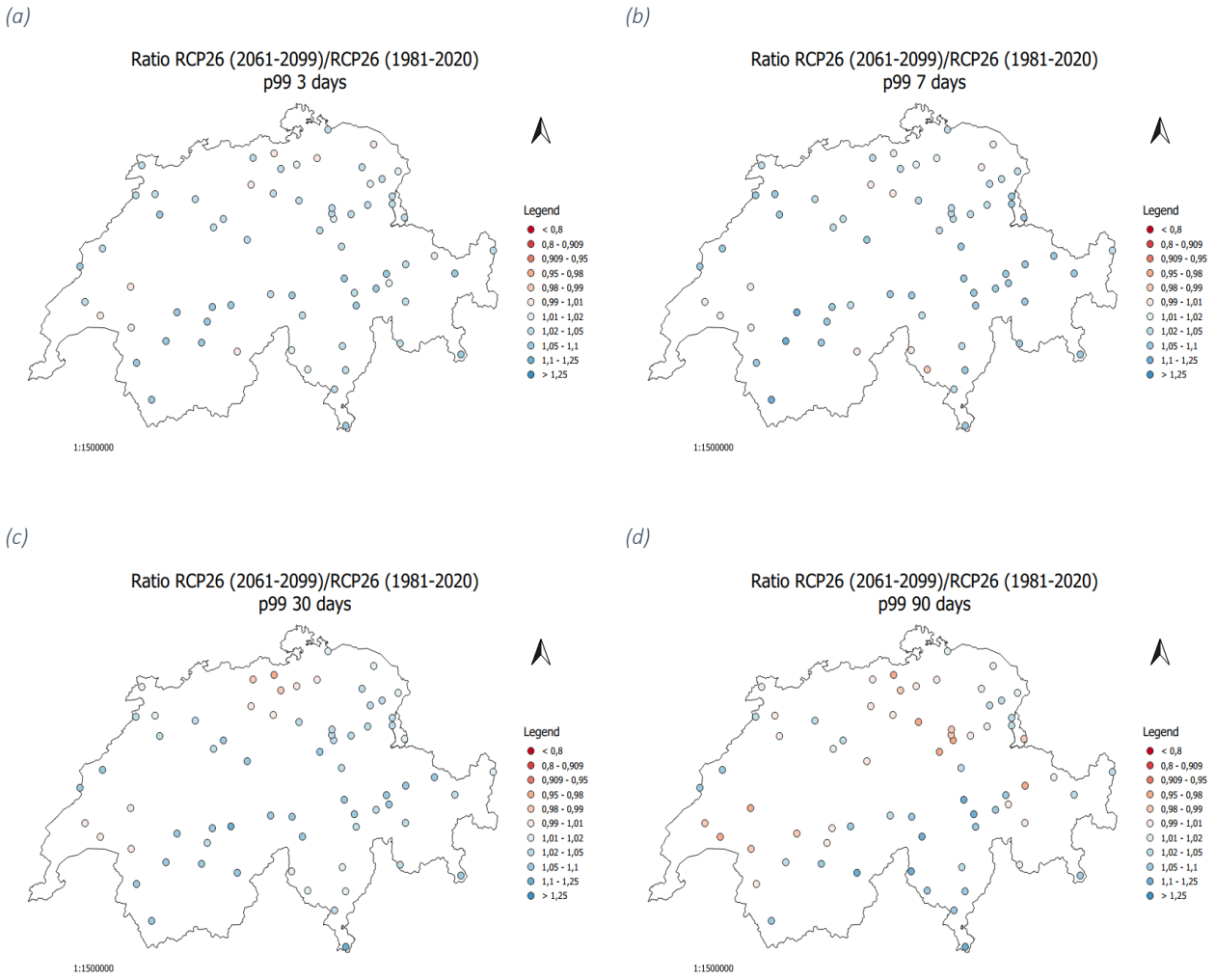

Figure 47 - Maps showing the ratio of the 99th percentile of the 3 (a), 7 (b), 30 (c) and 90 day precipitation (d) for the RCP2.6 scenario of the CH2018 simulations (mean of all ten models) for the period between 2061 and 2099 and the RCP2.6 scenario of the CH2018 simulation (mean of all ten models) for the control period (1981 – 2020). Values larger than 1 indicate an overestimation (blue) and values less than 1 an underestimation (red).

Figure 47 presents the spatial analysis for scenario 2.6. For the 3, 7 and 30 day time windows, some stations north of the alps and in Ticino show a slight tendency to be in line with the PC results, while the rest of Switzerland is overestimated. The 90 days time window is the only one with underestimates for some stations along the alpine range.

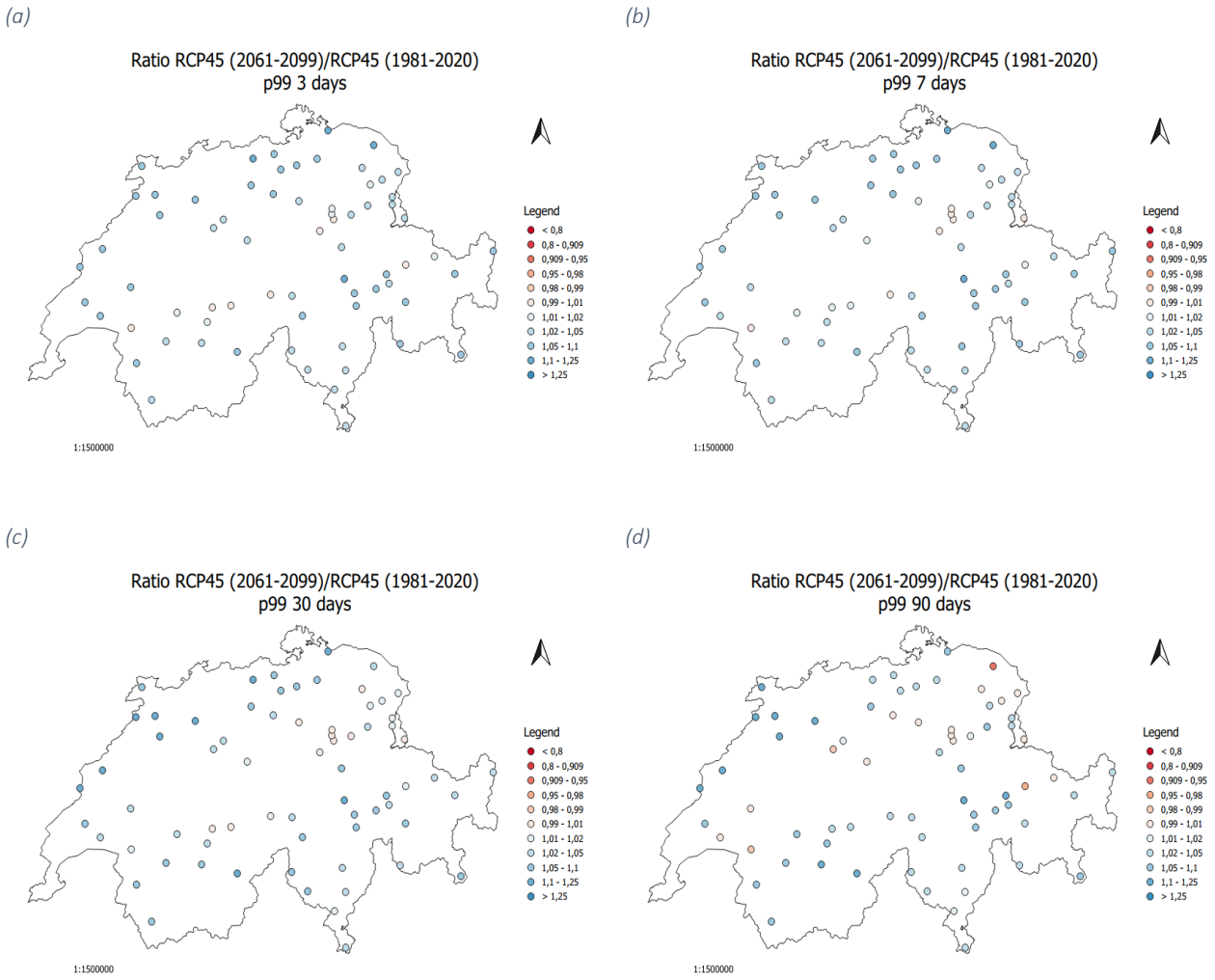

Figure 48 - Maps showing the ratio of the 99th percentile of the 3 (a), 7 (b), 30 (c) and 90 day precipitation (d) for the RCP4.5 scenario of the CH2018 simulations (mean of all ten models) for the period between 2061 and 2099 and the RCP4.5 scenario of the CH2018 simulation (mean of all ten models) for the control period (1981 – 2020). Values larger than 1 indicate an overestimation (blue) and values less than 1 an underestimation (red).

Figure 48 collects all the results of the spatial analysis of scenario 4.5 . The Alps for the most part are in line with the PC results while the rest of Switzerland is overestimated.

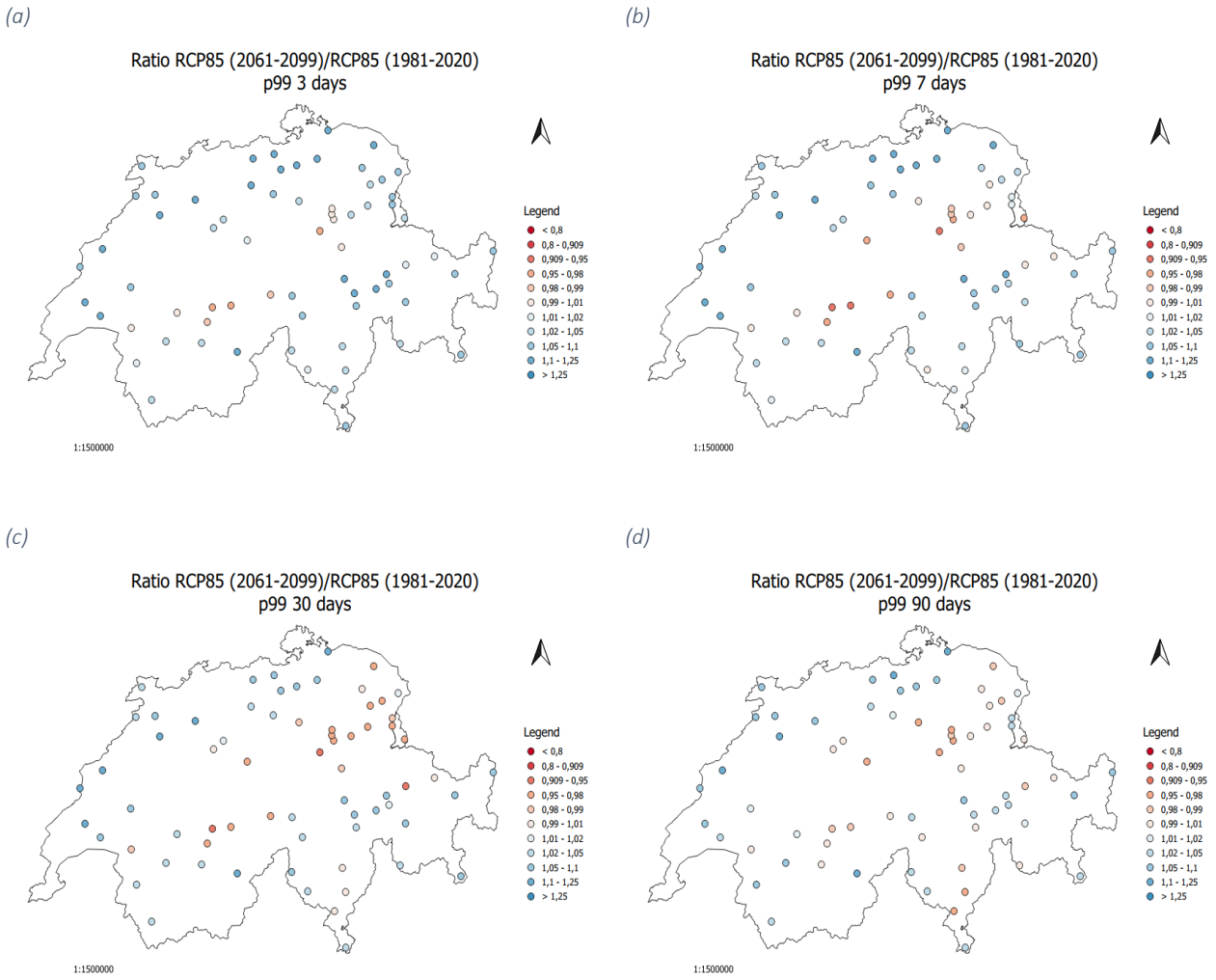

Figure 49 - Maps showing the ratio of the 99th percentile of the 3 (a), 7 (b), 30 (c) and 90 day precipitation (d) for the RCP8.5 scenario of the CH2018 simulations (mean of all ten models) for the period between 2061 and 2099 and the RCP8.5 scenario of the CH2018 simulation (mean of all ten models) for the control period (1981 – 2020). Values larger than 1 indicate an overestimation (blue) and values less than 1 an underestimation (red).

Finally, the spatial analysis of the RCP8.5 presented in Figure 49 shows a tendency to underestimate along the Alpine arc more pronounced for the time windows of 7 and 30 days. The rest of Switzerland on the other hand tends to overestimate the PC results.

Last, the spatial analysis for maxima. RCP2.6 presents an overestimation in the walensee area for the 3 and 7 days time windows while the rest of the territory is mostly underestimated with some exceptions where the results are in line with the PC. The 30 and 90 days time windows are generally underestimated except for Ticino where the trend is of overestimation.

RCP4.5 presents instead an underestimation of the whole territory, with few exceptions of results in line with the PC. These exceptions are more visible for long time windows.

For RCP8.5 the same considerations made for RCP4.5 apply.

5 Discussion

Expectations for PC are that of a general underestimation of SMN data, since the tendency of models is to underestimate the frequency of clustering (Leckebusch et al., 2008).

Expectations for F1 and F2, on the other hand, are dependent on the constraints of each scenario. For RCP2.6 being the scenario that foresees the decrease of greenhouse gases in order to keep the global temperature increase below 2 °C, it is expected that the simulations present lower values than the precipitation analyzed during the PC or at least are in line with it, resulting in an underestimation. This is mainly due to the fact that the trend of extreme precipitation in the past is not particularly displayed, i.e. the analysis of the history of extreme precipitation does not present these events in a significant way and for this reason also in the future it can be expected that these events are not expressed. Additionally, even if it is a long shot one could assume that with the decrease in greenhouse gases and global temperature more or less at the same temperatures today that the trend of increasing extremes of events would remain unchanged or at least not increase dramatically. On the other hand, talking about RCP4.5 scenario, being a scenario that foresees a decrease in greenhouse gases but without being able to maintain the increase in global warming below 2° C, it is expected that the trend of extreme events tends to increase as suggested by the literature (which records an increase in the trend for some years). What is expected is then a trend like the analysis for the past with a slight tendency to mitigate the underestimation expected for RCP2.6, while for the scenario RCP8.5, which involves unabated conditions, regarding the decrease of greenhouse gases is expected that the model overestimates the one in the control period. It must also be taken into account that even if the changes in GHG emission management differ, the effects will still be somewhat delayed compared to the decision, i.e. the effects described above are likely to be only slightly detectable.

5.1 Historic data

The results of multi-day precipitation products for median values are shown to be more reliable for larger time windows (30 and 90 days): short time windows (3 and 7 days), do not effectively simulate extreme events that are becoming less rare in the last year (Huber at al., 2011). In fact, the median analysis, does not consider extreme events and has a good correlation with the PC observations. Correlation that increases as the time window analyzed increases.

Moreover, the chain model simulations show much more than what the real data present. The SMN observations in fact do not show particular spatial inclinations or inclinations in general, the precipitations are equally distributed over the whole territory with the same flow rates in millimeters, while for the 30 and 90 days simulations the impact of the Alpine arc is evident.

Extremes, on the other hand, are accurate despite the tendency of models to underestimate clustering frequency (Leckebusch et al., 2008).

The 95th percentile shows a good correlation between the observed data and the CH2018 chain model simulations, and unlike the median, the extremes are best visualized in the 90-day time window. It should be noted that the clearest spatial analysis pattern can be seen in the 30-day time window, where the effect of the Alps is more pronounced than in the 90-day time window.

The third statistical value, the ratio of the 99th percentile to the SMN network observation, is overall greater than one, this means that the chain model simulation slightly overestimates the actual data even though the correlation analysis for stations does not show the accuracy between data sets as for the 95th percentile; therefore, it can be concluded that the most extreme events are not perceived very well by the model simulations.

For the 3- and 90-day time windows, the spatial analysis shows that the simulations underestimate Ticino and the Neuchatel area while overestimating the Alps. Underestimation that extends to the entire north of Switzerland.

SMN observations of maxima show that the wider the time window, the less extreme precipitation is evident. However, in Ticino and the Walensee area the precipitation is slightly higher than in the rest of Switzerland.

In contrast, the spatial analysis of the chain simulations for the maxima presents a clearer spatial pattern based on a 30-day time window, while the other time windows show spatial inconsistencies.

5.2 Future

5.2.1 First future period (2021-2060)

In F1, according to CH2018 chain model simulations, there is a good correlation between the simulation results for the control period and those for F1. RCP4.5 has the highest standard deviation of all scenarios particularly for the short time window, the low value of the difference does not allow for further assumptions.

The spatial analysis of the simulated median for F1 is affected by topography particularly visible in the 30-day time window, where a fairly good estimate is seen over the Alpine arc and an overestimation over the rest of the territory. Overall, the difference between observed data and simulation outputs from the CH2018 chain model is not optimal for the median, meaning that even if future simulations agree with those from the control period, reliability is not ideal.

The 95th percentile analysis shows that the simulations are consistent with the past and are influenced by topography (more specifically of the Alps), except for RCP2.6 where the impact of topography is less evident.

However, the analyses for correlation between the two datasets are quite good for the 3-day time window, except for RCP2.6, which also shows good correlation over the 30-day time window.

From the future analysis there is a general overestimation for all scenarios, however the long time window has a better correlation than the short time window.

This pattern does not show up in the correlation analysis of the different stations taken individually, because even though the correlation is good, the standard deviation for the long time window is larger than in the short time window. In addition, the spatial distribution shows the impact of topography more visible for the long time window and particularly for RCP8.5.

On the other hand, from the analysis of future simulations, RCP2.6 is the only one with some differences in the arrangement of maxima that is not due to topography, as there are both overestimates and underestimates along the Alps. In eastern Switzerland, only the Walensee area, part of Graubünden near Ticino, and some stations located in the cantons of Valais and Neuchatel do not have overestimates.

This trend becomes less apparent when increasing the time window under analysis. The 90-day window shows a large overestimate and an unclear spatial distribution.

Scenario 4.5 shows slight predispositions for Ticino and Valais (three stations) visible on the 90 days but not visible on the other time windows, while the differences for scenario 8.5 are not visible because the maxima are always underestimated, and it is not possible to extrapolate a spatial distribution that could indicate if the simulation is effective.

5.2.2 Second future period (2061-2099)

The results of the multi-day precipitation products for the median values show good correlation although they show a slight overestimation of the results in the PC. Standard deviations are highest for RCP8.5, medium for RCP4.6, and small for RCP2.6.

Due the tendency to standardize the data, it is not surprising that the scenario 2.6 has a lower standard deviation since its constraints are designed to improve the situation of extreme events. RCP4.5 in fact presents values for the standard deviation between RCP2.6 and RCP8.5 having constraints similar to RCP2.6 but less drastic. RCP8.5, instead, presents the highest standard deviation of all because its constraints do not imply changes, reason why simulations on long time scale, having the simulations tendency to standardize data, are more distant from PC simulations.

The spatial analysis, on the other hand, shows trends with values that are too low to develop further hypotheses.

For the 95th and 99th percentiles in general, the SMN data are overestimated. Correlations are good and standard deviations are lower than the median.

Heavy rains are best simulated for long time windows (30 and 90 days) since they have more stations recording them. The spatial analysis for RCP2.6 does not show particular trends, RCP4.6 has a good estimate

over the Alps but in general overestimates the PC results, while RCP8.5 underestimates the Alps and Ticino and overestimates the rest of the territory.

The maxima as opposed to the other statistical variables are generally underestimated. The 3-, 7-, and 30-day time windows for RCP2.6 are closer to having a good estimate of the PC results. Standard deviations are quite high, particularly for the short time windows (3 and 7 days).

Finally, the spatial analysis for RCP2.6 overestimates Ticino and the Walensee area while underestimating all the rest of Switzerland. RCP4.5 and RCP8.5, on the other hand, have a general underestimation in the whole territory.

5.3 Cautions approach

Despite every best effort to have the most accurate outcome, it is impossible to avoid uncertainty. It occurs in the natural sciences, medicine, or computer science (Skeels et al., 2010). The knowledge we have about an object on the Earth's surface is always subject to some kind of uncertainty, whether it is about the object's location, its existence, or its description (Shi, 2010).

Moreover, besides the uncertainty and the most obvious limitations, such as error and statistical conjectures, mishandling of data or observer error, observational network resolution and instrumental issues may result in erroneous data for climate scenario, making also CH2018 data problematic for multi day precipitation estimations.

Scientific uncertainty, according to Jiang et al. (2016) is multifaceted and as an impact on the trustworthiness of climate projections since it involves is uncertainty in both scientific modeling and climate sensitivity. If formal detection and attribution assessments suggest that an observed change has been impacted by human activities and the projection is compatible with attribution, confidence in certain parts of the future climate change projection improves. However, a human first reaction might not yet have him urged from deniers of natural climate variability, in many cases especially at the regional scales included in this evaluation although it is projected to do so in the future. If the fundamental physical causes of changes are well understood confidence in such projection without attribution may still be strong under higher scenario.

Multiple variables contribute to scientific uncertainty (Wright et al., 2015). The first is parametric uncertainty, which refer to GCM ability to mimic processes on spatial or temporal scale that are smaller than they can resolve (Prudhomme et al., 2002). The second is structural uncertainty, which examines weather GCMs accurately represent all of the important physical processes that occur on scales that can resolve structural uncertainty, can develop when a process is not yet recognized, such as abrupt change processes, or when it is recognized but not well enough understood to be effectively described (Prudhomme et al., 2002). Third factor is climate sensitivity, which is the measurement of the planet's response to rising CO2 levels, defined as the change in equilibrium precipitation coast by a doubling of CO2 levels in the atmosphere

compared to preindustrial level (Mitchell, 1989). Finally, long term precipitation estimates are influenced by differences in emission throughout time (Groisman et al., 1999).

6 Conclusion

Precipitation data play an important role in getting a clearer view of future predictions of how the climate will evolve. Recent changes in the frequency of extreme events leads to an increasing need for predictions that are as accurate as possible in order to be able to make decision for their consequences or to warn the population in time. Until now, precipitation products have been mainly analyzed in terms of daily precipitation, but problematic events such as floods rather than droughts are the consequence of several consecutive days with or without rain. This raises the following questions: What is the reliability of climate models for Switzerland, in terms of different precipitation signatures and precipitation distributions, and since floods, respectively droughts often occur in response to long periods with and without precipitation, are the models able to correctly simulate extreme events with enough accuracy?

To answer these questions, an analysis was first conducted with past data, in order to verify the accuracy of the chain model simulations composing CH2018 by comparing the data with those obtained from SwissMetNet observations for the period 1981 to 2020 and further on by comparing the future outputs with the one from the period in which we have also the observations. In order to achieve the goal, the correlations between the two datasets have been studied using scatterplot and boxplot, moreover for two stations an analysis of the frequency distribution has been done to get an idea of how the extremes were perceived locally and finally the data have been analyzed also at spatial level to evaluate if the topography had some effect on the prediction of the simulations, i.e. areas better simulated than others.

The results of this analysis show how the simulations are not yet able to accurately predict extreme events, in fact they tend to standardize the data, you can get an idea of how rainfall will evolve, but not satisfactorily to prevent disasters such as floods or droughts. The multi-day analysis turns out to optimize this lack of warning, since it turns out to monitor the sequence of days with precipitation (or lack of it) that are the discriminant for predicting problematic situations, in this particular work, related to precipitation (whether there are present or not).

Although these considerations are valid and can be used for future studies, the limitations of the work should not be forgotten. There are only 69 stations analyzed, the amount of data provided may therefore be a limitation to the overall understanding with respect to the low visibility of extreme data from the CH2018 simulations. Also, like many other data, those used for the work are surrounded by uncertainty. Therefore simulations for describing weather events are an ongoing process and they are constantly reviewed with studies and research.

In conclusion, beside its challenges and careful approaches to read the results, this work shows that it is also worthwhile to do multi-day precipitation analysis. Their knowledge can help to improve the warning and prediction of extreme events that in recent years are becoming less and less rare. Moreover, it turns out

to be a valid solution to have an overview of the general trend of heavy rains and thus improve the management of their consequences, and possibly also make the reading of CH2018 more sensitive to the sequence of multiple rainy days or their absence.

6.1 Future work

Since this work was completed with a limited number of data a possible follow up of this work could be to redo the analysis with more data, for example start analyzing the most recent period in order to have more stations available. Also the integration with the outputs of the DATA-GRIDDED could be a possibility to enrich the results. Regarding the analysis, it could be possible to have a more detailed analysis of the simulated areas with less precision and maybe add the analysis of other meteorological factors in order to have a clearer view of the discriminants and have more warnings in the future to predict any extreme events. Moreover, for the different scenario it would be interesting to use different analysis for each scenario due their different constraints.

7 Literature

Addor, N. and Seibert, J., 2014. Bias correction for hydrological impact studies–beyond the daily perspective. Hydrological Processes, 28(17), pp.4823-4828.

AghaKouchak, A., Cheng, L., Mazdiyasni, O. and Farahmand, A., 2014. Global warming and changes in risk of concurrent climate extremes: Insights from the 2014 California drought. Geophysical Research Letters, 41(24), pp.8847-8852.

Allen, M.R. and Ingram, W.J., 2002. Constraints on future changes in climate and the hydrologic cycle. Nature, 419(6903), pp.228-232.

Alexander, L.V., Zhang, X., Peterson, T.C., Caesar, J., Gleason, B., Klein Tank, A.M.G., Haylock, M., Collins, D., Trewin, B., Rahimzadeh, F. and Tagipour, A., 2006. Global observed changes in daily climate extremes of temperature and precipitation. Journal of Geophysical Research: Atmospheres, 111(D5).

Anderson, G., Md Kootval, H.K., Kull, D.W., Clements, J., Consulting, S., Fleming, G., Éireann, M., Frei, T., Lazo, J.K., Letson, D. and Mills, B.K., 2015. Valuing weather and climate: Economic assessment of meteorological and hydrological services (No. 115204, pp. 1-308). The World Bank.

Aon Benfield, 2017. 2016 Annual global climate and catastrophe report. 72. Retrieved from http://thoughtleadership.aonbenfield.com/Documents/20170117-ab-if-annual-climate-catastrophe-report.pdf

Ayar, P.V., Vrac, M., Bastin, S., Carreau, J., Déqué, M. and Gallardo, C., 2016. Intercomparison of statistical and dynamical downscaling models under the EURO-and MED-CORDEX initiative framework: present climate evaluations. Climate dynamics, 46(3-4), pp.1301-1329.

Bader, S. and Bantle, H., 2004. Das Schweizer Klima im Trend: Temperatur-und Niederschlagsentwicklung 1864-2001. MeteoSchweiz.

Bader, S. and Fukutome, S., 2015. Milde und kalte Bergwinter. MeteoSchweiz.

Ban, N., Schmidli, J. and Schär, C., 2015. Heavy precipitation in a changing climate: Does short-term summer precipitation increase faster?. Geophysical Research Letters, 42(4), pp.1165-1172.

Bellprat, O., Kotlarski, S., Lüthi, D., De Elía, R., Frigon, A., Laprise, R. and Schär, C., 2016. Objective calibration of regional climate models: application over Europe and North America. Journal of Climate, 29(2), pp.819-838.

Beniston, M., Diaz, H. F., & Bradley, R. S., 1997. Climatic change at high elevation sites: an overview. Climatic Change, 36(3), 233–251. https://doi.org/10.1023/A:1005380714349

Beniston, M., Stephenson, D.B., Christensen, O.B., Ferro, C.A., Frei, C., Goyette, S., Halsnaes, K., Holt, T., Jylhä, K., Koffi, B. and Palutikof, J., 2007. Future extreme events in European climate: an exploration of regional climate model projections. Climatic change, 81(1), pp.71-95.

Boberg, F. and Christensen, J.H., 2012. Overestimation of Mediterranean summer temperature projections due to model deficiencies. Nature Climate Change, 2(6), pp.433-436.

Bosshard, T., Kotlarski, S., Zappa, M. and Schär, C., 2014. Hydrological climate-impact projections for the Rhine River: GCM–RCM uncertainty and separate temperature and precipitation effects. Journal of Hydrometeorology, 15(2), pp.697-713.

Buytaert, W., Vuille, M., Dewulf, A., Urrutia, R., Karmalkar, A. and Célleri, R., 2010. Uncertainties in climate change projections and regional downscaling in the tropical Andes: implications for water resources management. Hydrology and Earth System Sciences, 14(7), p.1247.

CH2018, 2018. CH2018 - Climate Scenarios for Switzerland, Technical Report. Zurich: National Centre for Climate Services,Zürich,271pp. ISBN 978-3-9525031-4-0.

Collins, M., AchutaRao, K., Ashok, K., Bhandari, S., Mitra, A.K., Prakash, S., Srivastava, R. and Turner, A., 2013. Observational challenges in evaluating climate models. Nature Climate Change, 3(11), pp.940-941.

Dai, A., and J. Slingo, 1999: Diurnal and semidiurnal variations in global surface wind and divergence fields. J. Geophys. Res. Atmos., 104, 31 109–31 125, https://doi.org/10.1029/ 1999JD900927

Ebert, E.E. and McBride, J.L., 2000. Verification of precipitation in weather systems: Determination of systematic errors. Journal of hydrology, 239(1-4), pp.179-202.

Eden, J.M., Widmann, M., Maraun, D. and Vrac, M., 2014. Comparison of GCM-and RCM-simulated precipitation following stochastic postprocessing. Journal of Geophysical Research: Atmospheres, 119(19), pp.11-040.

Edwards, P.N., 2011. History of climate modeling. Wiley Interdisciplinary Reviews: Climate Change, 2(1), pp.128-139.

Flato, G., Marotzke, J., Abiodun, B., Braconnot, P., Chou, S.C., Collins, W., Cox, P., Driouech, F., Emori, S., Eyring, V. and Forest, C., 2014. Evaluation of climate models. In Climate change 2013: the physical science basis. Contribution of Working Group I to the Fifth Assessment Report of the Intergovernmental Panel on Climate Change (pp. 741-866). Cambridge University Press.

Frei, C., & Schär, C., 2001. Detection Probability of Trends in Rare Events: Theory and Application to Heavy Precipitation in the Alpine Region. Journal of Climate, 14(7), 1568–1584. https://doi.org/10.1175/1520-0442(2001)014<1568:DPOTIR>2.0.CO;2

Goody, R., Anderson, J., Karl, T., Miller, R. B., North, G., Simpson, J., & Washington, W. (2002). Why monitor the climate?. Bulletin of the American Meteorological Society, 83(6), 873-878.

Gordon, H.B., Whetton, P.H., Pittock, A.B., Fowler, A.M. and Haylock, M.R., 1992. Simulated changes in daily rainfall intensity due to the enhanced greenhouse effect: implications for extreme rainfall events. Climate Dynamics, 8(2), pp.83-102.

Groisman, P.Y., Karl, T.R., Easterling, D.R., Knight, R.W., Jamason, P.F., Hennessy, K.J., Suppiah, R., Page, C.M., Wibig, J., Fortuniak, K. and Razuvaev, V.N., 1999. Changes in the probability of heavy precipitation: important indicators of climatic change. In Weather and Climate Extremes (pp. 243-283). Springer, Dordrecht.

Hakala, K., Addor, N., Teutschbein, C., Vis, M., Dakhlaoui, H. and Seibert, J., 2019. Hydrological modeling of climate change impacts. Encyclopedia of water: Science, technology, and society, pp.1-20.

Huber, D.G. and Gulledge, J., 2011. Extreme weather and climate change: Understanding the link, managing the risk. Arlington: Pew Center on Global Climate Change.

Jain, S.K., Singh, V.P., 2003. Water resources systems planning and management. Elsevier.

Jiang, D., Tian, Z. and Lang, X., 2016. Reliability of climate models for China through the IPCC Third to Fifth Assessment Reports. International Journal of Climatology, 36(3), pp.1114-1133.

Jones, B. (2021). Torrential rain causes flooding and landslides in Japan. https://www.theguardian.com/weather/2021/aug/19/torrential-rain-causes-flooding-and-landslides-in-japan. [13.09.2021]

Katz, R.W. and Brown, B.G., 1992. Extreme events in a changing climate: variability is more important than averages. Climatic change, 21(3), pp.289-302.

Kay, A.L., Davies, H.N., Bell, V.A. and Jones, R.G., 2009. Comparison of uncertainty sources for climate change impacts: flood frequency in England. Climatic change, 92(1-2), pp.41-63.

Kendon, E.J., Ban, N., Roberts, N.M., Fowler, H.J., Roberts, M.J., Chan, S.C., Evans, J.P., Fosser, G. and Wilkinson, J.M., 2017. Do convection-permitting regional climate models improve projections of future precipitation change?. Bulletin of the American Meteorological Society, 98(1), pp.79-93.

Kilsby, C.G., Cowpertwait, P.S.P., O'connell, P.E. and Jones, P.D., 1998. Predicting rainfall statistics in England and Wales using atmospheric circulation variables. International Journal of Climatology: A Journal of the Royal Meteorological Society, 18(5), pp.523-539.

Kothavala, Z., 1997. Extreme precipitation events and the applicability of global climate models to the study of floods and droughts. Mathematics and computers in simulation, 43(3-6), pp.261-268.

Kotlarski, S. and Rajczak, J., 2018. Documentation of the localized CH2018 datasets. Transient Daily Time Series at the Local Scale: DAILY-LOCAL, DAILY-GRIDDED. Version, 1.

Lafon, T., Dadson, S., Buys, G. and Prudhomme, C., 2013. Bias correction of daily precipitation simulated by a regional climate model: a comparison of methods. International Journal of Climatology, 33(6), pp.1367-1381.

Leckebusch, G.C., Weimer, A., Pinto, J.G., Reyers, M. and Speth, P., 2008. Extreme wind storms over Europe in present and future climate: a cluster analysis approach. Meteorologische Zeitschrift, 17(1), pp.67-82.

Lendvai, A., Ranzi, R. and Peretti, G., 2014. Misura delle precipitazioni nevose mediante i pluviometri. AINEVA–Neve e Valanghe, 84, pp.12-21.

Luo, L., Wood, E.F. and Pan, M., 2007. Bayesian merging of multiple climate model forecasts for seasonal hydrological predictions. Journal of Geophysical Research: Atmospheres, 112(D10).

Mailhot, A., Kingumbi, A., Talbot, G. and Poulin, A., 2010. Future changes in intensity and seasonal pattern of occurrence of daily and multi-day annual maximum precipitation over Canada. Journal of Hydrology, 388(3-4), pp.173-185.

Maraun, D., Shepherd, T.G., Widmann, M., Zappa, G., Walton, D., Gutiérrez, J.M., Hagemann, S., Richter, I., Soares, P.M., Hall, A. and Mearns, L.O., 2017. Towards process-informed bias correction of climate change simulations. Nature Climate Change, 7(11), pp.764-773.

MeteoSwiss, 2021. Available from: https://www.meteosvizzera.admin.ch/home/tempo/termini-meteo/precipitazioni.html [12.09.2021]

Mishra, V., Kumar, D., Ganguly, A.R., Sanjay, J., Mujumdar, M., Krishnan, R. and Shah, R.D., 2014. Reliability of regional and global climate models to simulate precipitation extremes over India. Journal of Geophysical Research: Atmospheres, 119(15), pp.9301-9323.

Moron, V., Barbero, R., Evans, J.P., Westra, S. and Fowler, H.J., 2019. Weather types and hourly to multiday rainfall characteristics in tropical Australia. Journal of Climate, 32(13), pp.3983-4011.

Manabe, S., Wetherald, R.T. and Stouffer, R.J., 1981. Summer dryness due to an increase of atmospheric CO 2 concentration. Climatic Change, 3(4), pp.347-386.

Mitchell, J.F., 1989. The "greenhouse" effect and climate change. Reviews of Geophysics, 27(1), pp.115-139.

National Centre for Atmospheric Science, 2020. Available from: https://ncas.ac.uk/learn/what-is-a-climate-model/ [31.08.2021]

National Research Council, 2011. Advancing the science of climate change. National Academies Press.

Neelin, J.D., 2010. Climate change and climate modeling. Cambridge University Press.

Prein, A.F. and Gobiet, A., 2017. Impacts of uncertainties in European gridded precipitation observations on regional climate analysis. International Journal of Climatology, 37(1), pp.305-327.

Prudhomme, C., Reynard, N. and Crooks, S., 2002. Downscaling of global climate models for flood frequency analysis: where are we now?. Hydrological processes, 16(6), pp.1137-1150.

QGIS.org, 2021. QGIS Geographic Information System. QGIS Association. http://www.qgis.org/.

Rind, D., Goldberg, R. and Ruedy, R., 1989. Change in climate variability in the 21st century. Climatic change, 14(1), pp.5-37.

RStudio Team (2021). RStudio: Integrated Development Environment for R. RStudio, PBC, Boston, MA URL http://www.rstudio.com/.

Sahoo, S.P. and Panda, K.C., 2020. Prediction of Climate Change Using Statistical Downscaling Techniques. In New Frontiers in Stress Management for Durable Agriculture (pp. 311-328). Springer, Singapore.

Santer, B.D., Taylor, K.E., Wigley, T.M., Penner, J.E., Jones, P.D. and Cubasch, U., 1995. Towards the detection and attribution of an anthropogenic effect on climate. Climate Dynamics, 12(2), pp.77-100.

Shi, W. (2010). Principles of Modeling Uncertainties in Spatial Data and Spatial Analysis. CRC Press.

Shine, K.P., Derwent, R.G., Wuebbles, D.J., Morcrette, J.J., Hougton, J., Jenkins, G. and Ephraums, J., 1990. Climate change: the IPCC scientific assessment. Cambridge University. London.

Skeels, M., Lee, B., Smith, G., & Robertson, G. G. (2010). Revealing uncertainty for information visualization. In: Information Visualization, 9(1), S. 70-81.

Smith, J.B., Hulme, M., Jaagus, J., Keevallik, S., Mekonnen, A. and Hailemariam, K., 1998. Climate change scenarios. UNEP Handbook on Methods for Climate Change Impact Assessment and Adaptation Studies, 2, pp.3-1.

Sun, Q., Miao, C., Duan, Q., Ashouri, H., Sorooshian, S. and Hsu, K.L., 2018. A review of global precipitation data sets: Data sources, estimation, and intercomparisons. Reviews of Geophysics, 56(1), pp.79-107.

Trenberth, K.E., 2005. The impact of climate change and variability on heavy precipitation, floods, and droughts. Encyclopedia of hydrological sciences, 17.

Weisheimer, A. and Palmer, T.N., 2014. On the reliability of seasonal climate forecasts. Journal of the Royal Society Interface, 11(96), p.20131162.

Wilby, R.L., 2010. Evaluating climate model outputs for hydrological applications. Hydrological Sciences Journal–Journal des Sciences Hydrologiques, 55(7), pp.1090-1093.

Wilby, R.L. and Wigley, T.M., 1997. Downscaling general circulation model output: a review of methods and limitations. Progress in physical geography, 21(4), pp.530-548.

Wilhelm, B., Arnaud, F., Enters, D., Allignol, F., Legaz, A., Magand, O., et al., 2012. Does global warming favour the occurrence of extreme floods in European Alps? First evidences from a NW Alps proglacial lake sediment record. Climatic Change, 113(3), 563–581. https://doi.org/10.1007/s10584-011-0376-2

Woldemeskel, F.M., Sharma, A., Sivakumar, B. and Mehrotra, R., 2014. A framework to quantify GCM uncertainties for use in impact assessment studies. Journal of Hydrology, 519, pp.1453-1465.

Wood, A.W., Leung, L.R., Sridhar, V. and Lettenmaier, D.P., 2004. Hydrologic implications of dynamical and statistical approaches to downscaling climate model outputs. Climatic change, 62(1-3), pp.189-216.

Wright, A.N., Hijmans, R.J., Schwartz, M.W. and Shaffer, H.B., 2015. Multiple sources of uncertainty affect metrics for ranking conservation risk under climate change. Diversity and Distributions, 21(1), pp.111-122.

Yuan, X., Wood, E.F., Luo, L. and Pan, M., 2011. A first look at Climate Forecast System version 2 (CFSv2) for hydrological seasonal prediction. Geophysical research letters, 38(13).

Zhang, X., Zwiers, F.W., Li, G., Wan, H. and Cannon, A.J., 2017. Complexity in estimating past and future extreme short-duration rainfall. Nature Geoscience, 10(4), pp.255-259.

8 Appendix

CH2018 Simulation Name	*tas*	*tasmax*	*tasmin*	*pr*	*rsds*	*hurs*	*sfcWind*
CLMCOM-CCLM4_ECEARTH_EUR11_RCP45	X	X	X	X	X	X	
CLMCOM-CCLM4_ECEARTH_EUR11_RCP85	X	X	X	X	X	X	
CLMCOM-CCLM4_HADGEM_EUR11_RCP45	X	X	X	X	X	X	
CLMCOM-CCLM4_HADGEM_EUR11_RCP85	X	X	X	X	X	X	
CLMCOM-CCLM4_HADGEM_EUR44_RCP85	X	X	X	X	X	X	X
CLMCOM-CCLM4_MPIESM_EUR11_RCP45	X	X	X	X	X	X	
CLMCOM-CCLM4_MPIESM_EUR44_RCP45	X	X	X	X	X	X	
CLMCOM-CCLM4_MPIESM_EUR11_RCP85	X	X	X	X	X	X	
CLMCOM-CCLM4_MPIESM_EUR44_RCP85	X	X	X	X	X	X	
CLMCOM-CCLM5_ECEARTH_EUR44_RCP85	X	X	X	X	X	X	X
CLMCOM-CCLM5_MIROC_EUR44_RCP85	X	X	X	X	X	X	X
CLMCOM-CCLM5_MPIESM_EUR44_RCP85	X	X	X	X	X	X	X
CLMCOM-CCLM5_HADGEM_EUR44_RCP85	X	X	X	X	X	X	X
DMI-HIRHAM_ECEARTH_EUR11_RCP26	X	X	X	X	X	X	X
DMI-HIRHAM_ECEARTH_EUR11_RCP45	X	X	X	X	X	X	X
DMI-HIRHAM_ECEARTH_EUR44_RCP45	X	X	X	X	X	X	X
DMI-HIRHAM_ECEARTH_EUR11_RCP85	X	X	X	X	X	X	X
DMI-HIRHAM_ECEARTH_EUR44_RCP85	X	X	X	X	X	X	X
ICTP-REGCM_HADGEM_EUR44_RCP85	X	X	X	X	X		
KNMI-RACMO_ECEARTH_EUR44_RCP45	X	X	X	X	X	X	X
KNMI-RACMO_ECEARTH_EUR44_RCP85	X	X	X	X	X	X	X
KNMI-RACMO_HADGEM_EUR44_RCP26	X	X	X	X	X	X	X
KNMI-RACMO_HADGEM_EUR44_RCP45	X	X	X	X	X	X	X
KNMI-RACMO_HADGEM_EUR44_RCP85	X	X	X	X	X	X	X
MPICSC-REMO1_MPIESM_EUR11_RCP26	X	X	X	X	X	X	
MPICSC-REMO1_MPIESM_EUR44_RCP26	X	X	X	X	X	X	
MPICSC-REMO1_MPIESM_EUR11_RCP45	X	X	X	X	X	X	
MPICSC-REMO1_MPIESM_EUR44_RCP45	X	X	X	X	X	X	
MPICSC-REMO1_MPIESM_EUR11_RCP85	X	X	X	X	X	X	
MPICSC-REMO1_MPIESM_EUR44_RCP85	X	X	X	X	X	X	
MPICSC-REMO2_MPIESM_EUR11_RCP26	X	X	X	X	X	X	
MPICSC-REMO2_MPIESM_EUR44_RCP26	X	X	X	X	X	X	
MPICSC-REMO2_MPIESM_EUR11_RCP45	X	X	X	X	X	X	
MPICSC-REMO2_MPIESM_EUR44_RCP45	X	X	X	X	X	X	
MPICSC-REMO2_MPIESM_EUR11_RCP85	X	X	X	X	X	X	
MPICSC-REMO2_MPIESM_EUR44_RCP85	X	X	X	X	X	X	
SMHI-RCA_ECEARTH_EUR11_RCP26	X	X	X	X	X	X	X
SMHI-RCA_ECEARTH_EUR44_RCP26	X	X	X	X	X	X	X
SMHI-RCA_ECEARTH_EUR11_RCP45	X	X	X	X	X	X	X
SMHI-RCA_ECEARTH_EUR44_RCP45	X	X	X	X	X	X	X
SMHI-RCA_ECEARTH_EUR11_RCP85	X	X	X	X	X	X	X

CH2018 Simulation Name	*tas*	*tasmax*	*tasmin*	*pr*	*rsds*	*hurs*	*sfcWind*
SMHI-RCA_ECEARTH_EUR44_RCP85	X	X	X	X	X	X	X
SMHI-RCA_IPSL_EUR11_RCP45	X	X	X	X	X	X	X
SMHI-RCA_IPSL_EUR44_RCP45	X	X	X	X	X	X	X
SMHI-RCA_IPSL_EUR11_RCP85	X	X	X	X	X	X	X
SMHI-RCA_IPSL_EUR44_RCP85	X	X	X	X	X	X	X
SMHI-RCA_HADGEM_EUR44_RCP26	X	X	X	X	X	X	X
SMHI-RCA_HADGEM_EUR11_RCP45	X	X	X	X	X	X	X
SMHI-RCA_HADGEM_EUR44_RCP45	X	X	X	X	X	X	X
SMHI-RCA_HADGEM_EUR11_RCP85	X	X	X	X	X	X	X
SMHI-RCA_HADGEM_EUR44_RCP85	X	X	X	X	X	X	X
SMHI-RCA_MPIESM_EUR44_RCP26	X	X	X	X	X	X	X
SMHI-RCA_MPIESM_EUR11_RCP45	X	X	X	X	X	X	X
SMHI-RCA_MPIESM_EUR44_RCP45	X	X	X	X	X	X	X
SMHI-RCA_MPIESM_EUR11_RCP85	X	X	X	X	X	X	X
SMHI-RCA_MPIESM_EUR44_RCP85	X	X	X	X	X	X	X
SMHI-RCA_CCCMA_EUR44_RCP45	X	X	X	X	X	X	X
SMHI-RCA_CCCMA_EUR44_RCP85	X	X	X	X	X	X	X
SMHI-RCA_CSIRO_EUR44_RCP45	X	X	X	X	X	X	X
SMHI-RCA_CSIRO_EUR44_RCP85	X	X	X	X	X	X	X
SMHI-RCA_MIROC_EUR44_RCP26	X	X	X	X	X	X	X
SMHI-RCA_MIROC_EUR44_RCP45	X	X	X	X	X	X	X
SMHI-RCA_MIROC_EUR44_RCP85	X	X	X	X	X	X	X
SMHI-RCA_NORESM_EUR44_RCP26	X	X	X	X	X	X	X
SMHI-RCA_NORESM_EUR44_RCP45	X	X	X	X	X	X	X
SMHI-RCA_NORESM_EUR44_RCP85	X	X	X	X	X	X	X
SMHI-RCA_GFDL_EUR44_RCP45	X	X	X	X	X	X	X
SMHI-RCA_GFDL_EUR44_RCP85	X	X	X	X	X	X	X
TOTAL	68	68	68	68	67	47	68

Table 8 – EURO-CORDEX climate model used in CH2018 with their possible variables. The first column is the simplified CH2018 simulation identifier used in the CH2018 data files. The scheme follows the rule as [RCM]_[GCM]_[RESOLUTION]_[SCENARIO] (Kotlarski et al., 2018). [RCM] and [GCM] are the abbreviation taken by CH2018 for the CORDEX model names; [RESOLUTION] refers to the two possible spatial resolution, EUR11 and EUR44, with respectively 12 and 50 km and finally the [SCENARIO] stays for the three possible greenhouse gar scenario RCP2.6, RCP4.5 and RCP8.5. Moreover, "REMO1" and "REMO2" are the same GCM-RCM model chain but with different initial conditions. As far as the abbreviation for the meteorological variable covered by CH2018 see next table.

Variable name	Abbreviation	Unit
Daily mean 2m temperature	*tas*	°C
Daily maximum 2m temperature	*tasmax*	°C
Daily minimum 2m temperature	*tasmin*	°C
Daily precipitation sum	*pr*	mm/day
Daily mean global radiation	*rsds*	W/m2
Daily mean relative humidity	*hurs*	%
Daily mean near-surface wind speed	*sfcWind*	m/s

Table 9 - List of meteorological variables which CH2018 datasets DAILY-LOCAL and DAILY-GRIDDED includes and their unit.

8.1 Historic data

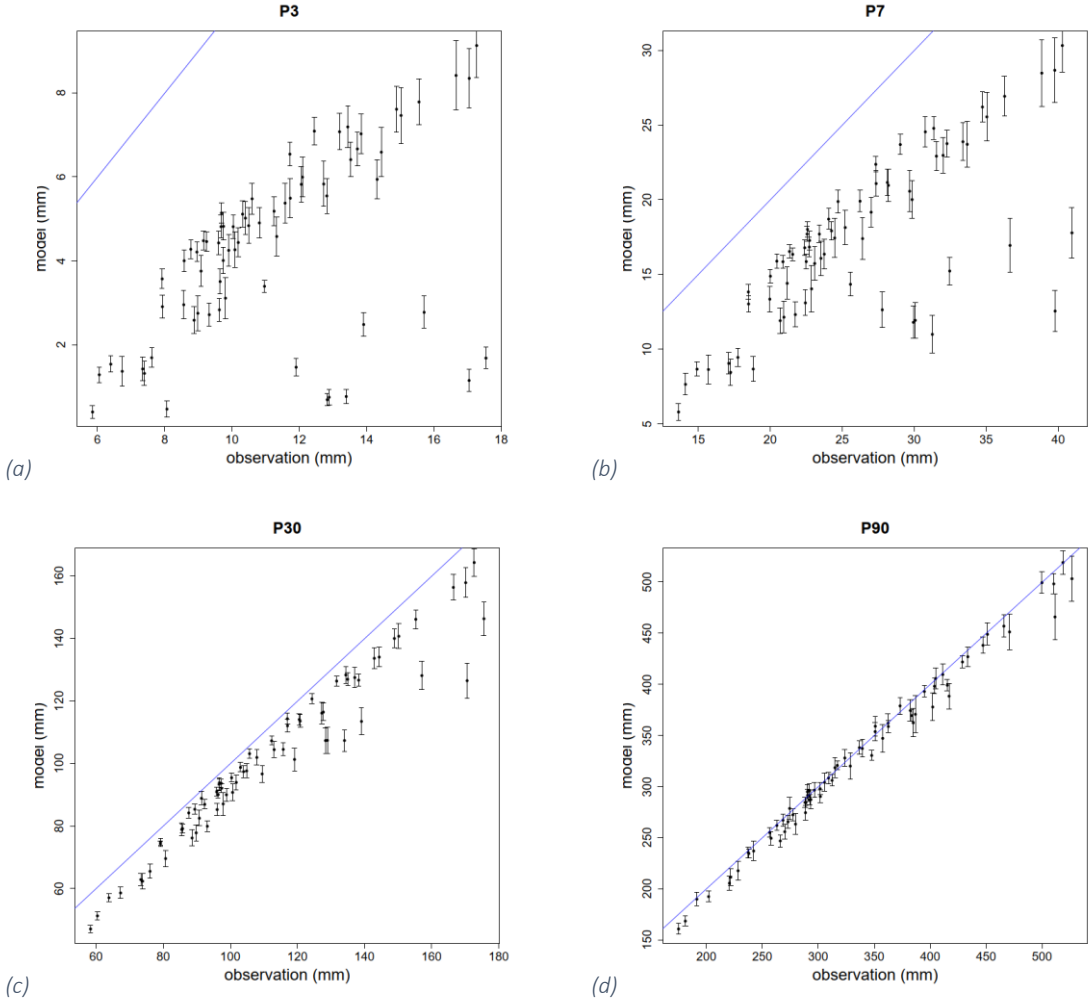

Figure 50 - Correlation of median or 50th percentile precipitation for the time windows of 3 (a), 7 (b), 30 (c) and 90 days precipitation (d) in millimeters for all 69 selected stations. for the period between 1981 and 2020. The blue line displays the 1:1 line between the two data sets while the error bars indicate the standard deviation of CH2018 different model results.

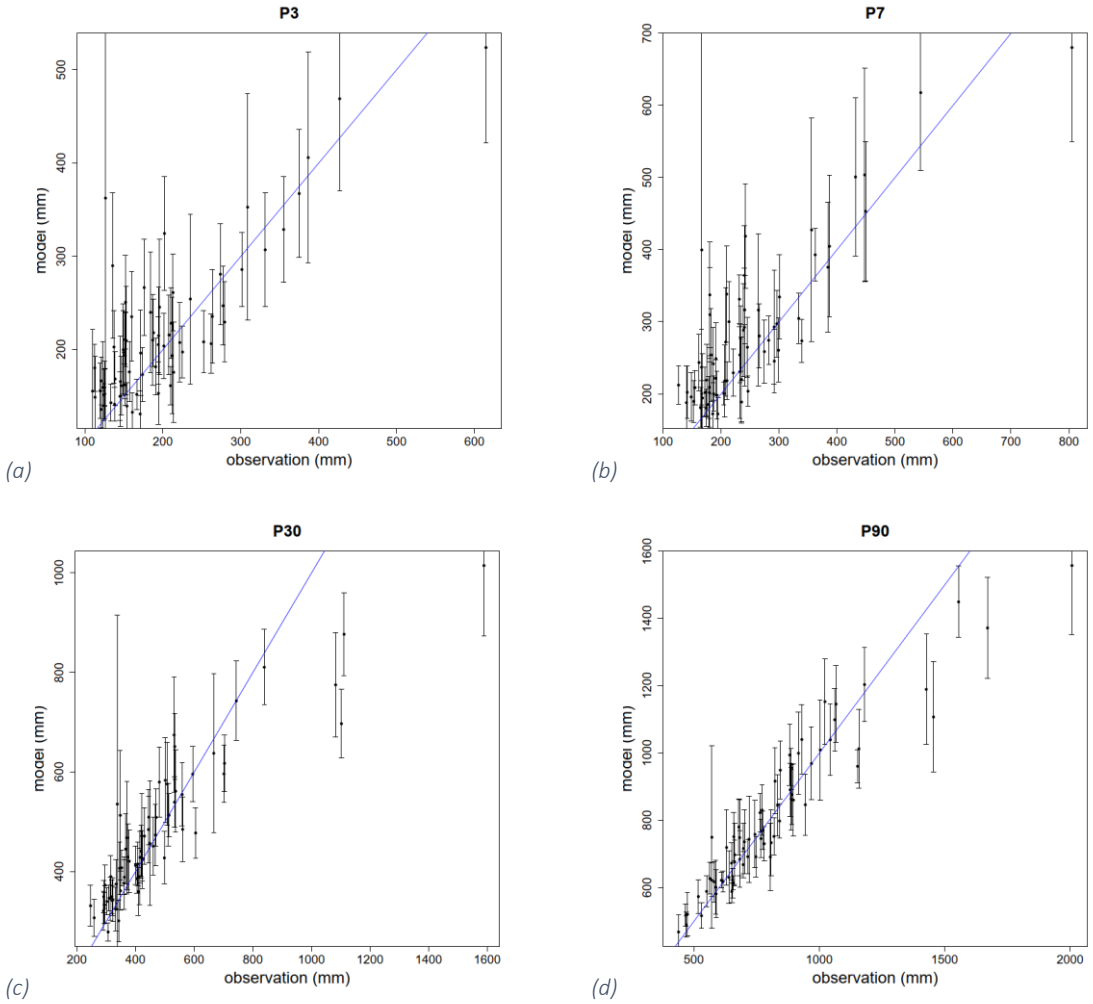

Figure 51 - Correlation between the maximum observed and simulated 3 (a), 7 (b), 30 (c) and 90 day precipitation (d) in millimeters for the 69 stations for the period between 1981 and 2020. The blue line displays the 1:1 line while the error bars indicate the standard deviation of the ten CH2018 model results.

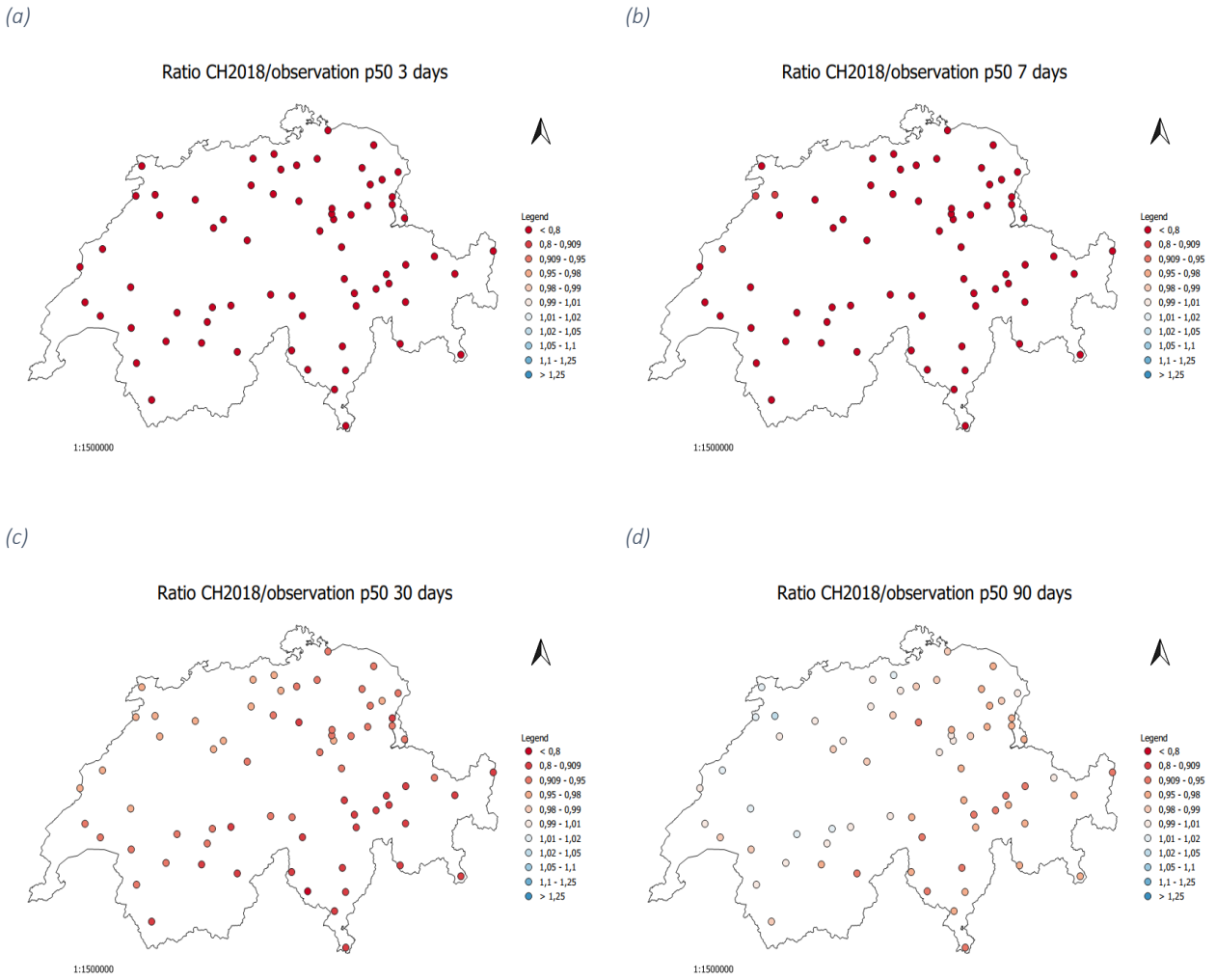

Figure 52 - Maps showing the ratio of the median of the 3 (a), 7 (b), 30 (c) and 90 day precipitation (d) for the CH2018 simulations (mean of all ten models) and the observations for the period between 1981 and 2020. Values larger than 1 indicate an overestimation (blue) and values less than 1 an underestimation (red).

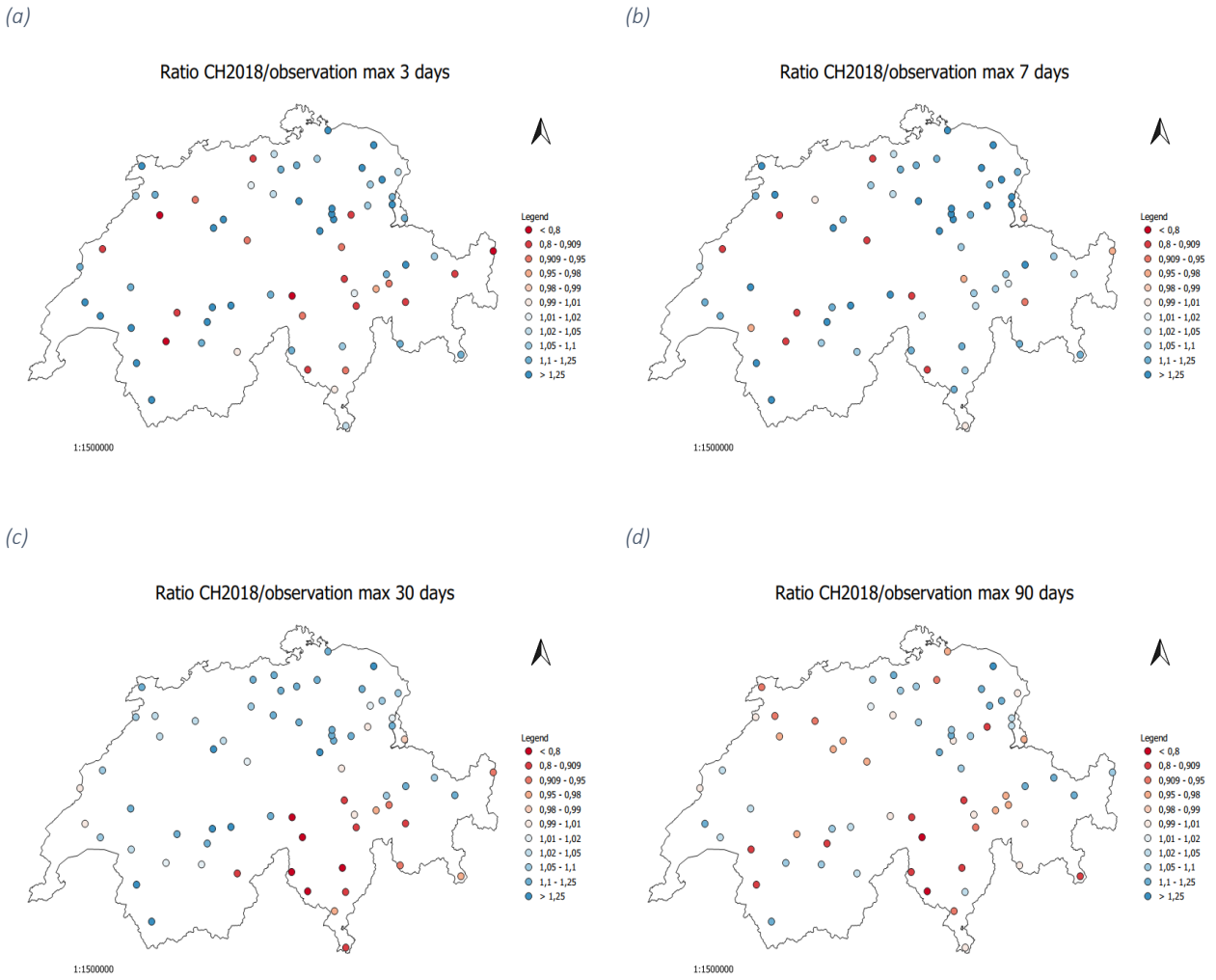

Figure 53 - Maps showing the ratio of the maximum 3 (a), 7 (b), 30 (c) and 90 day precipitation (d) for the CH2018 simulations (mean of all ten models) and the observations for the period between 1981 and 2020. Values larger than 1 indicate an overestimation (blue) and values less than 1 an underestimation (red).

8.2 First future period (2021-2060)

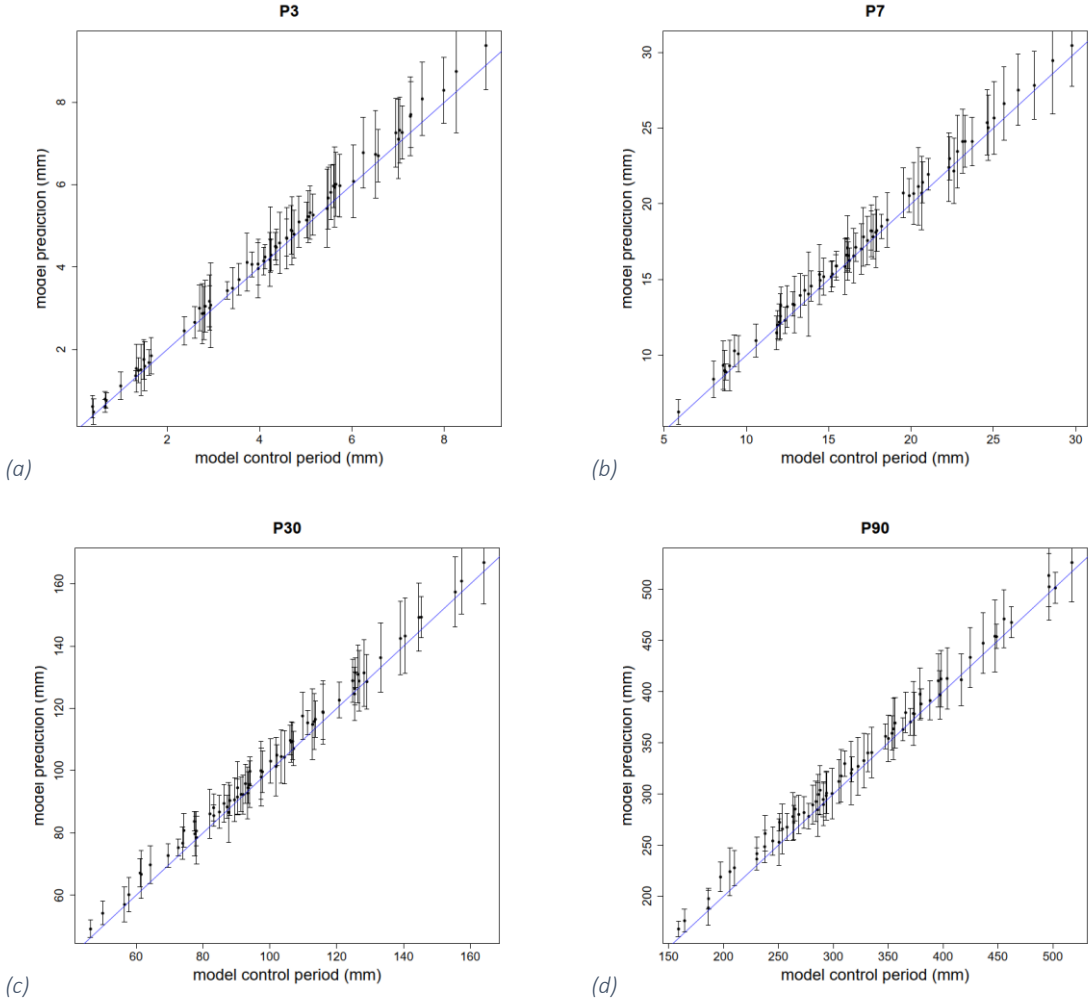

Figure 54 - Correlation between the mean of RCP2.6 (2021 – 2060) and RCP2.6 (1981 – 2020) of the 3 (a), 7 (b), 30 (c) and 90 day precipitation (d) in millimeters for the 69 stations analyzed. The blue line displays the 1:1 line while the error bars indicate the standard deviation of CH2018 model results.

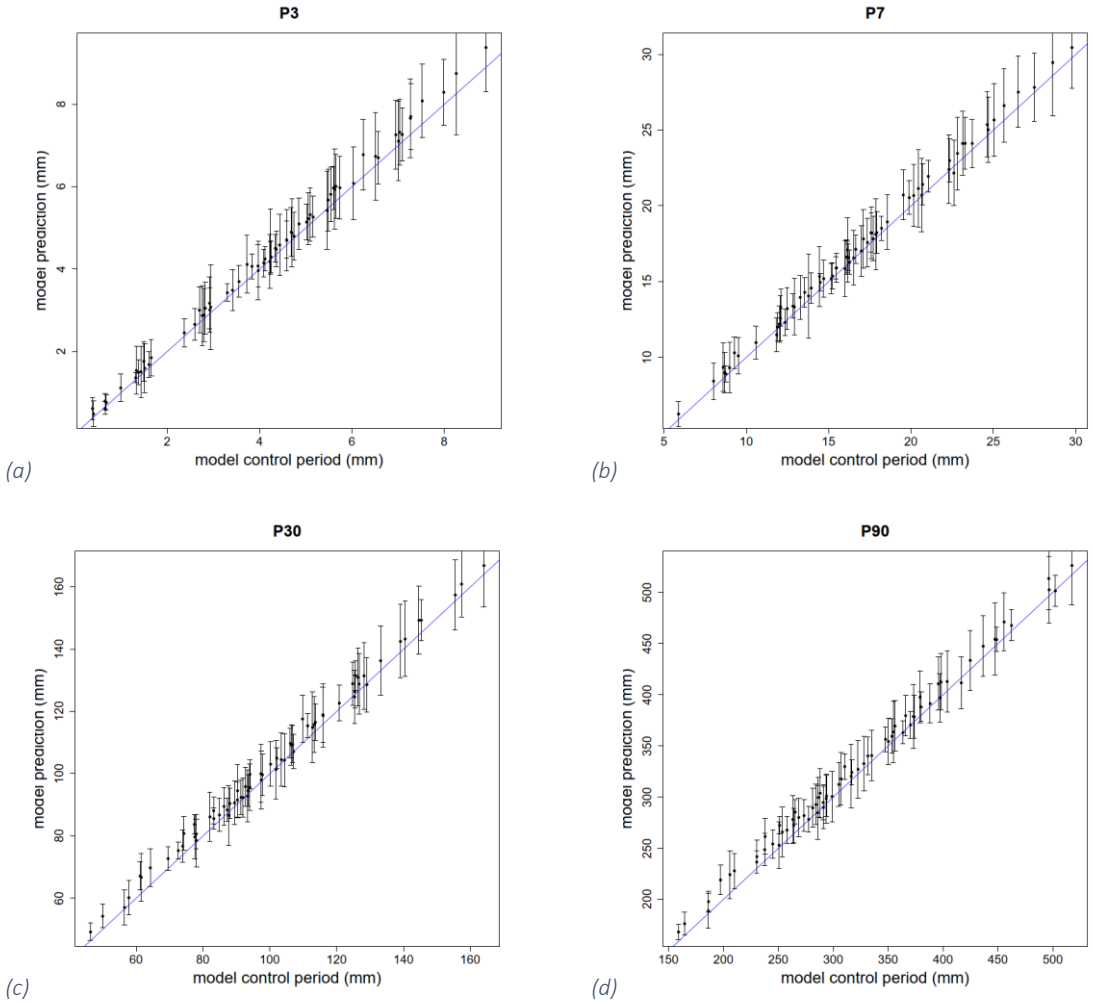

Figure 55 - Correlation between the mean of RCP4.5 (2021 – 2060) and RCP4.5 (1981 – 2020) of the 3 (a), 7 (b), 30 (c) and 90 day precipitation (d) in millimeters for the 69 stations analyzed. The blue line displays the 1:1 line while the error bars indicate the standard deviation of CH2018 model results.

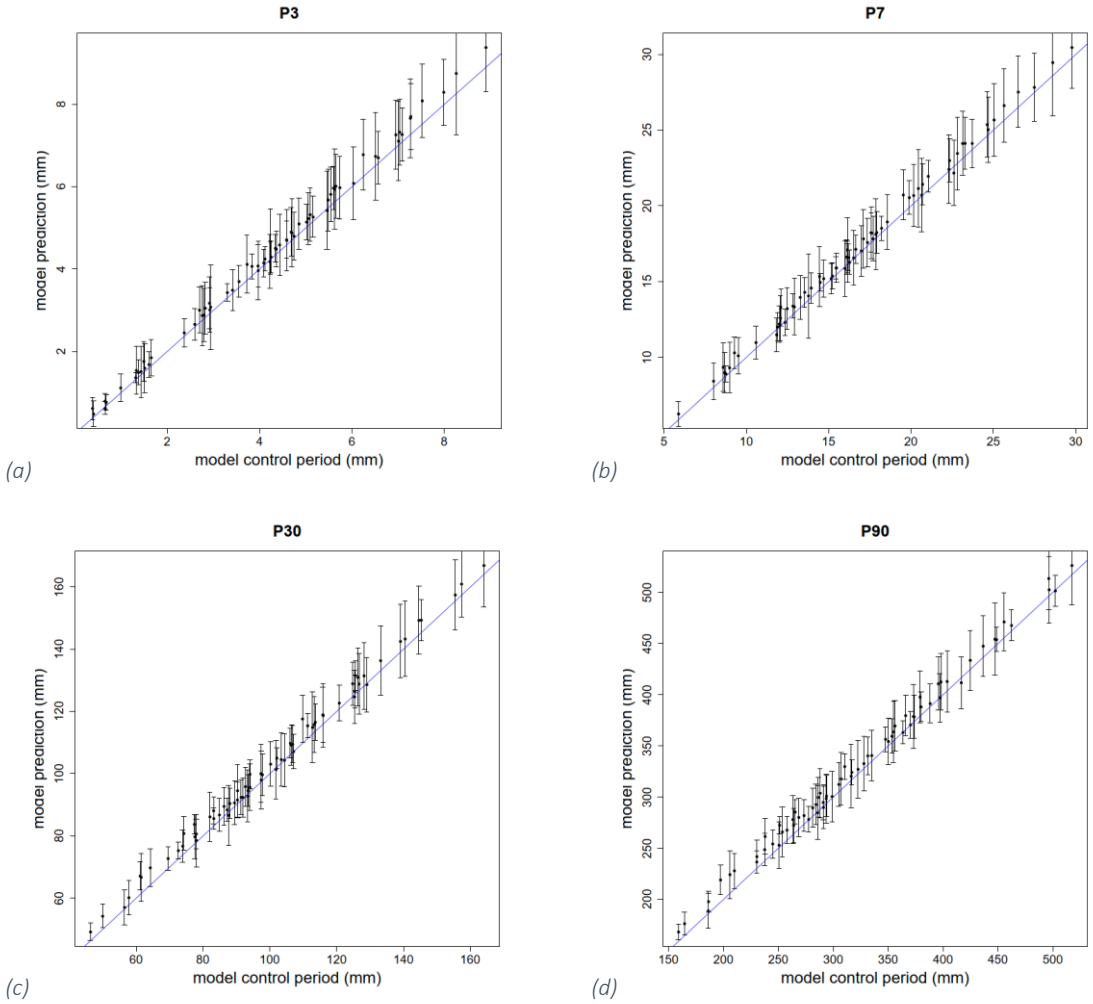

Figure 56 - Correlation between the mean of RCP8.5 (2021 – 2060) and RCP8.5 (1981 – 2020) of the 3 (a), 7 (b), 30 (c) and 90 day precipitation (d) in millimeters for the 69 stations analyzed. The blue line displays the 1:1 line while the error bars indicate the standard deviation of CH2018 model results.

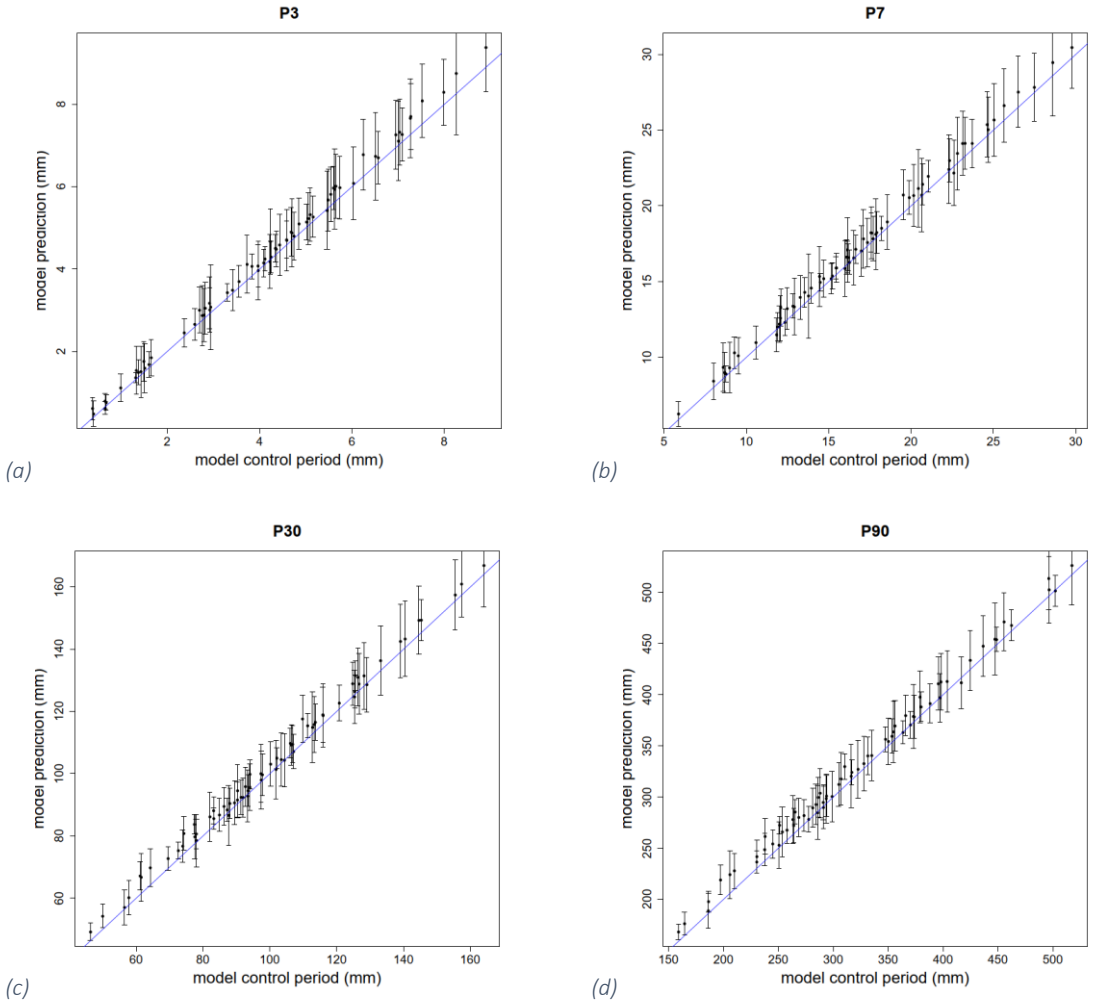

Figure 57 - Correlation between the maximum of RCP2.6 (2021 – 2060) and RCP2.6 (1981 – 2020) of the 3 (a), 7 (b), 30 (c) and 90 day precipitation (d) in millimeters for the 69 stations analyzed. The blue line displays the 1:1 line while the error bars indicate the standard deviation of CH2018 model results.

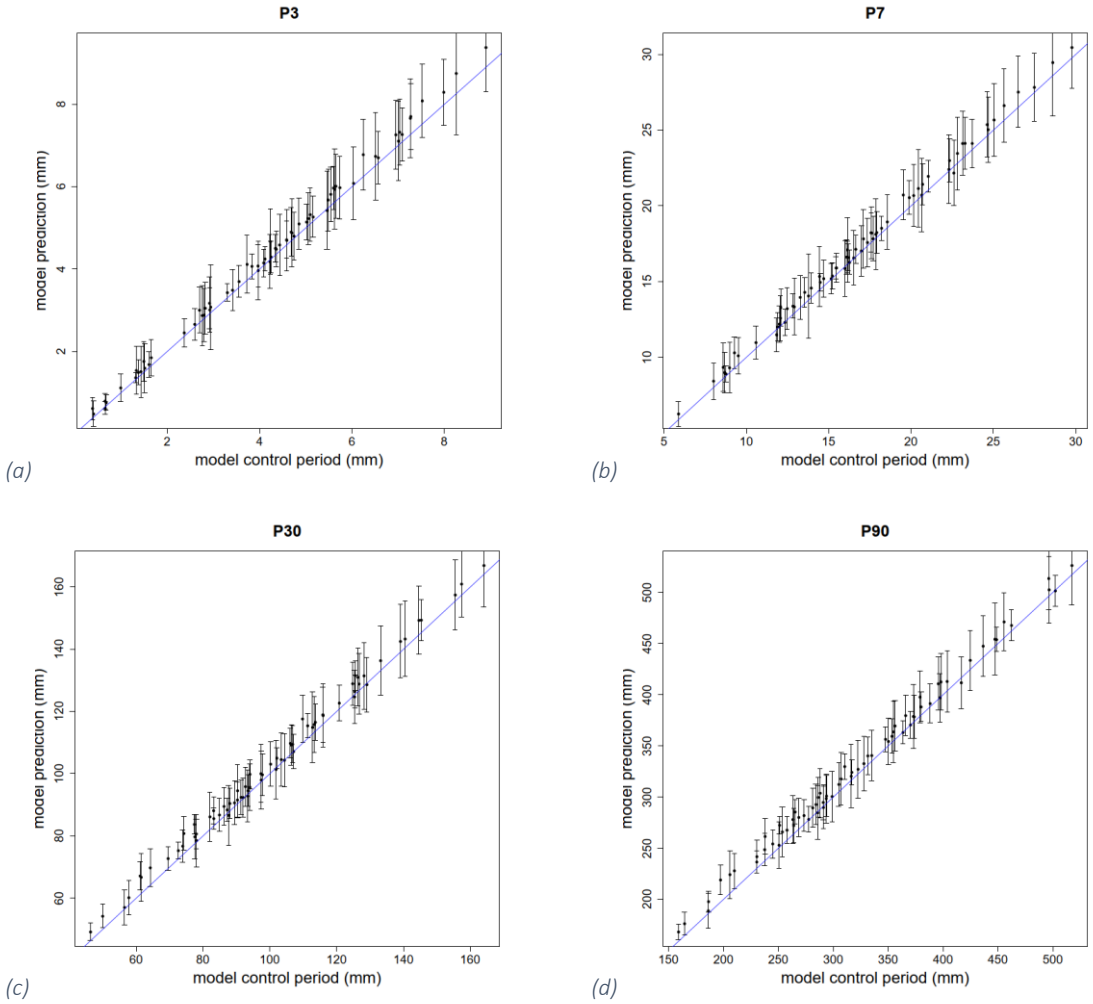

Figure 58 - Correlation between the maximum of RCP4.5 (2021 – 2060) and RCP4.5 (1981 – 2020) of the 3 (a), 7 (b), 30 (c) and 90 day precipitation (d) in millimeters for the 69 stations analyzed. The blue line displays the 1:1 line while the error bars indicate the standard deviation of CH2018 model results.

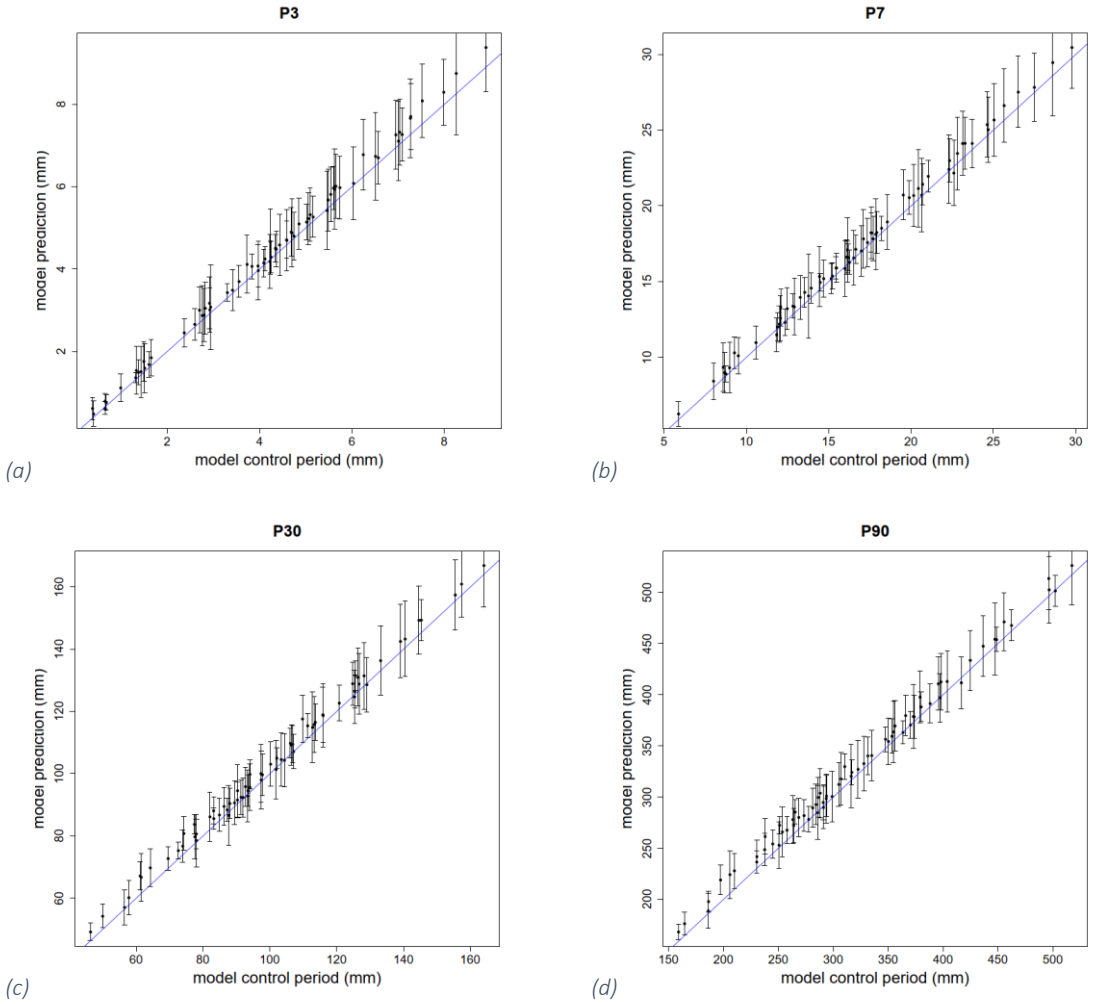

Figure 59 - Correlation between the maximum of RCP8.5 (2021 – 2060) and RCP8.5 (1981 – 2020) of the 3 (a), 7 (b), 30 (c) and 90 day precipitation (d) in millimeters for the 69 stations analyzed. The blue line displays the 1:1 line while the error bars indicate the standard deviation of CH2018 model results.

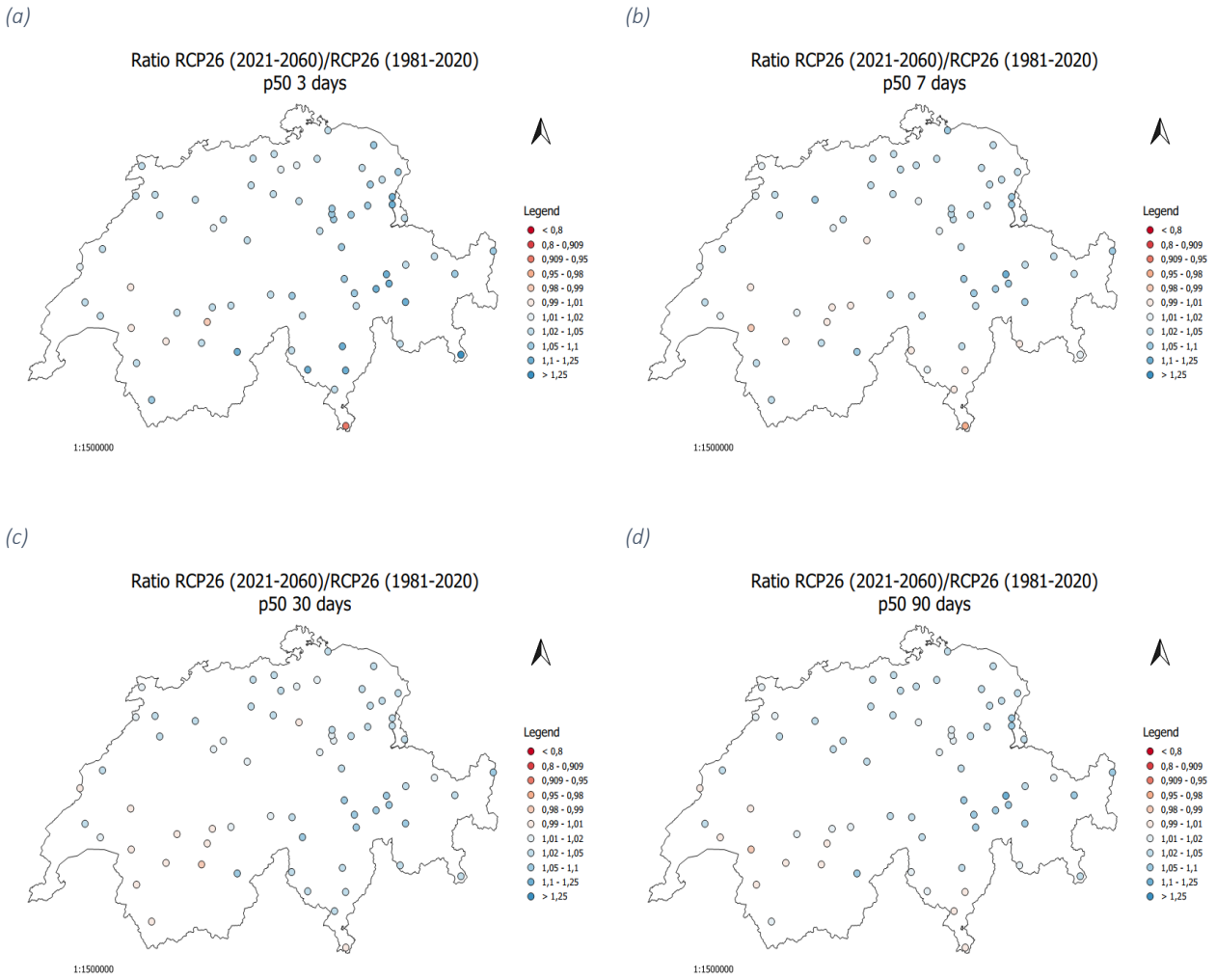

Figure 60 - Maps showing the ratio of the median or 50th percentile of the 3 (a), 7 (b), 30 (c) and 90 day precipitation (d) for the RCP2.6 scenario of the CH2018 simulations (mean of all ten models) for the period between 2021 and 2060 and the RCP2.6 scenario of the CH2018 simulation (mean of all ten models) for the control period (1981 – 2020). Values larger than 1 indicate an overestimation (blue) and values less than 1 an underestimation (red).

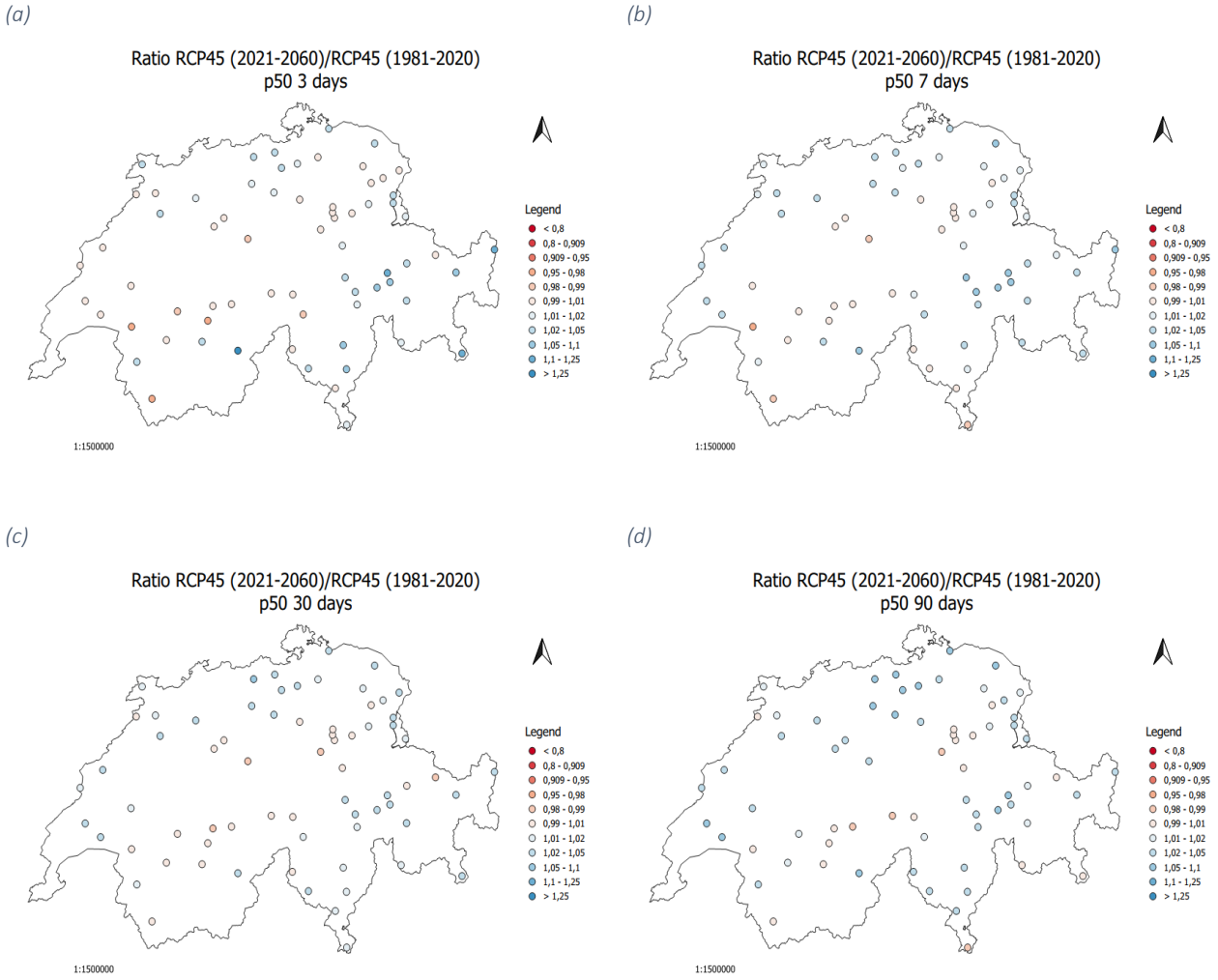

Figure 61 - Maps showing the ratio of the median or 50th percentile of the 3 (a), 7 (b), 30 (c) and 90 day precipitation (d) for the RCP4.5 scenario of the CH2018 simulations (mean of all ten models) for the period between 2021 and 2060 and the RCP4.5 scenario of the CH2018 simulation (mean of all ten models) for the control period (1981 – 2020). Values larger than 1 indicate an overestimation (blue) and values less than 1 an underestimation (red).

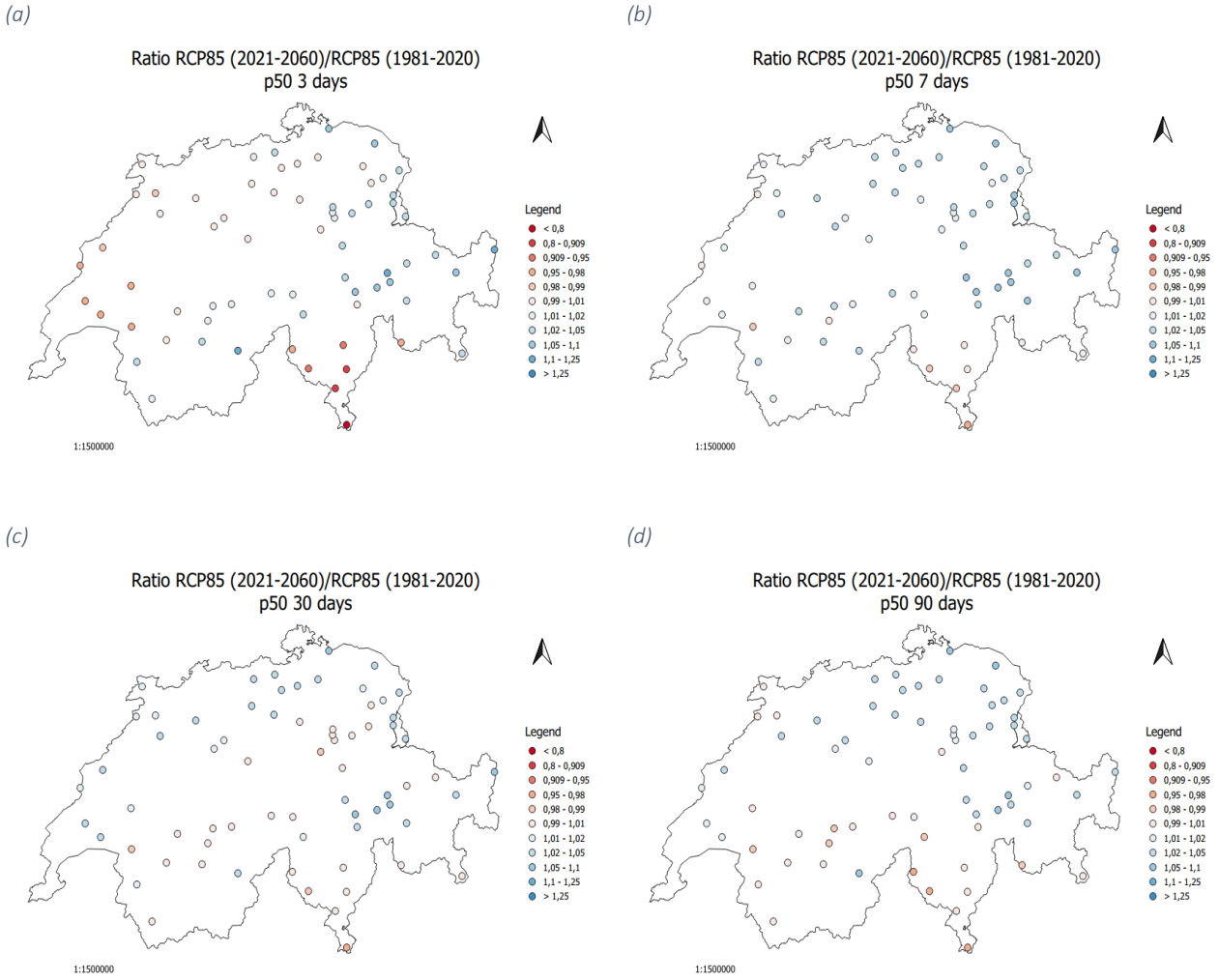

Figure 62 - Maps showing the ratio of the median or 50th percentile of the 3 (a), 7 (b), 30 (c) and 90 day precipitation (d) for the RCP8.5 scenario of the CH2018 simulations (mean of all ten models) for the period between 2021 and 2060 and the RCP8.5 scenario of the CH2018 simulation (mean of all ten models) for the control period (1981 – 2020). Values larger than 1 indicate an overestimation (blue) and values less than 1 an underestimation (red).

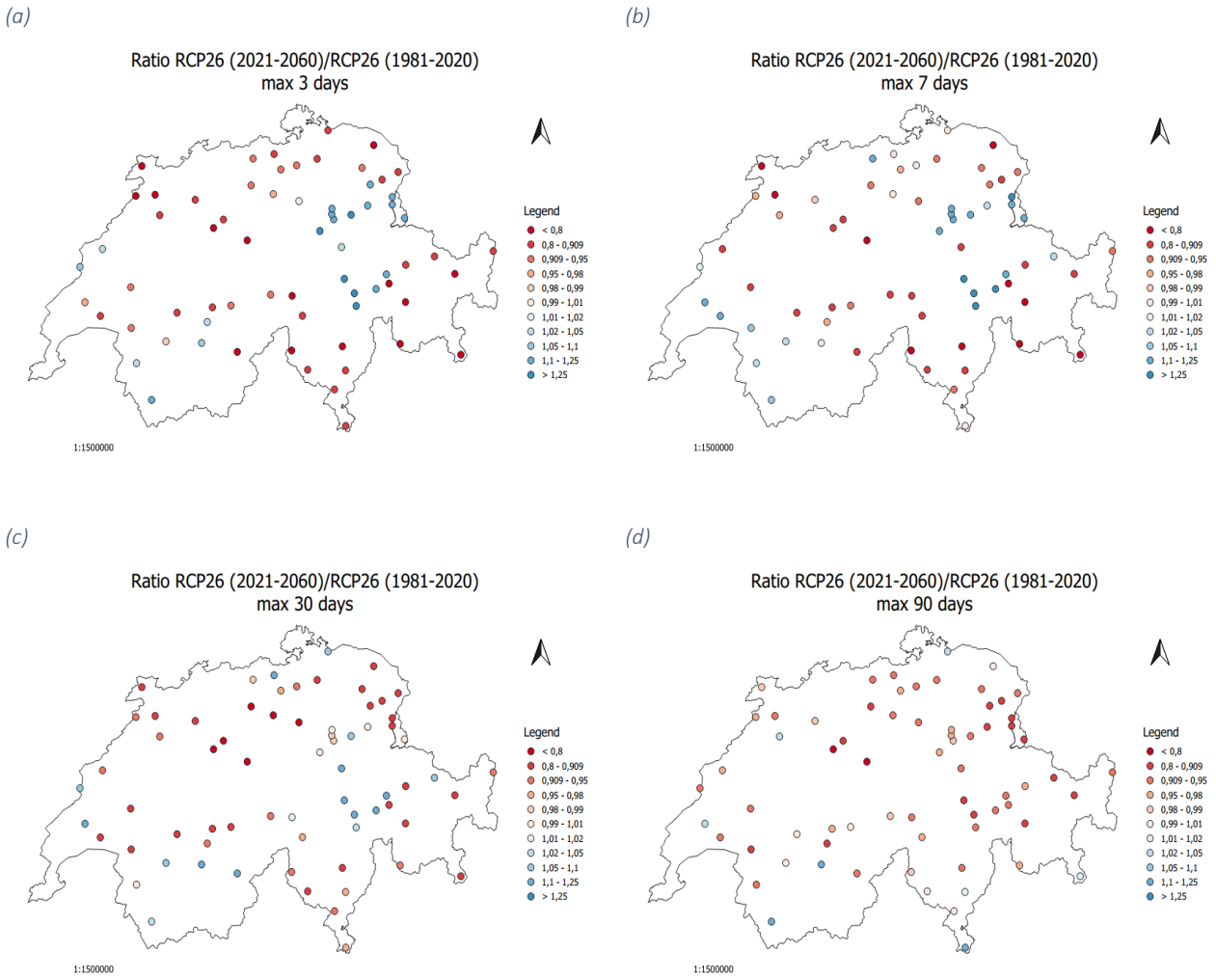

Figure 63 - Maps showing the ratio of the maximum of the 3 (a), 7 (b), 30 (c) and 90 day precipitation (d) for the RCP2.6 scenario of the CH2018 simulations (mean of all ten models) for the period between 2021 and 2060 and the RCP2.6 scenario of the CH2018 simulation (mean of all ten models) for the control period (1981 – 2020). Values larger than 1 indicate an overestimation (blue) and values less than 1 an underestimation (red).

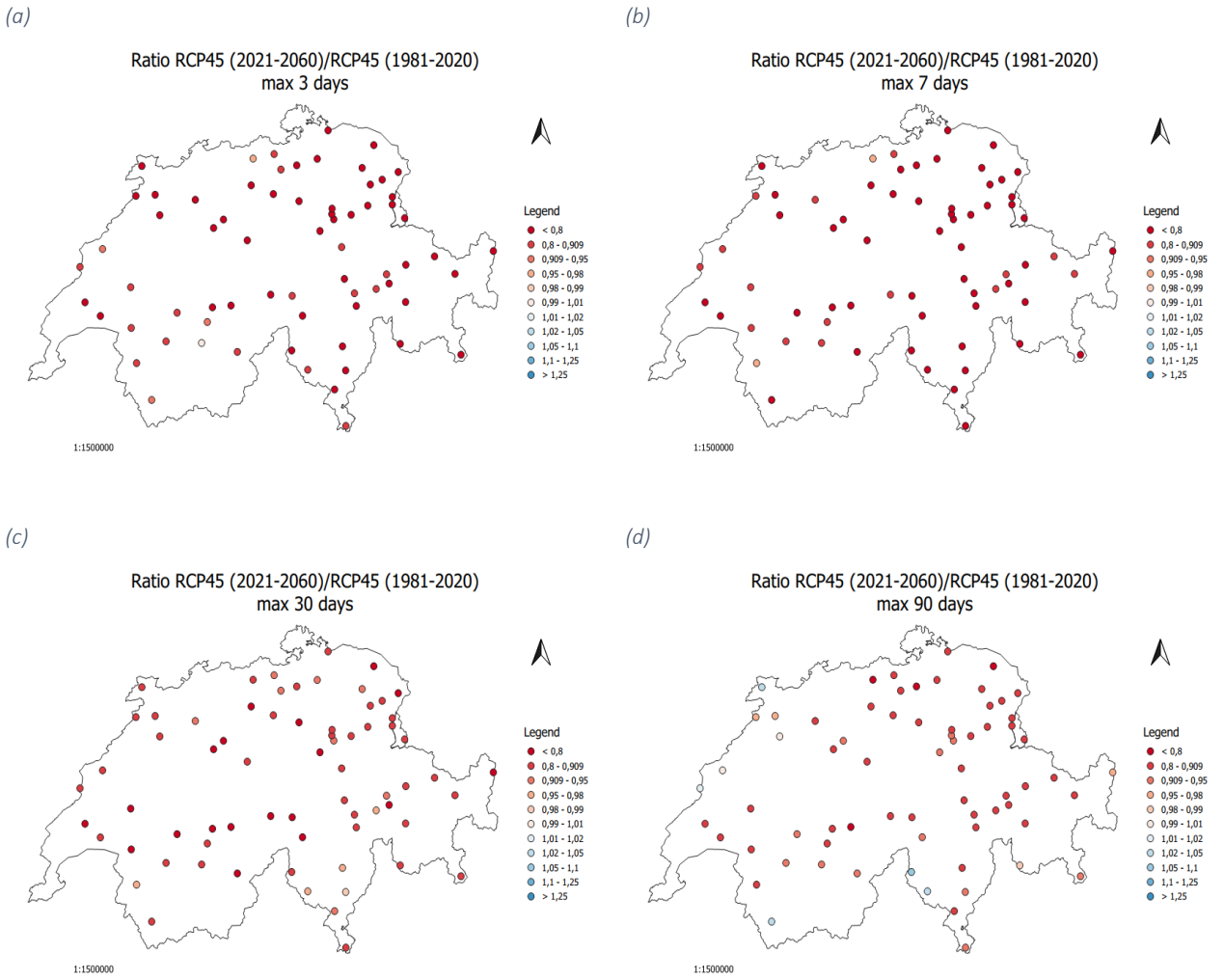

Figure 64 - Maps showing the ratio of the maximum of the 3 (a), 7 (b), 30 (c) and 90 day precipitation (d) for the RCP4.5 scenario of the CH2018 simulations (mean of all ten models) for the period between 2021 and 2060 and the RCP4.5 scenario of the CH2018 simulation (mean of all ten models) for the control period (1981 – 2020). Values larger than 1 indicate an overestimation (blue) and values less than 1 an underestimation (red).

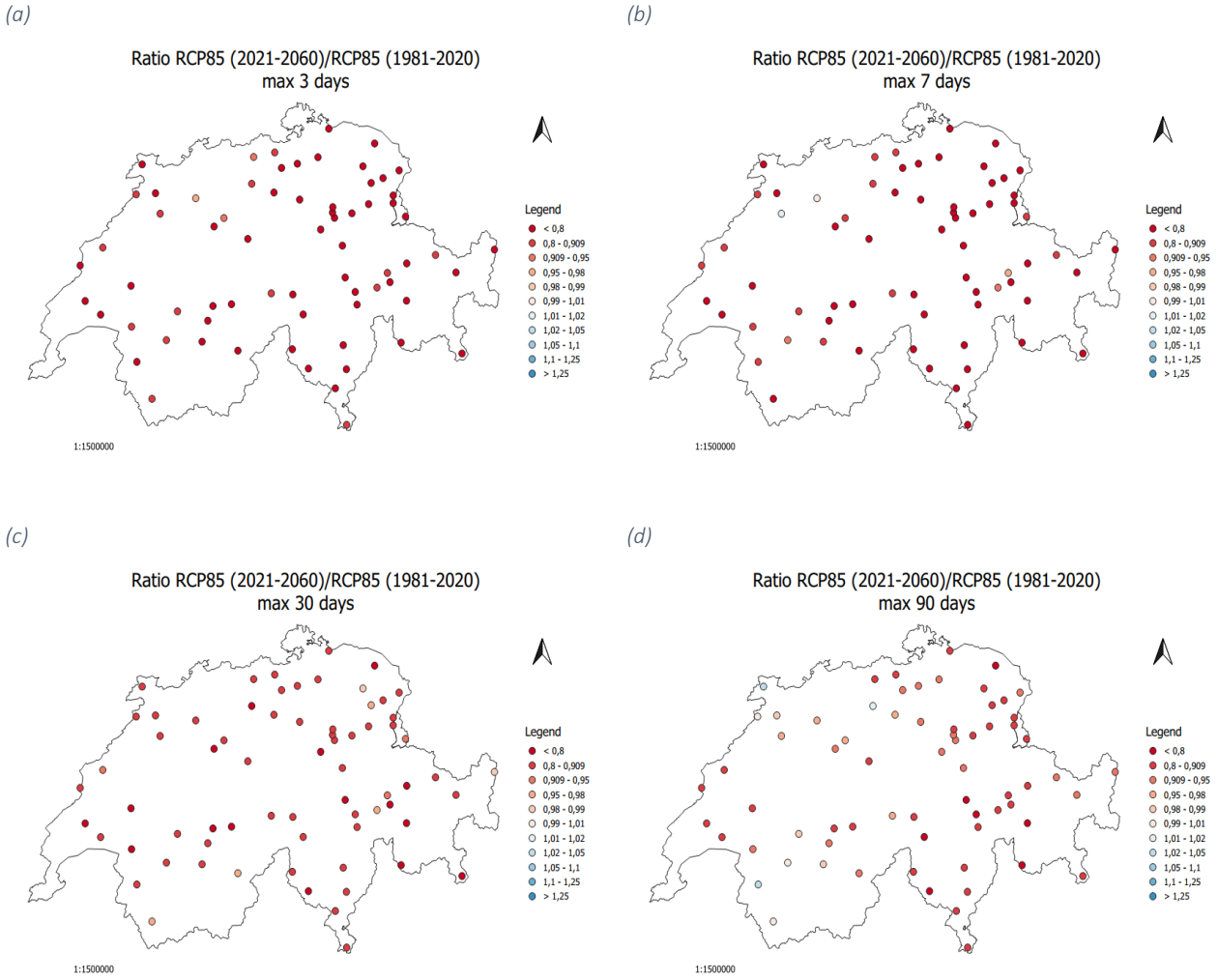

Figure 65 - Maps showing the ratio of the maximum of the 3 (a), 7 (b), 30 (c) and 90 day precipitation (d) for the RCP8.5 scenario of the CH2018 simulations (mean of all ten models) for the period between 2021 and 2060 and the RCP8.5 scenario of the CH2018 simulation (mean of all ten models) for the control period (1981 – 2020). Values larger than 1 indicate an overestimation (blue) and values less than 1 an underestimation (red).

8.3 Second future period (2021-2099)

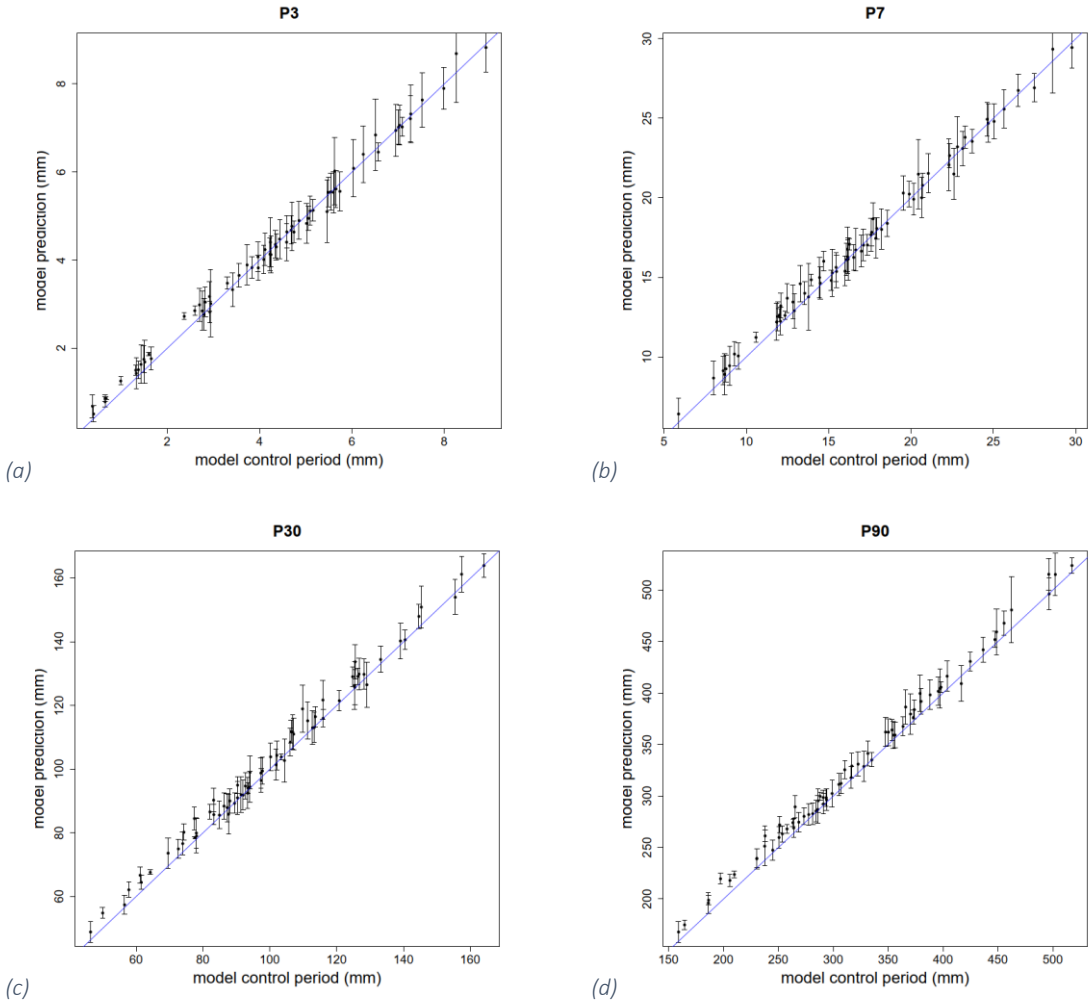

Figure 66 - Correlation between the mean of RCP2.6 (2061 – 2099) and RCP2.6 (1981 – 2020) of the 3 (a), 7 (b), 30 (c) and 90 day precipitation (d) in millimeters for the 69 stations analyzed. The blue line displays the 1:1 line while the error bars indicate the standard deviation of CH2018 model results.

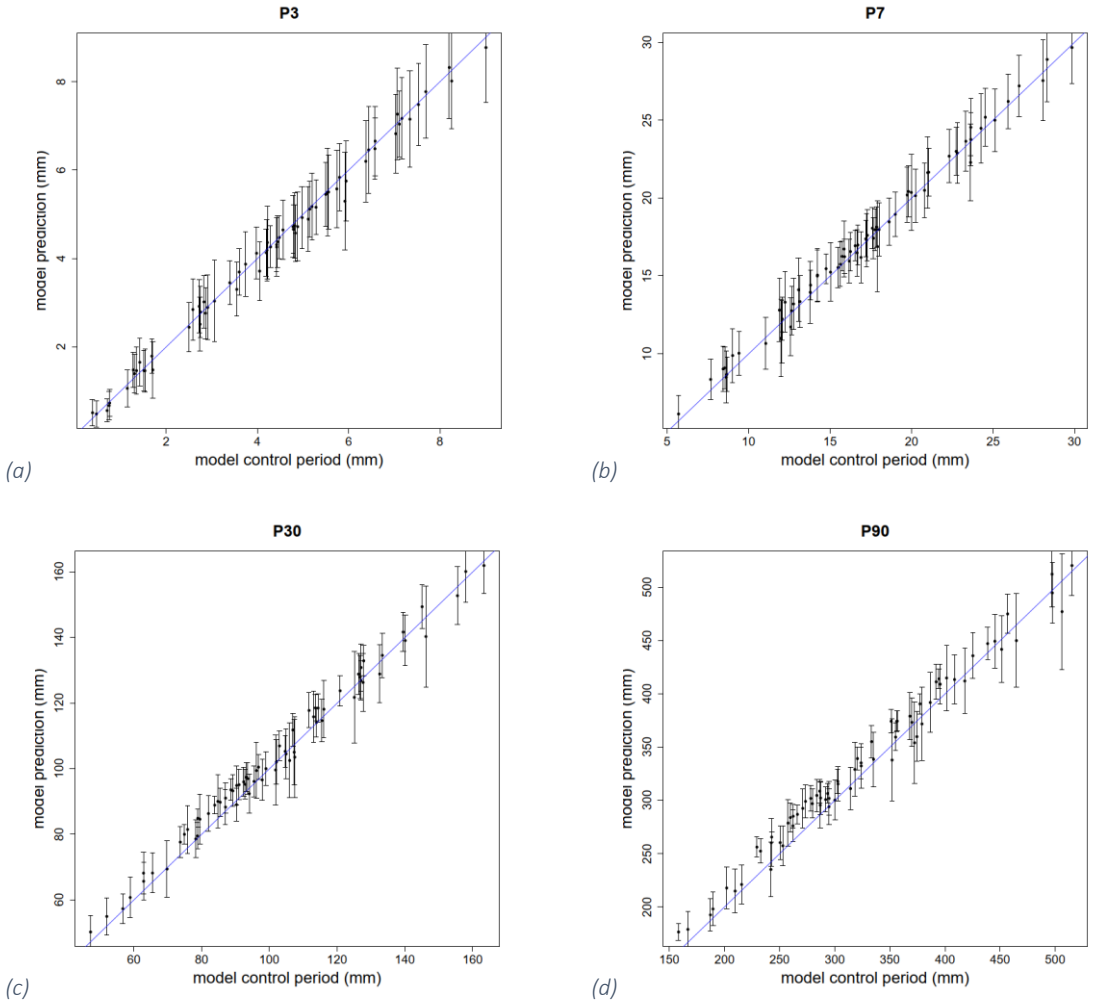

Figure 67 - Correlation between the mean of RCP4.5 (2061 – 2099) and RCP4.5 (1981 – 2020) of the 3 (a), 7 (b), 30 (c) and 90 day precipitation (d) in millimeters for the 69 stations analyzed. The blue line displays the 1:1 line while the error bars indicate the standard deviation of CH2018 model results.

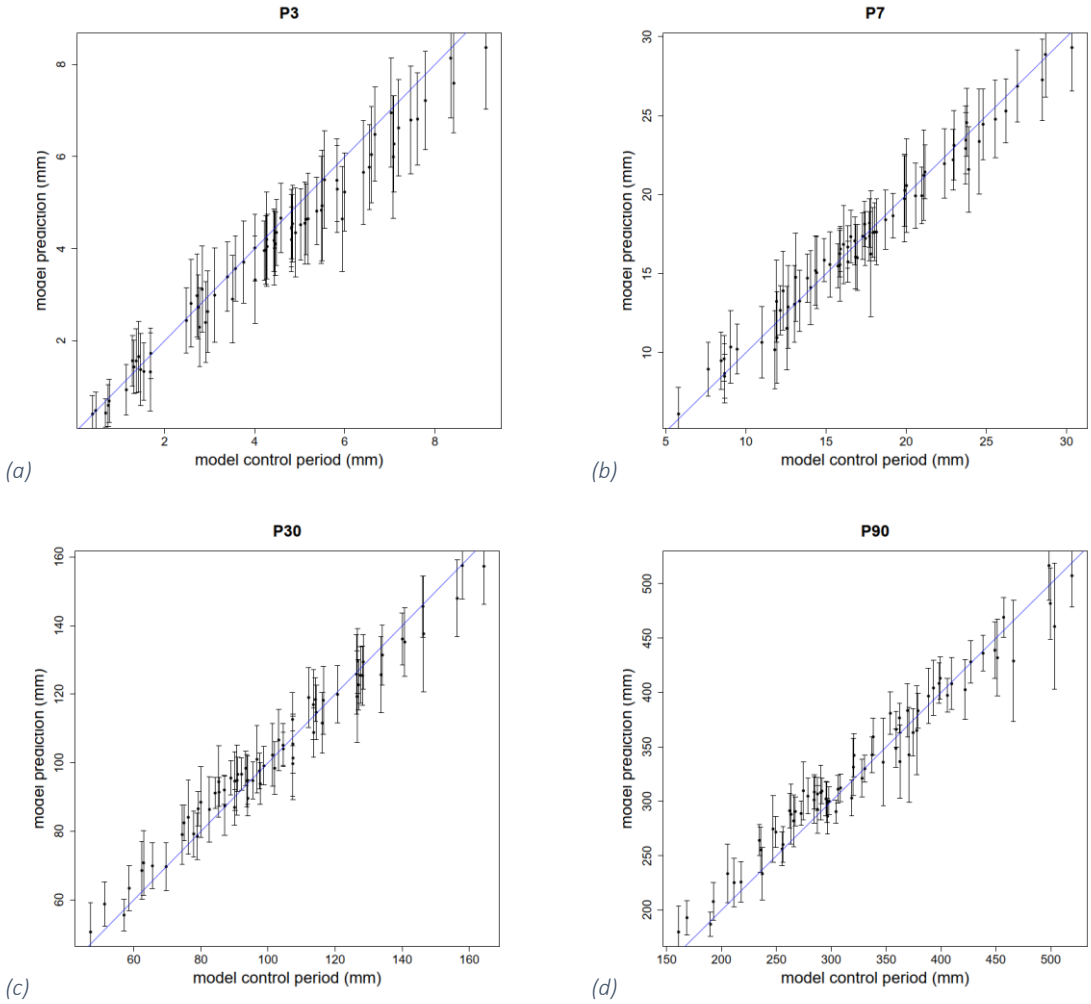

Figure 68 - Correlation between the mean of RCP8.5 (2061 – 2099) and RCP8.5 (1981 – 2020) of the 3 (a), 7 (b), 30 (c) and 90 day precipitation (d) in millimeters for the 69 stations analyzed. The blue line displays the 1:1 line while the error bars indicate the standard deviation of CH2018 model results.

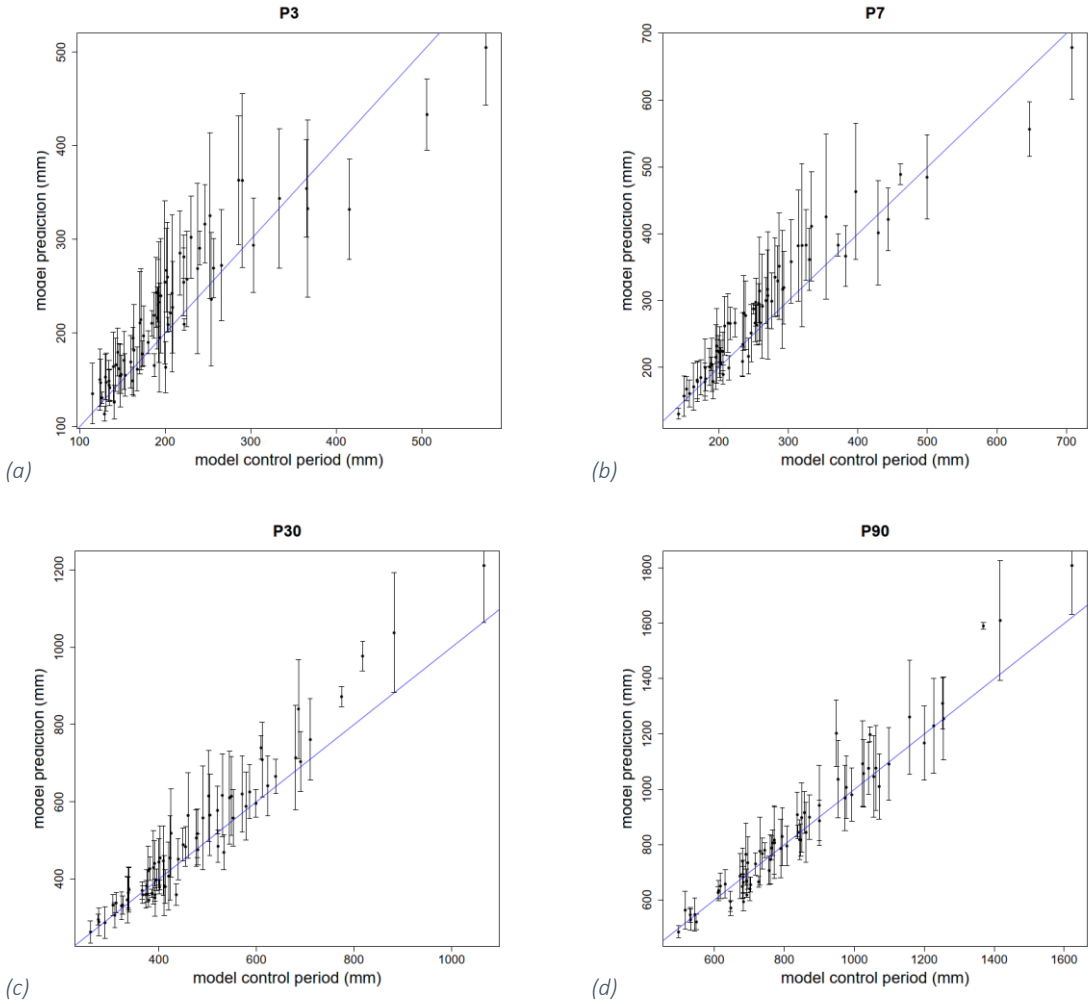

Figure 69 - Correlation between the maximum of RCP2.6 (2061 – 2099) and RCP2.6 (1981 – 2020) of the 3 (a), 7 (b), 30 (c) and 90 day precipitation (d) in millimeters for the 69 stations analyzed. The blue line displays the 1:1 line while the error bars indicate the standard deviation of CH2018 model results.

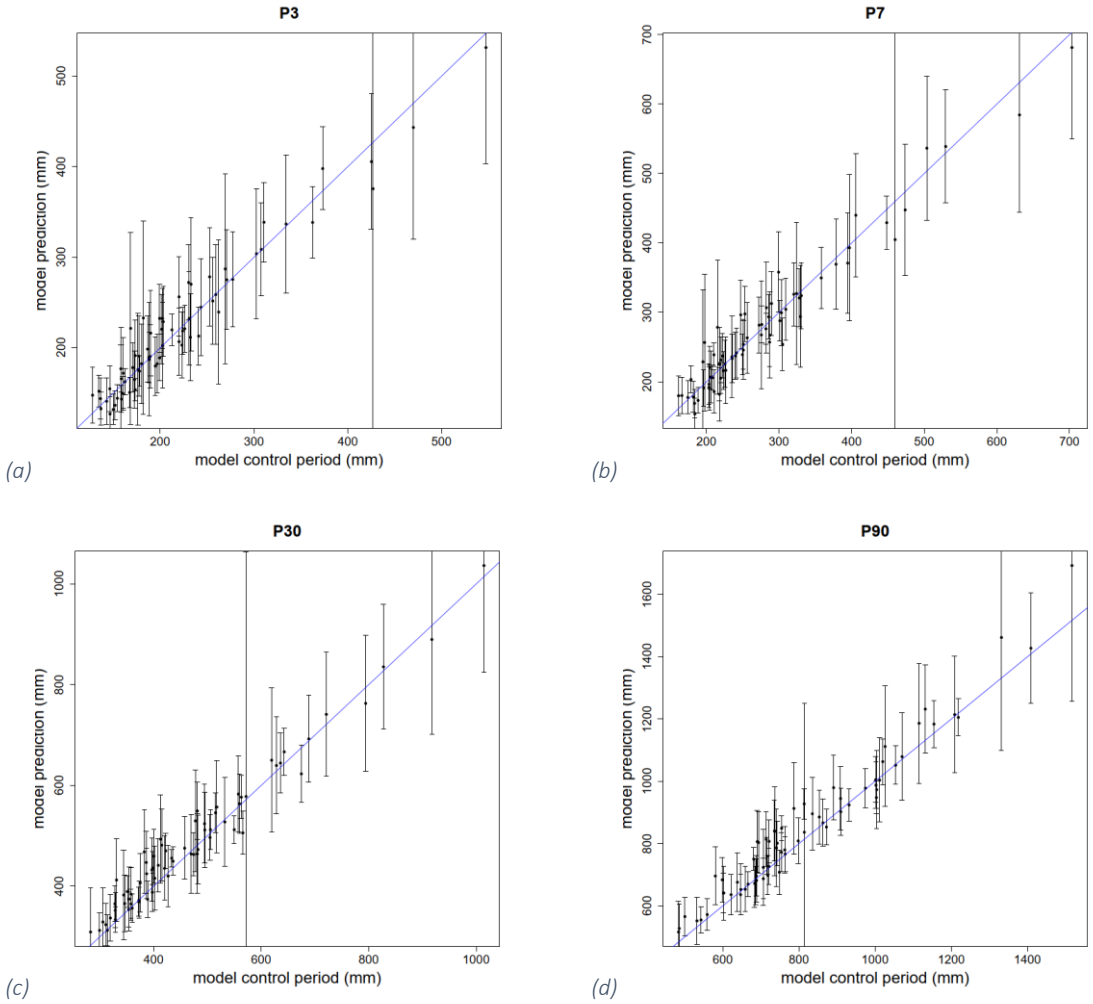

Figure 70 - Correlation between the maximum of RCP4.5 (2061 – 2099) and RCP4.5 (1981 – 2020) of the 3 (a), 7 (b), 30 (c) and 90 day precipitation (d) in millimeters for the 69 stations analyzed. The blue line displays the 1:1 line while the error bars indicate the standard deviation of CH2018 model results.

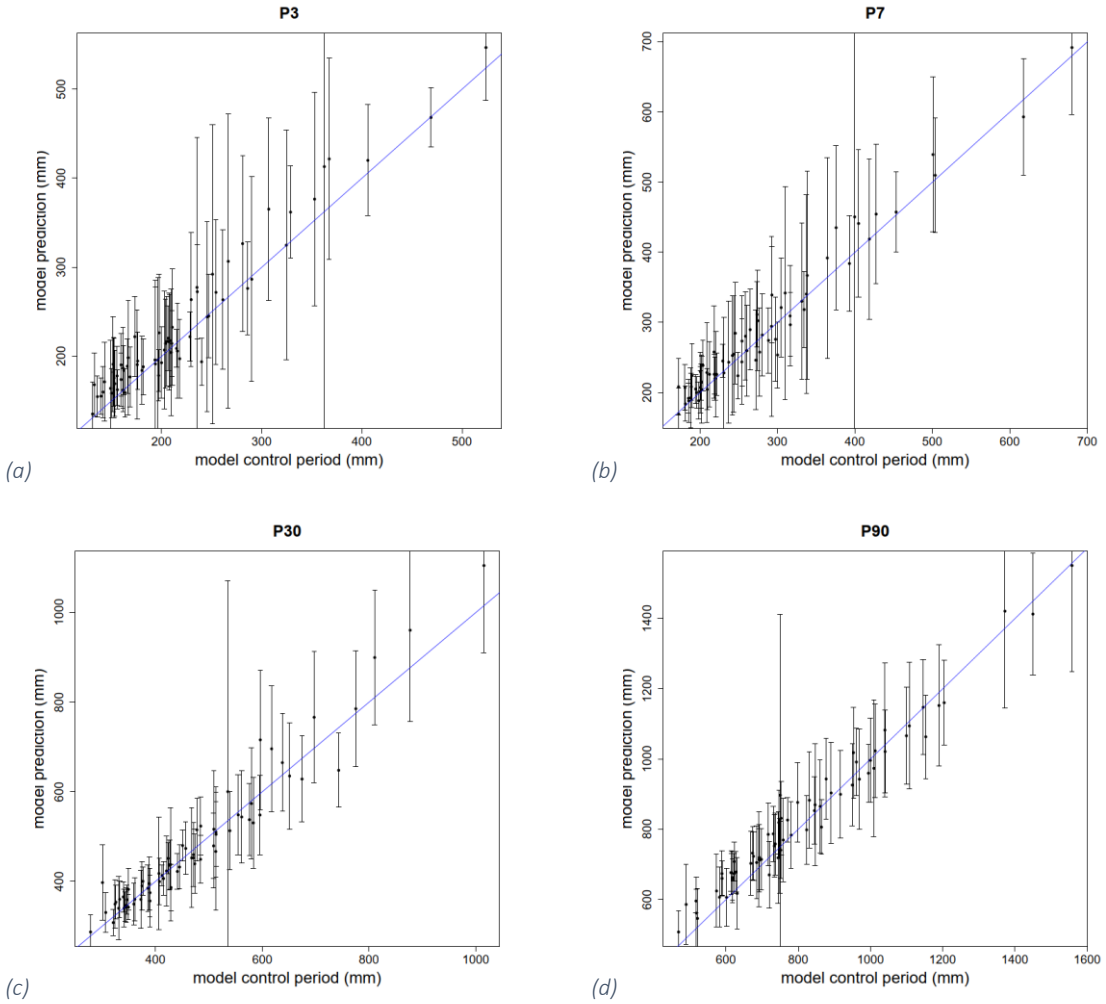

Figure 71 - Correlation between the maximum of RCP8.5 (2061 – 2099) and RCP8.5 (1981 – 2020) of the 3 (a), 7 (b), 30 (c) and 90 day precipitation (d) in millimeters for the 69 stations analyzed. The blue line displays the 1:1 line while the error bars indicate the standard deviation of CH2018 model results.

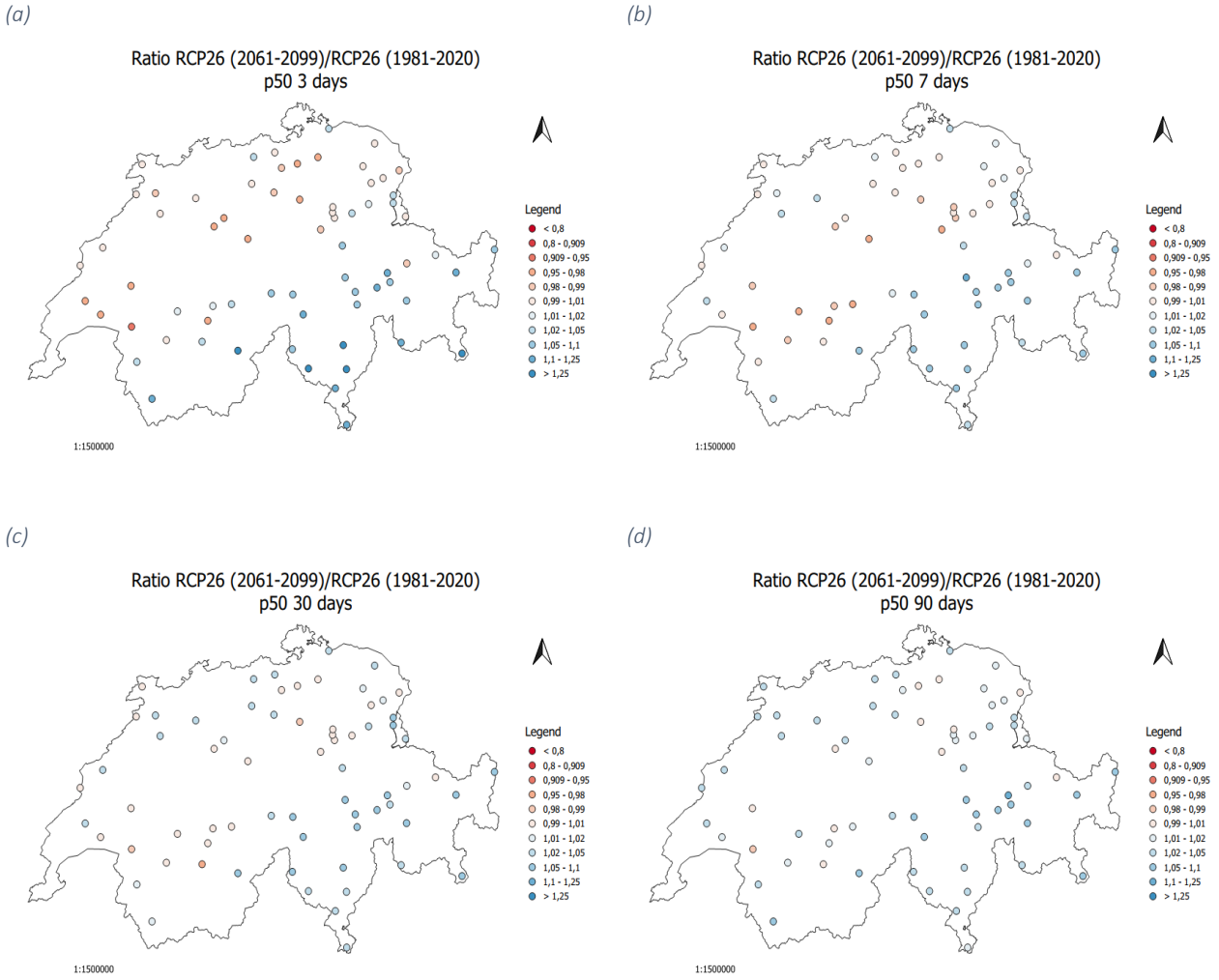

Figure 72 - Maps showing the ratio of the median or 50th percentile of the 3 (a), 7 (b), 30 (c) and 90 day precipitation (d) for the RCP2.6 scenario of the CH2018 simulations (mean of all ten models) for the period between 2061 and 2099 and the RCP2.6 scenario of the CH2018 simulation (mean of all ten models) for the control period (1981 – 2020). Values larger than 1 indicate an overestimation (blue) and values less than 1 an underestimation (red).

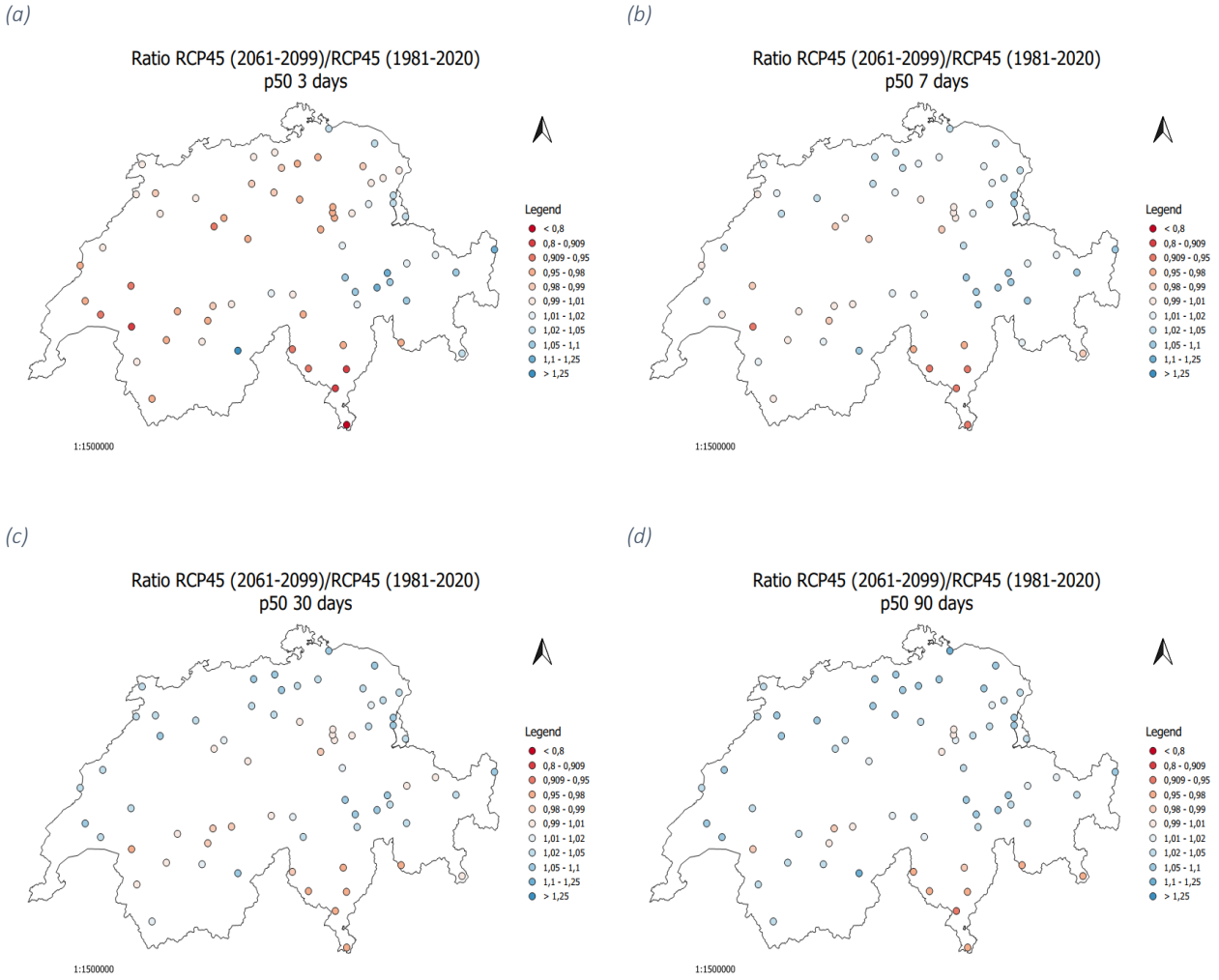

Figure 73 - Maps showing the ratio of the median or 50th percentile of the 3 (a), 7 (b), 30 (c) and 90 day precipitation (d) for the RCP4.5 scenario of the CH2018 simulations (mean of all ten models) for the period between 2061 and 2099 and the RCP4.5 scenario of the CH2018 simulation (mean of all ten models) for the control period (1981 – 2020). Values larger than 1 indicate an overestimation (blue) and values less than 1 an underestimation (red).

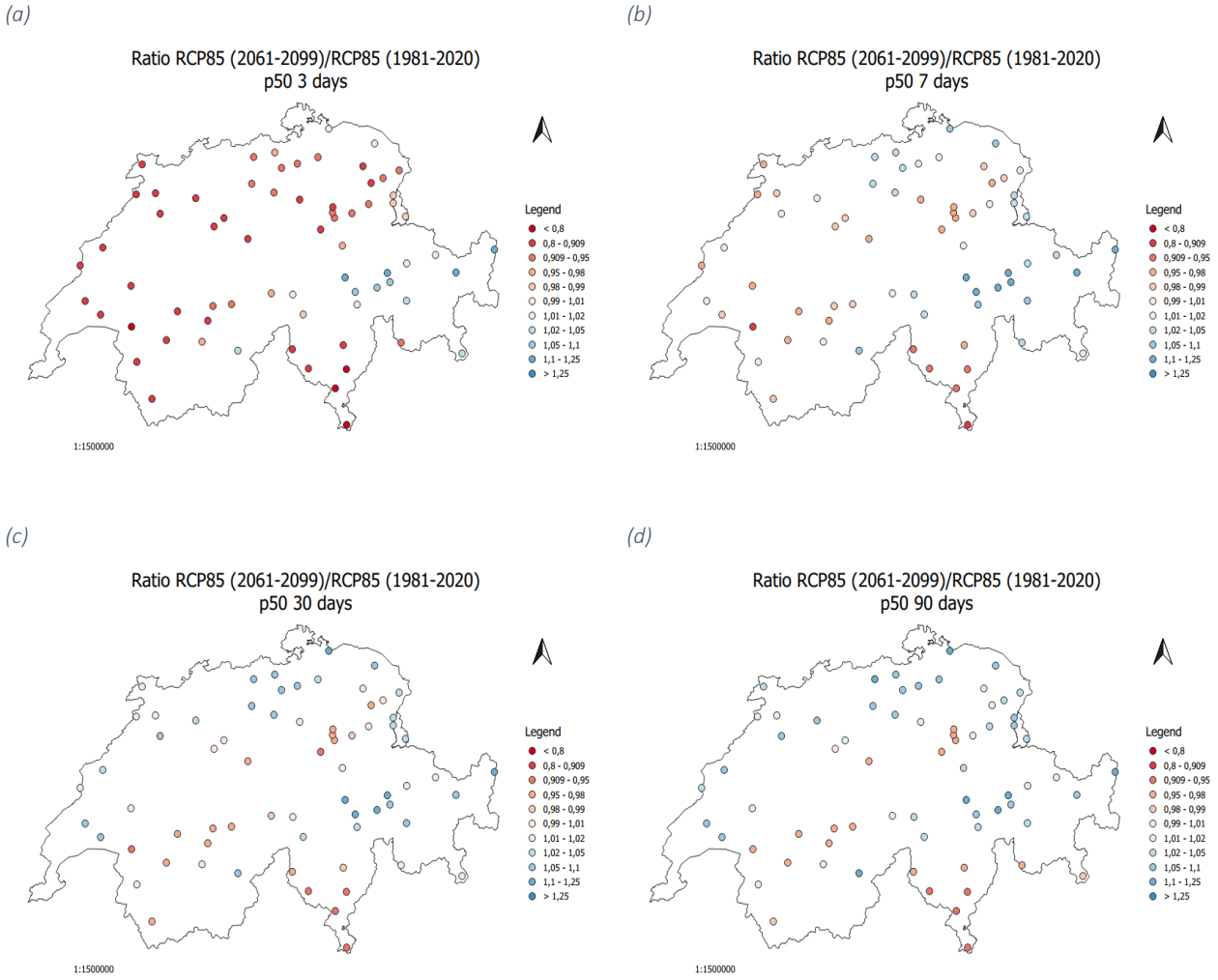

Figure 74 - Maps showing the ratio of the median or 50th percentile of the 3 (a), 7 (b), 30 (c) and 90 day precipitation (d) for the RCP8.5 scenario of the CH2018 simulations (mean of all ten models) for the period between 2061 and 2099 and the RCP8.5 scenario of the CH2018 simulation (mean of all ten models) for the control period (1981 – 2020). Values larger than 1 indicate an overestimation (blue) and values less than 1 an underestimation (red).

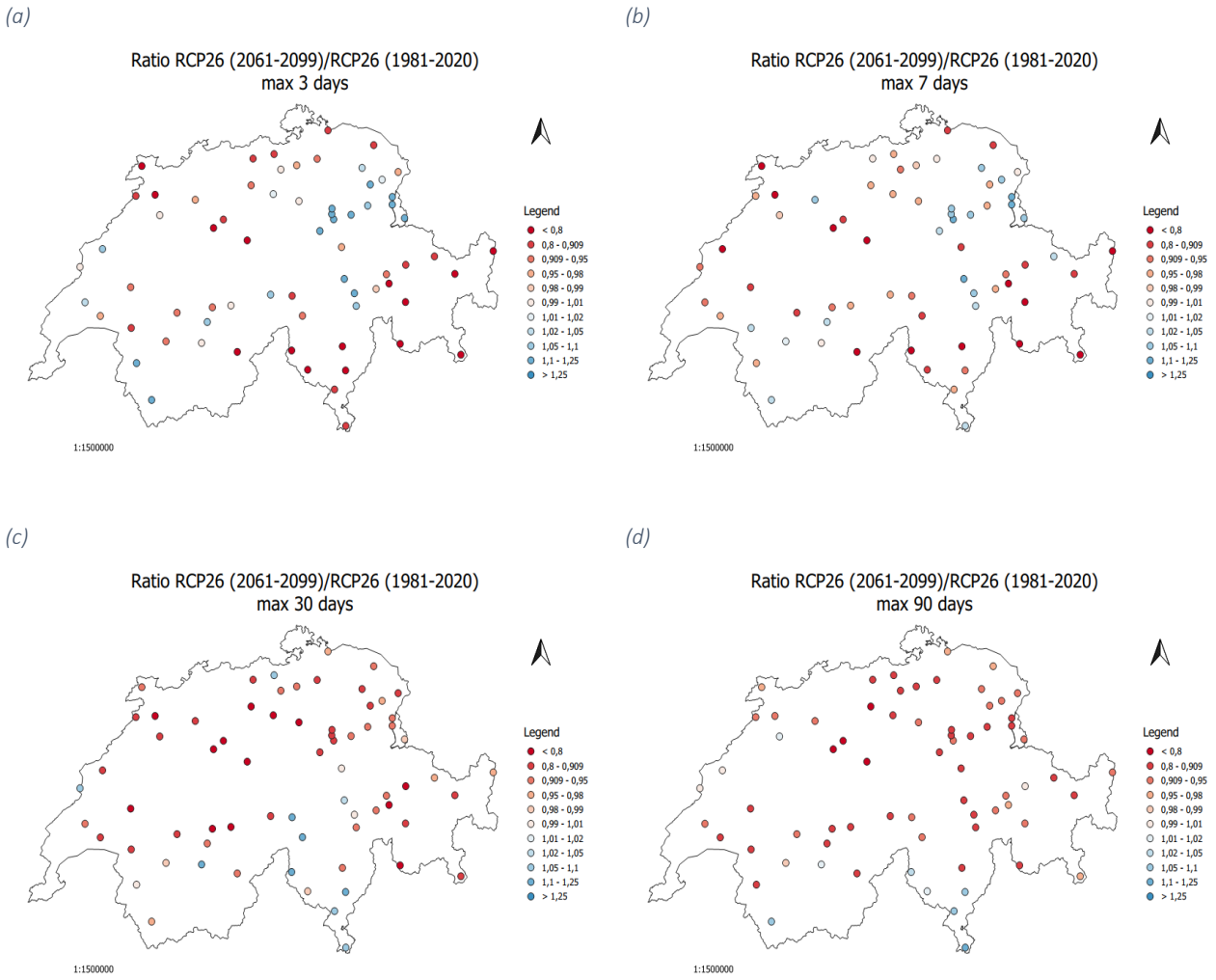

Figure 75 - Maps showing the ratio of the maximum of the 3 (a), 7 (b), 30 (c) and 90 day precipitation (d) for the RCP2.6 scenario of the CH2018 simulations (mean of all ten models) for the period between 2061 and 2099 and the RCP2.6 scenario of the CH2018 simulation (mean of all ten models) for the control period (1981 – 2020). Values larger than 1 indicate an overestimation (blue) and values less than 1 an underestimation (red).

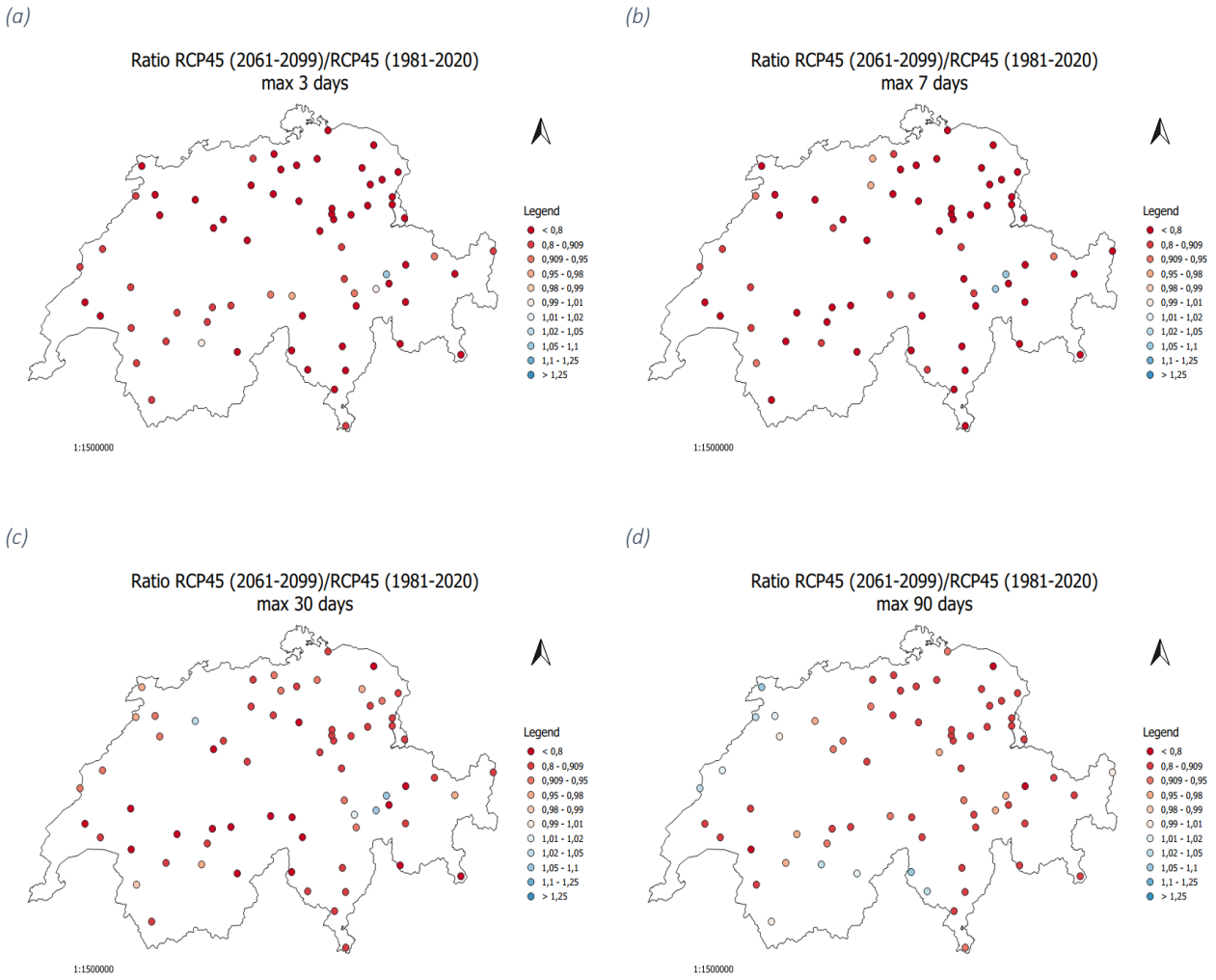

Figure 76 - Maps showing the ratio of the maximum of the 3 (a), 7 (b), 30 (c) and 90 day precipitation (d) for the RCP4.5 scenario of the CH2018 simulations (mean of all ten models) for the period between 2061 and 2099 and the RCP4.5 scenario of the CH2018 simulation (mean of all ten models) for the control period (1981 – 2020). Values larger than 1 indicate an overestimation (blue) and values less than 1 an underestimation (red).

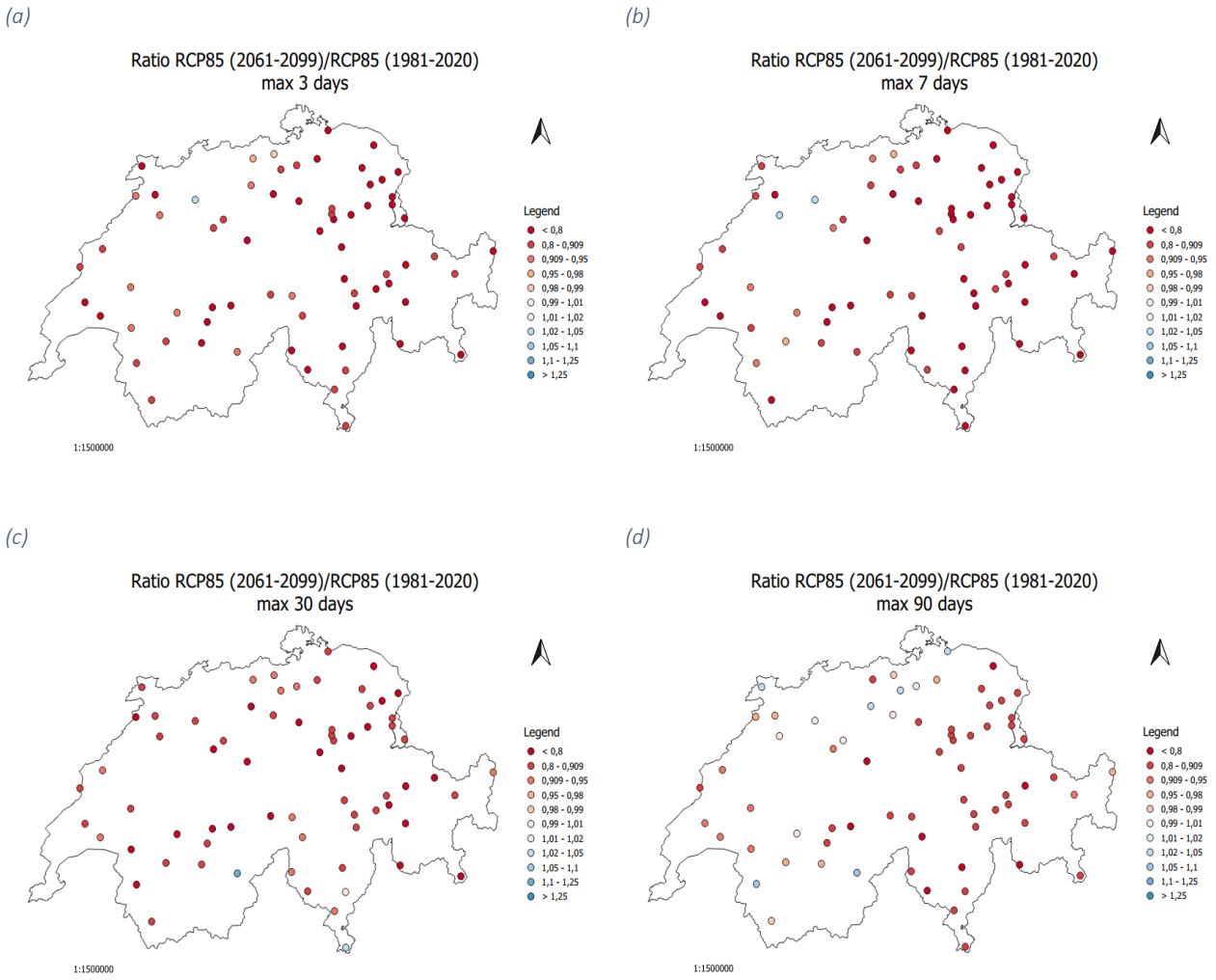

Figure 77 - Maps showing the ratio of the maximum of the 3 (a), 7 (b), 30 (c) and 90 day precipitation (d) for the RCP8.5 scenario of the CH2018 simulations (mean of all ten models) for the period between 2061 and 2099 and the RCP8.5 scenario of the CH2018 simulation (mean of all ten models) for the control period (1981 – 2020). Values larger than 1 indicate an overestimation (blue) and values less than 1 an underestimation (red).

Zürich, 30th September 2021

Declaration of Originality

I hereby declare that the submitted thesis is the result of my own, independent work.
All external sources are explicitly acknowledged in the thesis.

Désirée Montalbetti